Imperial College London

CELL-BASED GENE THERAPY FOR MENDING INFARCTED HEARTS

By

Bhawana Poudel

A Dissertation Submitted for the Examination
for the Transfer of Status to the Degree of
Doctor of Philosophy

Supervisors

Professor Nadia Rosenthal

Dr. Maria Paola Santini

Harefield Heart Science Centre

National Heart and Lung Institute

Imperial College London

2011

ABSTRACT

The goal of this study was to analyse the efficiency of a combinatorial cell/growth factor therapy to improve function of infarcted murine hearts. The Insulin-like Growth Factor-1 (IGF-1) isoform, IGF-1Ea, has been shown to reduce scar formation and decrease cell death after MI. The present study utilized P19Cl6-derived, *IGF-1Ea* over-expressing cardiomyocytes to achieve its goal.

The P19Cl6 cells were stably transduced with *IGF-1Ea* using a lentiviral vector and investigated first *in vitro* for their feasibility for *in vivo* cell therapy. The engineered pluripotent cells over-expressing *IGF-1Ea* survived better to hypoxia-induced injury than the control cells. The cells maintained their pluripotency and efficient differentiation capacity towards ventricular cardiomyocyte lineage, generating large quantities of cardiomyocytes optimal for the transplantation study. The generated cardiomyocytes were functionally active and exhibited a mature phenotype.

Transplantation of the cardiomyocytes into allogeneic wild type murine infarcted hearts conferred a tendency for maintenance of function at short-term time point. At long-term however, this effect was lost, returning to the level of the control infarcted hearts. Cell tracing assessment revealed engraftment of both IGF-1Ea- and empty-cells, although the cells failed to couple with the recipient tissue. Scar size and capillary density analyses revealed no significant difference between the cells transplanted compared to the saline treated hearts, corroborating with the long-term functional data. Interestingly, the IGF-1Ea-cell transplanted hearts expressed significantly higher amount of VEGFa compared to the controls, albeit no change in capillary density. Further investigation revealed that the enhanced VEGFa expression in IGF-1Ea-cells transplanted hearts was associated with reduced hypertrophy, marked by reduced cell cross-sectional area at the border-zone, aSK and bMHC expression compared to the control hearts. Nonetheless, modulation of hypertrophic response and transplantation of IGF-1Ea-cells were not able to confer lasting functional preservation, possibly due to lack of sufficient engraftment and coupling of the transplanted cells.

ACKNOWLEDGEMENT

I would like to thank my family in Nepal and in Germany for all their love, support and care. My special gratitude goes to Lars who has gone through all the ups and downs with me during this PhD experience. Thank you for being so understanding, for all the valuable input on my work and most importantly for taking time to edit my thesis! Without your love, encouragement, support and trust I would not have made this far.

I cannot thank enough my supervisors. Nadia, you are an inspiration to me and you will always be! I shall always cherish the moments in your labs in Harefield and Rome! Thank you for giving me the opportunities to explore various labs and attend wonderful conferences. I feel very lucky and honoured to have worked with you. Maria Paola, I cannot thank you enough for all the things you have taught me and the brilliant project that I could work on because of you. Thank you for being a wonderful teacher.

My supervisors and I would like to extend our special gratitude to Professor Christine Mummery for providing us with P19Cl6 cells. Thank you to all the Molecular and Cellular Biology, Cardiac Regeneration, Electrophysiology and Developmental Dynamics Group members at Harefield and Nadia Rosenthal lab in Monterotondo for being such wonderful people and for helping me with various projects and techniques throughout my PhD experience. Thank you Esfir for taking care of me during my stay in Rome, Padmini for helping me with histological analyses, Elham for all your encouragement, support and being a true friend, Leanne and Rene for teaching me the real time PCR, statistics and hypoxia assays, Roland and Jan for helping me with microscopes, Tommasso for continuing my work and Cesare for teaching me electrophysiological techniques and most importantly for his moral support as a mentor. Thank you to Kalyani, Jonas and Borggia for sharing their PhD experience and fun times with me.

My special thank you goes to EMBO Short-term Fellowship for providing me the opportunity to conduct a part of my PhD work at EMBL, Monterotondo. Most importantly, thank you to Imperial College London and the Harefield Heart Science Centre, UK for giving me the wonderful PhD opportunity to work at two of the world's most prestigious institutes for research.

ABBREVIATIONS

CVDs	Cardiovascular Diseases
TBX5	T-Box transcription factor 5
Gata4	Gata-binding protein 4
MI	Myocardial Infarction
IL8	Interleukin 8
Mac-1-ICAM-1	Macrophage-1 antigen, Inter-Cellular Adhesion Molecule 1
IL-1	Interleukin-1
TNFα	Transforming Growth Factor alpha
PEUU	Polyester Urethane Urea
MSC	Mesenchymal Stem Cell
CSC	Cardiac Stem Cell
ESC	Embryonic Stem Cell
iPS cells	induced Pluripotent Stem cells
MCP-3	Monocyte Chemotactic Protein-3
SDF-1	Stromal-derived Factor-1
LVEF	Left Ventricular Ejection Fraction
BOOST	Bone Marrow Transfer to Enhance ST-Elevation Infarct Regeneration
Klf4	Kruppel-like factor 4
CHF	Chronic Heart Failure
LV	Left Ventricle
Bcl-2	B-cell lymphoma 2
VEGF	Vascular Endothelial Growth Factor
IGF-1	Insulin-like Growth Factor-1
P19EC	Embryonal Carcinoma-derived stem cells
P19Cl6	Clonal derivative of P19EC
GFP	Green Fluorescent Protein
MLC-2v	Myosin Light Chain-2 ventricular
MLC-1	Myosin Light Chain-1
MLC-2	Myosin Light Chain-2
CMV	Cytomegalovirus
DMSO	Dimethylsulfoxide

EB	Embroid Body
MEF2c	Myocyte Enhancer Factor 2c
BMP	Bone Morphogenic Protein
αMHC	alpha Myosin Heavy Chain
βMHC	beta Myosin Heavy Chain
IGF-1Ea	Insulin-like Growth Factor-1 Ea isoform
IGF-2	Insulin-like Growth Factor-2
IGF-1R	Insulin-like Growth Factor-1 Receptor
IGF-2R	Insulin-like Growth Factor-2 Receptor
IGFBP	Insulin-like Growth Factor Binding Protein
DNA	Deoxyribonucleic Acid
RNA	Ribonucleic Acid
mRNA	messenger RNA
MGF	Mechano Growth Factor
Gata2	Gata-binding protein-2
S-Phase	Synthesis Phase
PI-3 kinase	Phosphoinositide-3 kinase
DHP	Dihydropyridine
MAP kinase	Mitogen Activated Protein kinase
IRS	Insulin Receptor Substrate
SHC	Src-homology containing protein
Grb2	Growth factor receptor-bound protein 2
SOS	Sons of Sevenless
ERK	Extracellular Regulated Kinase
Rb	Retinoblastoma protein
MEF	Myocyte Enhancer Factor
PDK-1	Phosphoinositide-dependent protein kinase-1
NF-ATc	Nuclear Factor of Activated T cells
Tet	Tetracycline
TetR	Tet Repressor
TetO2	Tetracycline Operator
qRT-PCR	quantitative Real Time-Polymerase Chain Reaction
αSK	alpha Skeletal actin
HT1080	Human connective tissue fibrosarcoma cell line

HEK(293)	human embryonic kidney cell line
EMEM	Eagle's Minimum Essential Medium
FBS	Fetal Bovine Serum
DMEM	Dulbecco's Modified Eagle Medium
NEAA	Non-Essential Amino Acids
LDH	Lactate Dehydrogenase
INT	2-(4-iodophenyl)-3-(4-nitrophenyl)-5-phenyltetrazolium chloride
FACS	Fluorescence Activated Cell Sorting
PI	Propidium Iodide
EF	Ejection Fraction
FAC	Fractional Area Change
FS	Fractional Shortening
PFA	Paraformaldehyde
WGA	Wheat Germ Agglutinin
LCA/LAD ligation	Left-anterior Descending Coronary Artery ligation
SEM	Standard Error of the Mean
SD	Standard Deviation
ROS	Reactive Oxygen Species
CICR	Calcium Induced Calcium Release
NCX	Na+/Ca2+ exchanger
SERCA	Sarco(endo)plasmic Ca2+-ATPase
Rhod	Rhodamine based
WT	Wild Type
ECG	Echocardiogram
VEGFR	Vascular Endothelial Growth Factor Receptor
BM-MNC	Bone Marrow-Mononuclear Cells
LVAD	Left Ventricular Assist Device

TABLE OF CONTENTS

TABLE OF TABLES

TABLE OF FIGURES

CHAPTER 1

1.1 SECTION I: GENERAL INTRODUCTION

1.1.1 Cardiovascular diseases

Cardiovascular diseases (CVDs) are among the top killers in the western world and the majority of people who suffer from cardiac diseases is exposed to several risk factors [1]. CVDs are disorders of the blood vessels and the heart. In 2004 alone CVDs claimed 17.1 million lives worldwide, representing 29% of all global deaths. Among these deaths, 7.2 million were caused by coronary heart disease and 5.7 million by stroke [2]. CVDs are either innate or acquired defects of the heart. Congenital heart defect, which is one of the CVDs, is a result of malformation of the heart or blood vessels near the heart during development of the organ. The causes of congenital heart defects are not completely known. However, environmental factors such as exposure to toxic substances [3] or viruses like measles during pregnancies have been implicated in causing congenital heart defects [4]. Progress has been made on understanding the underlying mechanisms and pathways of the congenital heart defects. Research has shown the involvement of a number of transcription factors such as TBX5 [5], Nkx2-5 [6], Gata4 [7] among others in causing different kinds of defects. With a better understanding of the underlying molecular pathways and improved surgical interventions, many of the existing defects can be corrected today. However, these interventions generally only repair the symptoms rather than the cause. Therefore, patients who suffer from congenital heart defects may develop other problems during their adult lives.

During adulthood, people may develop other CVDs such as the valvular heart diseases, inflammatory heart diseases, hypertensive heart diseases and atherosclerosis. The valvular heart diseases affect one or several of the heart valves. Some examples of valvular heart disease are aortic valve stenosis, mitral valve prolapse and valvular cardiomyopathy [8, 9]. The inflammatory heart disease as the name implies, is caused by inflammation of the heart muscle or other tissue within the organ. Some examples of such diseases are endocarditis, inflammatory cardiomegaly and myocarditis [10, 11]. The hypertensive heart disease is one of the largest groups among the acquired CVDs. It is caused by high blood pressure and includes left ventricular hypertrophy, coronary heart disease, congestive heart failure, hypertensive cardiomyopathy and cardiac arrythmias [12]. Another common cardiovascular disease is atherosclerosis. Atherosclerosis is marked by the thickening of the blood vessels through deposition of lipid plaques, extreme form of which restricts

blood supply to certain parts of the heart causing ischemic injury. Ischemic injury can also result from blockade of blood vessels by blood clots. Prolonged ischemia then causes myocardial infarction (MI). MI, which is marked by necrotic death of cardiomyocytes, consequently leads to heart failure, 'the inability of heart to pump blood efficiently'. MI causes inflammatory cell infiltration and remodelling of the affected region, which often results in cardiac arrest and death of the patient [13]. Being one of the most common types of CVDs, the focus of this study is ischemic injury leading to myocardial infarction.

1.1.2 Inflammatory cell infiltration, phagocytosis and fibrosis following ischemic injury

A myocardial injury is rapidly accompanied by an inflammatory reaction. Inflammatory reaction involves complement cascade and tissue resident mast and/or macrophage cells activation, infiltration of circulating leukocytes in the affected tissue, which mediate cellular destruction and phagocytosis of degenerating cardiomyocytes. Mast cells reside in essentially all tissue types throughout the body (reviewed in [14]). Upon activation by injury or infection, they release cytokines and molecules such as TNFα, IL-6, IL-1, histamine, serotonin and newly synthesized platelet-activating factor (PAF), leukotrienes. The mediators affect either the vasculature to either express endothelial adhesion molecules for inducing rolling and infiltration of the leukocytes, activate leukocytes directly and/or affect both events (reviewed in [14]). The activation of mast cells upon injury or infection is driven by various factors such as bradykinins, complement system, bacterial toxins etc (reviewed in [14]). Hill and Ward [15] were the first to report that the myocardial ischemic injury activated the complement cascade, which are capable of activating mast cells or have a direct impact on neutrophil infiltration via chemotaxis. Upon infiltration into injured tissue, neutrophils conduct cellular destruction of damaged or infected cells. They can however, exacerbate muscle injury by damaging uninjured myocytes via generation of proteolytic enzymes and reactive oxygen species or by directly binding to cardiomyocytes, which is dependant on the Mac-1-ICAM-1 (Macrophage-1 antigen, Inter-Cellular Adhesion Molecule 1) interaction [16, 17]. The myocytes have to be stimulated by cytokines such as IL-1 (Interleukin-1), TNFα (Tumor Necrosis Factor alpha) and IL-6 (Interleukin-6) to induce ICAM-1 expression and neutrophils stimulated by IL8 or PAF to show Mac-1 [16]. The infiltrated neutrophils, the macrophages together with the resident mast cells mediate inflammation, cellular destruction and phagocytosis of the injured tissue.

The inflammatory response in the myocardial injury eventually leads to the initiation of repair and healing processes, which in the heart result in formation of a scar. The infiltrated inflammatory cells attract fibroblast to the injury site to remodel the damaged tissue by recruiting a combination of cytokines that are secreted by the inflammatory cells themselves. During the healing process, mast cells together with macrophages provide cytokines and growth factors necessary to support fibroblast proliferation and new vessel formation [16]. Fibroblasts secrete high amounts of transforming growth factor-ß (TGF-ß), collagen and glycoproteins, which take part in forming the scar tissue (reviewed in [16, 18]).

Scar formation is crucial for rapidly resolving damage by secluding the lesion from the undamaged area and preventing uncontrolled damaging events [19]. Although scar formation represents a vital evolutionary adaptation of higher vertebrates to injury, it leads to restriction of regeneration. In addition, scar tissue does not possess biochemical, physical and functional properties of the original healthy tissue leading to adverse effects on overall function of the heart. Therefore, to restore cardiac function after an infarct, attenuation of scar size and replacement of contractile cardiac tissue is necessary**.**

1.1.3 Current available treatments for ischemic injury

Current interventions for ischemic injury are targeted at physical removal of the obstructions or reperfusion of the heart to restore blood flow to ischemic tissue. Physical removal of the obstruction re-establishes the blood flow. However, this intervention only transiently eliminates the symptom especially if the obstructions are lipid plaques, rather than permanently curing the problem. Reperfusion has the potential to rescue at-risk myocardium very quickly. If blood flow is restored rapidly, the loss of a few myocytes unlikely affects the overall function of the heart. However, for the myocardium that is unable to survive the injury, reperfusion is of little help. In fact reperfusion of the tissue leads to increased radical oxygen species production, which potentially causes adverse effects on the surviving myocardium [20]. There are other interventions that are targeted at improving mechanical function of an injured heart such as balloon pumps and left ventricular assist devices [21, 22], which however offer only temporary solutions. Currently the ultimate intervention to a failing heart is organ transplantation. The shortage of donors and the bigger challenge that is faced by organ transplantation, immune rejection, make organ transplantation unrealistic for a majority of patients. Moreover,

these solutions are mainly short-term solutions. Long-term solution must be focused at improving function via restoration of mechanical function of the injured heart itself.

1.1.4 Regeneration of mammalian hearts

Regeneration is a biological process that refers to replacement of body parts lost due to injury [23]. Invertebrates of the Planariidae family and Hydra genus have the potential to regenerate their whole bodies from small body parts or pieces, indicating their immortal existence [24-26]. In mammals however, regeneration of organs such as the cardiac muscle, appendages and spinal cord is very limited (reviewed in [23]). As the capacity for renewal of cardiac myocytes following injury is limited, mammalian hearts following myocardial infarction suffer from impairment of function due to permanent loss of contractile cell mass. Over the past decades, treatment for myocardial ischemia has made significant progress, however curing myocardial infarction remains still a challenge as the existing treatments for infarction fail to address the problem of contractile-cell loss.

The mechanical function of the heart can be separated into active (contractile) and passive (non-contractile) components, both of which should be targets for regenerative therapy [27, 28]. The active function is a result of contraction of individual myocytes and the passive component results from the cell-cell and cell to extracellular matrix interaction, which provides a compliant environment for contraction and relaxation. During myocardial infarction and heart failure both of these components are affected. The passive component is affected by formation of new non-contractile fibrotic tissue that replaces the contractile cells and extracellular matrix leading to a noncompliant stiff scar. Due to the introduction of stiff scar, the systolic contraction is decreased. In addition, the diastolic function is also affected as the heart is not able to relax completely. Both of these components should be addressed to improve mechanical properties of infarcted hearts.

1.1.5 Strategies to support regeneration and functional restoration

There are several strategies that can be exploited in mammals to potentially support regeneration of an injured heart. For improving the passive function, the lack of flexibility resulting from the scar tissue could be considered. Scar tissue is mainly composed of collagen and fibroblasts. Addition or inducing expression of elastin, an extracellular matrix protein, in the stiff scar tissue might improve flexibility of the stiff myocardium. Mizuno et al. showed that over-expression of elastin by endothelial cells preserved cardiac

function and decreased scar size compared with non-expressing control cells suggesting that elastin might replace the collagen or signal for decreasing collagen synthesis in the infarct region [29]. Matsubayashi et al. used a biopolymer scaffold seeded with vascular smooth muscle cells to replace scar tissue in the myocardium in a rat model [30]. Eight weeks post implantation of the scaffold they found increased extracellular elastin and fractional area shortening, without observing any mechanical activity in the patch region. This suggested that the functional improvement observed was due to compliance achieved through the implantation rather than restoration of contraction in the patch region. Similarly, Fujimoto et al. implanted a biodegradable polymer called the polyester urethane urea (PEUU) cardiac patch on the epicardial surface of sub-acutely infarcted rat LV wall, which resulted in increased number of smooth muscle cells, fractional area shortening and tissue compliance in the infarct region [31]. Injection of mesenchymal stem cells (MSC) has also been shown to improve compliance by decreasing stiffness and fibrosis without transdifferentiating into cardiomyocytes [32]. All of these studies demonstrated that implantation of compliant material or cells in a scar region could potentially improve passive mechanical function by decreasing stiffness.

While improving the passive function of the infarcted heart possibly leads to overall improvement of heart function, it is vital to regenerate the stiff scar tissue with new contractile tissue to achieve an improvement of the active function of the infarcted region [28]. Mammalian tissue regeneration and active function are mainly impaired by failure of the damaged tissue to support survival, proliferation and/or differentiation of homing stem or progenitor cells. The hostile toxic microenvironment created by reactive oxygen species resulting from inflammation does not provide the cells with a favourable environment to home and reconstitute the lost contractile tissue. This significantly reduces the opportunity for the homing stem cells to regenerate the injured tissue and maintain mechanical function of the organ. There are several strategies that could be applied to counter this problem. A combinatorial cell and growth/survival factor therapy could be one of the approaches to utilize. This strategy could potentially (i) help reconstitute the lost tissue with the donor cells, (ii) with the growth/survival factor component, confer better survival of the transplanted cells and (iii) upon the release of the growth factor, create a favourable environment for engraftment of transplanted cells. In addition, with the release of the growth/survival factors, this approach could confer protection to the native cells; hence protect the at-risk cells from death. By creating a favourable microenvironment, the

combinatorial therapy might also enhance engraftment of endogenous stem cells that home into the injured organ. Alternatively, the regeneration of overall function could be obtained by non-combinatorial approach, which is independent of exogenous cell transplantation. This could be performed by supplementing the injured organ with factors, which could increase engraftment, survival, proliferation and differentiation of the endogenous progenitor cells to reconstitute the injured tissue. Although both of the combinatorial and non-combinatorial approaches will serve to improve overall function of the injured organ, a combinatorial approach might be more beneficial to patients who are elderly and have reduced levels of endogenous progenitor cells, for instance cardiac progenitor cells (CPCs) that have been reported to decline with age (reviewed in [33]).

The following figure outlines strategies that could be employed to regenerate mechanical function of the hearts following injury (Figure 1).

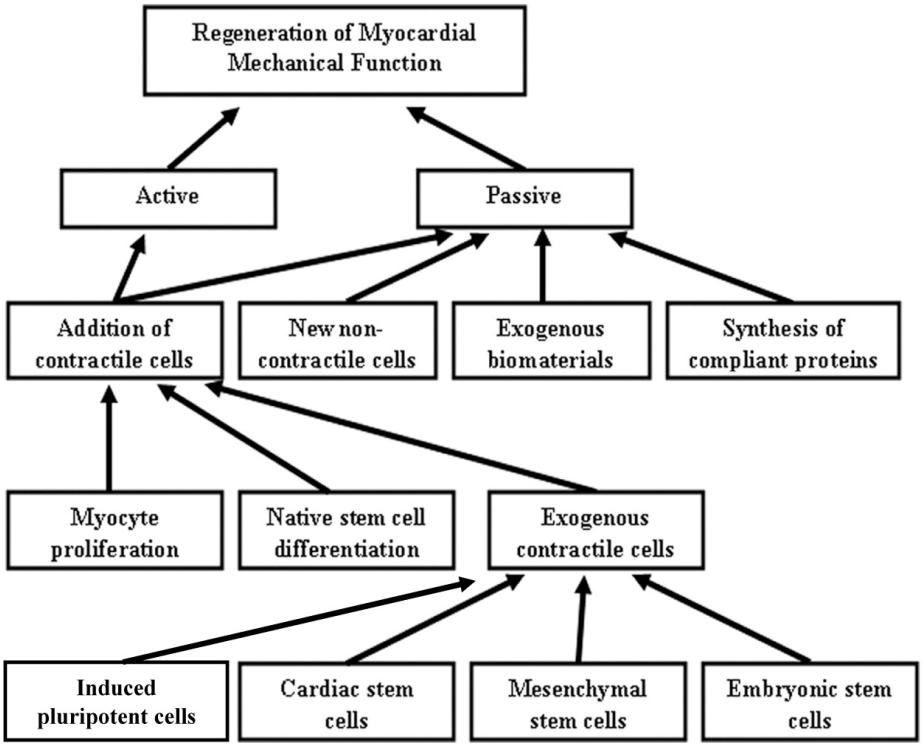

Figure 1. Regenerating Mechanical Function of Injured Hearts. Figure outlines various strategies for regenerating both the active and passive functions of injured hearts to obtain regeneration of the overall mechanical function. Figure adapted from Gaudette, G.R., Cardiac Regeneration: Materials Can Improve the Passive Properties of Myocardium, but Cell Therapy Must Do More, Circulation, Volume 114, Issue Number 24, Copyright (2006), with permission from Wolters Kluwer Health provided by Copyright Clearance Centre.

1.1.6 Improvement of active function

Improvement of active function of injured hearts can be achieved by (i) transplantation of cells that have the ability to contract and integrate with the recipient tissue, (ii) proliferation of adult cardiomyocytes or (iii) differentiation of endogenous progenitor cells into contractile cells. The following paragraphs will discuss in detail the different cell types that could be utilized for improving cardiac active function.

1.1.6.1 Cell therapy

1.1.6.1.1 An Ideal Cell for Therapy

For a successful regenerative strategy, the donor cells must possess a number of qualities. They should exhibit electrophysiological and contractile properties of cardiomyocytes and when delivered they should be able to integrate both physically and functionally within the host tissue. In order to engraft and synchronously beat with the host myocardium, they must possess adhesion and gap junction proteins such as N-cadherin and Connexin-43 respectively. Similarly, the implanted cells must possess all the cardiomyocyte specific proteins that are necessary for their mechanical (e.g. sarcomeric alpha-actinin, ventricular myosin heavy chain) and electrical functions (e.g. ion channel proteins). The proteins must also be functional. The cells should exhibit a calcium-induced calcium-release mechanism, which is ion channel dependent and is essential for excitation-contraction coupling. Both the calcium-induced calcium-release and excitation-contraction coupling are properties of functional cardiac myocytes. Upon delivery to the infarcted hearts, an ideal cell for regenerative therapy must improve overall heart functions. The functional improvement should ideally correlate with the regenerated muscle mass to demonstrate that the functional improvement is a direct effect of cell implantation. In addition, the donor cells must contract in synchrony with the native cells to circumvent arrhythmias.

All the methods for regeneration of muscle mass to improve active function of the heart must include addition of cell mass. This can be achieved through two different cell sources, namely the endogenous and the exogenous cells.

1.1.6.1.2 Cell Sources for Transplantation

An ideal cell for transplantation must have a high proliferative and differentiation capacity, an autologous origin and be readily available in large quantities for cell-based therapy. To date, five different cell types have been analysed and used in animal models.

These include Skeletal Myoblasts (SM), Mesenchymal Stem Cells (MSC) from bone marrow and adipose tissues, Cardiac Stem Cells (CSC), Embryonic Stem Cells (ESC) and induced Pluripotent Stem cells (iPS). Native adult cardiomyocytes could be induced to proliferate endogenously to regenerate the injured tissue. CSC and MSC are endogenous cell sources that could be recruited to the injury site to replenish the lost myocyte mass. ESC, SM and iPS cells are exogenous sources which have to be maintained and expanded in culture, and then delivered to the injured heart.

1.1.6.2 Endogenous cell sources for regeneration

1.1.6.2.1 Native adult Cardiomyocytes

In zebra fish and amphibians adult cardiomyocyte proliferation is a known phenomenon where amputation of their hearts leads to induction of mitotic cell division of native cardiomyocytes which then regenerates the entire heart [34, 35]. Studying further the cell cycle progression and regeneration mechanisms in lower vertebrates and invertebrates and applying these mechanisms in mammals could potentially help regenerate mammalian hearts after injury. However, unlike in the lower organisms, in higher vertebrates, scar formation seems to be favoured over cardiomyocyte proliferation, the reasons for which are not completely understood. Previously, there was a common understanding that cardiomyocytes were terminally differentiated cells that lacked the ability to proliferate. However, in 2001 Anversa et al. reported evidence on human cardiomyocytes at the border zone of an injured region dividing after myocardial infarction, suggesting that cardiomyocytes might re-enter cell cycle following injury. Their data showed approximately 4% of cardiomyocytes at the border zone positive for the proliferative cell marker Ki-67 [36]. Recently, Bergmann et al. became the first to produce evidence on renewal of cardiomyocytes in humans [37]. They took advantage of the carbon-14 integration into the DNA to establish the age of cardiomyocytes in humans. The carbon 14 level in the atmosphere increased after the Cold War due to bomb testings. They demonstrated that the DNA from cardiomyocytes from individuals born before the Cold War during which the atmospheric carbon-14 concentration was lower than after the Cold War, consisted of comparable level of carbon-14 to the after- Cold War subjects. This finding was the first to suggest in human, the renewal of cardiomyocytes. Considering the findings of these studies, the native cardiomyocytes appear to have the ability to replace lost tissues after injury. However, to develop a strategy for complete regeneration based

on stimulating this innate ability for proliferation, a better understanding of cell cycle and injury repair processes in mammals versus lower organisms is necessary.

1.1.6.2.2 Native Stem Cells

Native stem cells from the bone marrow, adipose tissue or the heart have a huge advantage over exogenous cell transplantation due to the circumvention of immune rejection. Potapova et al. showed that mesenchymal stem cells from the bone marrow have the ability to form cardiac myocytes when induced with 5-azacytidine, a DNA methylation agent. The resulting cardiac cells expressed cardiac specific proteins and formed sarcomeres [38]**.** Similarly, evidence suggests that cells from adipose tissue and heart differentiate into cardiomyocytes [39, 40]. The property of all these cells to differentiate into myocytes provides the possibility to develop a therapy to increase their homing to the injured region. Factors such as monocyte chemotactic protein-3 (MCP-3) [41] and stromal-derived factor-1 (SDF-1) [42] have been identified as homing molecules which could potentially be utilized to induce increased homing of the stem cell population to the injured site.

Transplantation of bone marrow cells improved cardiac function of infarcted hearts, indicated by increased left ventricular ejection fraction (LVEF) [43-48]. Meta-analyses on clinical studies on transplantation of bone marrow stem cells into patients reported a slight improvement in function, indicated by 3-4% mean absolute increase in left ventricular ejection fraction (LVEF) [49]**.** Reports from two groups show that the functional results are better in patients with low LVEF, or if cell infusion is delayed until at least 5 days post myocardial infarction. They observed an absolute increase in EF by 5.1% versus no increase if the infusion was done after 5 days or in the first 4 days after injury respectively [50] and [51]. However, another report by Bone Marrow Transfer to Enhance ST-Elevation Infarct Regeneration (BOOST) has reported that bone marrow cell transplantation had no long-term clinical benefit as the improved cardiac function declined at 18 months [46]. A nonrandomized trial with a 5-year follow-up time reported an improvement of global cardiac function, which was persistent with decreased mortality and infarct size and increased myocardial perfusion [52]. The functional improvement observed in these studies however has not been linked directly to the transplanted cells. Paracrine effects therefore have been suggested as a possible explanation for the improvement [48].

Cardiac stem cells are the next native stem cell type that has potential for cell-based cardiac repair. CSCs have innate capacity to differentiate into both cardiac and vascular lineages [53]**.** Human CSCs was obtained from myocardial biopsies and expanded in vitro. Upon expansion, the cells were transplanted into immunodeficient rat infracted hearts where they resulted in a chimera with human cardiomyocytes, coronary resistance arterioles and capillaries, showing clearly their cardiac and vascular lineage differentiation [53]. Therefore increasing their proliferation and differentiation into cardiomyocytes and vascular cells following injury would be a potential endogenous way to improve regeneration. However, the number of CSC declines with age, making it difficult to proliferate and differentiate them in large numbers in elderly patients [33]. Moreover, a better understanding and characterization of CSC is still lacking, which is vital to increase their efficiency of differentiation into cardiomyocytes for a cell therapy approach.

Promoting regeneration using endogenous cell populations seems promising due to their qualities to differentiate into cardiomyocytes and to avoid immune rejection. However, the biggest challenge in using them as a therapy is their low efficiency of differentiation into cardiomyocytes and/or the large number that needs to home into the injured site in order to regenerate the entire injured region. Due to these problems, alternative exogenous regeneration has received considerable attention in recent years. Exogenous regeneration aims at differentiating a stem cell population into cardiomyocytes in high quantities and delivering them into an injured site. To do so, the stem cells are expanded and driven towards cardiac lineage *in vitro* prior to their delivery.

1.1.6.3 Exogenous cell sources for regeneration

1.1.6.3.1 Skeletal Myoblast

Skeletal myoblasts are precursor cells for skeletal myocyte regeneration [54]. There are several features that make skeletal myoblasts an attractive cell type for cardiac cell transplantation. Skeletal myoblasts have an autologous origin, they more readily survive in the hostile post-infarct environment [55] and they have the capacity to regenerate. Due to their autologous origin, they are faced with no ethical problems. In addition they are available in abundance and they circumvent immune rejection that other cell types are faced with. Skeletal myoblasts differentiate into striated muscles, sharing similarity with cardiomyocytes, which are also striated. Due to their similarities, these cells were chosen to be the first cell type for cell therapy in myocardial infarction. The major limitation for

using skeletal myoblast for cell therapy however, is the lack of evidence of electromechanical coupling between the grafted cells and the native cardiomyocytes. *In vivo*: skeletal myoblasts lose their capability to express major adhesion and gap junction proteins like N-cadherin and Connexin-43 respectively when the cells differentiate into myotubes [56]. Connexin-43 and N-Cadherin are essential for electromechanical coupling of cardiomyocytes [56, 57], therefore transplantation of skeletal myoblasts and their differentiation into myocytes might not be ideal for coupling with native cardiomyocytes. Also, myoblasts have not been shown to transdifferentiate into cardiomyocytes *in vivo* therefore they cannot substitute lost host tissue completely. In clinical trial, transplantation of autologous skeletal myoblasts into infracted scars during bypass surgery into patients with severe post infarction LV dysfunction resulted in ventricular arrhythmia [58], and this study was confirmed in another nonrandomized study [59].

1.1.6.3.2 Induced Pluripotent Stem Cells

Until recently, reprogramming of differentiated cells into a pluripotent state was beyond imagination. Takahashi et al. however have remarkably realized this concept. They were able to successfully induce formation of ESC-like pluripotent cells from adult human fibroblasts by defined factors [60]. The group transfected human fibroblast cells with Oct3/4, Klf4, Sox2 and c-Myc containing viral vectors, which resulted in derivation of fibroblast cells into ESC-like cells that were named induced pluripotent cells (iPS cells) [60]. Following this work, two other groups were able to differentiate these iPS cells into cardiomyocytes [61, 62]. These were major advances in stem cell research, as they now allow researchers to derive and obtain pluripotent stem cells from somatic cells. iPS cells are important in research and potentially have therapeutic uses, bypassing the use of embryos, which is still ethically controversial. Because the iPS cells are derived from a patient's own somatic cells, they may be less prone to immune rejection than ESC. However, the transfection of the genes in these studies was conducted via retroviruses, which raised yet another important issue on safety of these cells for clinic as virus can cause cancers. In 2008, Okita et al. and Stadtfeld et al. individually demonstrated the generation of murine iPS cells without viral integration by using adenoviral vectors [63, 64]. The efficiency of reprogramming using this method however was very low. Similarly, Woltjen et al. utilized yet another method for obtaining iPS cells without viral integration called *piggyBac* transposition, which utilized the transposon/transposase system. This system was also successful in obtaining iPS cells, but with low efficiency similar to

previous findings [65]. While the efficiency of reprogramming somatic cells into iPS is making progress, the efficiency of differentiation of iPS cells into cardiac myocytes for therapeutic use is still inadequate. In addition, iPS cells still require improved methods of directed differentiation for generating homogenous populations, to be useful for cell therapy. Intramyocardial transplantation of iPS cells in the infarcted murine hearts attenuated ventricular remodelling and improved function compared to control cells injected hearts [66]. Although iPS cell transplantation has shown potential to improve function after transplantation, cells developed from the current methods have been shown to induce teratoma formation.

1.1.6.3.3 Embryonic Stem Cells

Embryonic stem cells represent a clear advantage for cell-based therapy. These cells have the capacity to create all body tissues and to differentiate efficiently into cardiomyocytes both *in vitro* and *in vivo*. Kolossov et al. transplanted undifferentiated ESC into mouse hearts and were able to find ESC-derived striated cardiac myocytes [67]. Several studies have shown that transplantation of embryonic stem cell-derived cardiomyocytes into rodent [68, 69], sheep [70] and pig [71] improved ventricular function and created new myocardial tissue after cardiac infarction. Moreover, human ESC-derived cardiomyocytes integrated functionally and structurally into the host myocardium, and survived following transplantation [71] and (reviewed in [72]). A factor limiting the use of ESCs is their inherent capacity to form teratomas when transplanted as undifferentiated cells. Therefore, in cell-based therapy, transplantation of a differentiated cell population is necessary. Even though it is very clear that ESC have great potential to regenerate and improve function of injured hearts, information is still lacking to correlate the number of engrafted cells with functional improvement observed in all these studies. Also, a complete regeneration and functional recovery is still not achieved. In addition, use of embryos for isolating ESC is still a matter of controversy and huge debate that scientist have to overcome.

1.1.6.4 Delivery of exogenous cells

Improving quantities and qualities of exogenous cells for transplantation is as important as improving methods of cell delivery into infarcted organs. Currently there are three routes that are being utilized for cell delivery, the intravascular, intracoronary and intramyocardial routes. Intravascular delivery is the least invasive route of delivery. However, the drawback with this route is its very low efficiency of cell delivery into the

heart due to entrapment of donor cells in the lungs [73]. The intracoronary delivery is efficient for direct delivery into the myocardium during angioplasty. However, following angioplasty when the blood flow is restored, the transplanted cells get washed away by the flow of blood, therefore intracoronary delivery of cells is also not a perfect way to deliver cells [74]. Although intramyocardial route shows discrepancies on cell engraftment [75] and it is a very invasive route, it is still more efficient to deliver cells than the intravascular and intracoronary routes. Hou et al. showed an 11% engraftment of delivered cells following this route [74]. Therefore, intramyocardial route was chosen as the method of delivery of P19Cl6-derived cardiac myocytes in this study.

1.1.7 Improvement of passive function

Passive function can be improved by (i) transplantation of cells that release paracrine factors that enhance function by increasing vessel density, reducing scar size and inflammation or enhancing engraftment of endogenous progenitor cells and (ii) direct supplementation of survival/ growth factors, angiogenic or anti-inflammatory and anti-fibrotic molecules by gene or pharmacotherapy.

1.1.7.1 Gene therapy

Regeneration of lost muscle mass seems possible with a cell therapy approach. However, an injured heart does not have a favourable environment for endo/exogenous cells to home and engraft. Inflammation is necessary as a first measure of defence to an injury to resolve injury as fast as possible, but the inflammatory cells produce radical oxygen species which are toxic and cause adverse effects on uninjured tissue and resident and/or homing stem cells. Therefore, for a successful regeneration and restoration of normal function of an injured heart, it seems necessary to combine cell therapy with cyto-protective survival factors that provide protection to both the donor cells and the recipient tissue. The factors could be delivered via either gene or pharmacotherapy. Pharmacotherapy usually is unspecific resulting in ectopic action of the factors that could have adverse effects. Gene therapy on the other hand can be utilized to express certain factors in a less ectopic manner. Unlike pharmacotherapy, in a gene therapy approach, a gene could be expressed in a regulated manner at a desired amount and specific site.

1.1.7.2 Ways to deliver genes

There are several ways to conduct gene therapy. The gene can be delivered as cDNA in a naked plasmid although this type of delivery is not efficient due to low transfection efficiency [76]. It can also be delivered via viral vectors. The issue with using virus would be the choice of virus. A virus for gene delivery must be safe and persistent. Adenoviruses are quite safe as they do not integrate into the genome of the cell when transduced into cells. However, because they are episomal they are also not very persistent. Lentiviruses and Adeno-associated Viruses are more persistent because of their integration into the genome of the cells. However, they are less safe compared to the Adeno virus as they permanently integrate into the genome of the recipient cells, possibly leading to adverse effects like mutations of DNA leading to generation of cancer cells. Nevertheless, for cardiac gene therapy, a viral vector must be able to integrate into non-dividing cells as cardiomyocytes are non-dividing cells and for this purpose, lentivirus and adeno-associated viruses make the best candidates [76].

1.1.7.3 Candidate genes for therapy

For cardiac gene therapy, one can use a few kinds of viral vectors but numerous genes to counter the resulting effects of injury. In Chronic Heart Failure (CHF) due to Myocardial Infarction, there are three instances where gene therapy could be utilized. It could be used to reduce the scar size, to attenuate left ventricular dilation or to treat CHF. Lowering scar size has to be performed immediately after occurrence of an infarct, therefore this could be a challenge for chronic myocardial infarction. However, left ventricular dilation and CHF proceed infarction hence these could be attenuated easily. The attenuation of LV dilation and treatment of CHF could be achieved by delivering transgenes that are anti-apoptotic (e.g Bcl-2), angiogenic (e.g. VEGF) or growth hormones such as Insulin-like Growth Factor-1 (IGF-1), which have multiple beneficial functions [77, 78]. Supplementation of these factors potentially protects at-risk myocardial cells from injury, inhibit expansion of scar, increase vessel formation and protect hearts from further functional impairment, preventing CHF.

1.1.8 Animal models of myocardial infarction

Due to the limited possibilities for controlled human studies, animal experimental models have become vital for studying myocardial infarction. The animal studies on myocardial infarction are targeted either at understanding the mechanisms underlying the injury or at

applying cell therapy approaches, testing pharmacological agents or devices for treating the injury. There are various ways to induce myocardial infarction in the animal hearts. Some of the commonly used techniques are: (i) occlusion of the left anterior descending coronary artery (LCA) either by physical ligation of the LCA [79] or by physical obstruction of the artery by placing a coil [80], (ii) chemical destruction of the tissue by injecting cardiotoxin [77], and (iii) physical destruction by cryo-injury i.e. applying metal probe chilled to -196°C locally to the LV wall [81]. Technique (i) involves ligation of the LCA that leads to the death of the cardiac tissue resulting from ischemia. Techniques (ii) and (iii) on the other hand do not involve occlusion of blood supply but direct death of the cardiac tissue by chemical and physical actions respectively. The advantages of using these latter models are that the injury obtained from them is localized, highly reproducible and the technique itself is comparatively less invasive than LCA ligation. However, cardiotoxin- and cryo-injuries do not occur naturally therefore, from clinical perspective these techniques are not the desired models for understanding human ischemia induced MI. Moreover, the LV remodelling events that occur after cryo-injury and injury induced by myocardial infarction and reperfusion are fairly different [82], suggesting that the outcomes of studies utilizing the cryo-injury model have to be carefully considered when the outcomes are to be translated into clinical studies. The LCA ligation model on the other hand involves occlusion of the coronary artery as it happens in humans, although the occlusion in humans occurs due to atherosclerotic plaques or blood clots in the arteries rather than physical ligation. The major disadvantage of using LCA ligation model is the massive variability on infarct size, which complicates comparison of animals within a group. In general, the use of healthy and young animals for studies is also a limiting factor faced by all these animal models. Patients with myocardial ischemia usually demonstrate spontaneous ischemia leading to infarction and this is not the case with young healthy animals. Therefore, neither of the techniques mentioned above mimics completely myocardial infarction as it happens in human hearts, thus better animal models need to be developed in order to capture fully, the disease model in animals. Despite these drawbacks, the available animal models contribute significantly to our understanding of the disease. And from the available models, the LCA ligation model currently represents the clinical scenario more closely than the others, therefore this model was chosen for establishing the myocardial ischemia in this study.

The following table provides a general overview on cell transplantation studies conducted on animal models of MI. The present study utilized Insulin-like Growth Factor-1Ea-gene therapy approach through transplantation of P19Cl6 cells, for a proof of principle. The objective behind using cell-based gene therapy was to obtain more than a single beneficial long-term effect from transplantation of the cells. For instance transplantation of SK with VEGF was shown to improve not only function and cell engraftment but also blood flow through generation of new vessels [83]. This study was inspired by combinatorial cell therapy approaches such as the SK-VEGF study and some others mentioned below, in order to obtain a long-term beneficial effect. The reasons for using particularly IGF-1Ea and P19Cl6 cells are described in 1.2 Section II.

1.1.9 Table 1: Overview of recent cell transplantation studies in animal models of MI

Cell Type	Number of cells administered per animal	Recipient	Setting	Objectives	Results	Follow-up	Reference
iPS cells	3*10^5 in 10µl DMEM	mice, female immunocompetent	acute MI by LCA ligation, intramyocardial transplantation	-effect of SK-derived iPS cells on regeneration of infracted hearts	-cells engrafted -teratoma observed in iPS cells injected but not in skeletal myoblast injected control	4 weeks	[84]
iPS cells	2*10^5 in 10µl differentiation media, injected in 4 spots, 2.5 µl/spot	mice, male 8-12 old, immunocompetent as well as athymic nude mice	acute MI by LCA ligation, intramyocardial transplantation	-test potential of iPS cells for heart disease therapy	-cells engrafted without detectable tumour -EF↑, FS↑, RSWT↑	4 weeks	[66]
CPCs	1*10^6 in 1ml PBS	rats, female 3 months old	1 month after MI by LCA ligation and reperfusion, intracoronary infusion	-clinical perspective on CPC transplantation, using a chronic MI model and intracoronary transplantation of cells as these methods are more clinically relevant	-cells engrafted -EF↑, LVEDP↓, dP/dt↑	35 days	[85]
CPCs with IGF-1	1*10^5 in 10 µl saline	rats, female 3 months old	acute MI by LCA ligation, intramyocardial transplantation	-to test whether transplantation of CPCs together with nanofiber coupled growth factor IGF-1 enhances repair after infarction	-detected myocardial regeneration - dP/dt↑, EF↑	1 month	[86]
CPC sheet	2.0 ± 0.2 × 10^6 per sheet	mice, male 3 months old	acute MI by LCA ligation, intramyocardial transplantation	-to understand the mechanism of improvement in function after CPC cell transplantation	-LVDd↓, LVDs↓, FS↑, LVEDP↓, +dP/dt↑	3, 4 weeks	[87]

SK expressing VEGF under hypoxia exposure, VEGF delivered via nanoparticles	1*10^7	rabbit, female	acute MI by LCA ligation, intramyocardial transplantation	-to test a promoter controlled expression of VEGF through cell therapy	-increased SK survival -increased blood vessels and blood flow - EF↑	max. 14 days, variable time points	[83]
Repeated injection of SK	average 329*10^6	pigs	chronic MI by vasculoembolization coil insertion, 6 weeks, intramyocardial transplantation	-to test sequential transplantation of cells to improve engraftment	- engraftment of cells - ↑dLVEF, - ↑tissue vasculogenesis, - ↓fibrosis	7 months	[80]
transgenic MSCs expressing GSK-3β	1*10^5 in 30 µl saline	mice, male 3 months old	acute MI by LCA ligation, intramyocardial injection	-to investigate the effect of GSK-3β on cardiac based cell therapy with MSC after MI	-increased survival and cardiomyocyte differentiation of MSC -increased vascularisation - LVEDD, LVESD and LVEDP not elevated, FS↑ -increased wall thickening	12 weeks	[88]
MSC with EPC	1*10^6 MSC and 1*10^6 EPC in 200 µl medium	rats	isoproterenol induced myocardial injury, cells transplantation 4 weeks after injury induction	-to test effects of transplantation of a cocktail of different cells on function improvement	-cells detected -↑ angiogenic growth factor expression, -↓ collagen deposition, - ↑ regional blood flow	12 weeks	[89]
ESC-derived CPCs	0.5-1.0*10^6 in saline in 30 µl saline	mice, female 8-10 weeks old	acute MI by LCA ligation	-to test if transplantation of ESC derived CPCs improve muscle generation and neovascularization	-cells engrafted -↓LVID, ↑EF, ↑FS, ↓ cardiac remodelling	4 weeks	[90]
human ESC-derived CM	1.5*10^6 in saline	rat	7-10 days after infarction	- to test ability of ESC-derived CM to engraft and improve impaired function	-FS↑, EDV↓	4 weeks	[91]
human ESC-derived CM with pro-survival factors	1*10^7 in saline	rat	4 days after MI by LCA ligation	-to improve efficiency of differentiation of hESC into CM, improve their purity and survival	-myocardial grafts observed -FS↑, EDV↓ -↑wall thickening	4 weeks	[92]
ESC-derived CM and BM	3*10^4-1*10^5	mice, male 12 weeks old	acute MI by LCA	-which cell is ideal for transplantation and understanding fate of ES-CM and BM cells upon transplantation	-BM cells no positive effect, ES-CM ↑ function -cells engrafted -no teratoma observed -EF↑, EDV↓	4-5 months for cell engraftment analysis 3-4 weeks function analysis	[67]

human ESC-derived CM	1*10^6	mice, 11-12 weeks old, immune compromised	acute MI by LCA	-long term analysis of hESC-derived CM transplantation	-cells engrafted -EF↑ at 4 weeks which became comparable to control at 12 weeks	12 weeks	[93]
mouse cardiac lineage committed ESC	3*10^7 in medium	sheep	14 days after myocardial injury caused by placing a coil	-to test heterogenous transplantation of ESC with the view that ESCs are immune priviledged	-cells engrafted -EF↑, variable	1 month	[70]

iPS: induced pluripotent cells, CPC: cardiac progenitor cells, SK: skeletal myoblasts, MSC: Mesenchymal Stem Cells, ESC: embryonic stem cells, CM: cardiomyocytes, EPC: endothelial progenitor cells, BM: bone marrow cells, VEGF: vascular endothelial growth factor, dP/dt: change in systolic pressure over time, LVEDP: left ventricular end diastolic pressure, LVESP: left ventricular end systolic pressure, LVEDD: left ventricular end diastolic diameter, LVESD: left ventricular end systolic diameter, EDV: end diastolic volume, LCA: left coronary artery, MI: myocardial infarction, EF: Ejection Fraction, FS: fractional shortening, ESV: end systolic volume, RSWT: regional septal wall thickness, LVDd: left ventricular diastolic diameter, LVDs: left ventricular systolic diameter, LVID: left ventricular internal diastolic diameter

1.2 SECTION II: THE CELL AND THE GENE OF CHOICE

1.2.1 The Cell: P19Cl6

1.2.1.1 P19 Embryonal Carcinoma-derived stem cells (P19EC)

P19EC are pluripotent cells like the ESCs. They are derived from teratocarcinoma. When injected into blastocysts, they are able to form tissues of all three germ layers [94]. Moreover, when treated with 1% DMSO they differentiate very efficiently into spontaneously beating cardiac myocytes. P19EC cells are very suitable for deriving clonal sub-lines [94-96]. P19Clone6 (P19Cl6) cells were made from P19EC cells with long-term culture of the cells under conditions promoting mesoderm differentiation [97]. P19Cl6 have even higher efficiency of differentiation into cardiac myocytes than P19EC and they are easier to maintain and manipulate in culture than embryonic or other candidate cells as they grow without feeder layer. Therefore P19Cl6 cells were chosen as the model system for cell therapy in this study. However, as these cells are derived from teratocarcinoma, this study only represents a proof of principle for cell therapy. To translate the outcome of this study to clinical applications, future investigations on safer model systems will be necessary.

1.2.1.2 Derivation and characteristics of P19Cl6 cells

P19Cl6 are a clonal derivative of pluripotent P19EC cells derived from teratocarcinoma. Teratocarcinomas are malignant tumors that arise from defective germ cells in the testis of mice and humans. They can also be derived artificially by transplanting early murine embryos from the uterus to ectopic sites [98, 99]. P19EC cells were isolated from teratocarcinoma formed after transplantation of a 7.5 day old embryo into murine testis [99]. The 7.5 day old embryo was derived from crossing C3H/He female mice with feral males carrying a number of variant alleles. The isolated undifferentiated P19EC cells had euploid male karyotype and the cells grew quickly in culture without feeder layer (reviewed in [98]). When these cells were injected into blastocysts of a different mouse strain, they formed tissues of all three germ layers in the resulting chimeric mice, proving their pluripotent potential [94]. P19EC cells are very suitable for deriving clonal sub-lines [94-96]. To select for ventricle specific cardiac myocytes, Moore et al. created a transgenic reporter cell line from P19Cl6, which expressed green fluorescent protein (GFP) under the transcriptional control of the rat myosin light chain-2v (MLC-2v)

promoter [100]. Myosin is a protein consisting of two heavy and two light chains, which are a major element of the contractile part of muscle cells [101]. The Myosin Light Chain (MLC) is of two types, MLC-1 and MLC-2. The MLC-2 is the regulatory chain [102] which is expressed in mouse and rat heart ventricles exclusively as MLC-2v [103]. To generate the MLC2v-GFP vector, Moore et al. cloned the 250bp rat MLC2v cDNA into a promoter free vector peGFP-N2 vector. This resulted in no detectable GFP expression in the P19Cl6 cells. Therefore they sub-cloned a ubiquitous CMV promoter in front of the MLC2v cassette, which then resulted in a higher expression of GFP in cardiomyocytes derived from P19Cl6 cells. This system provides an extra tool for positive selection of the ventricular cell population from a pool of differentiated cell lineages for various applications and studies [100]. The current study utilizes P19Cl6MLC2v-GFP cells generated by Moore et al. for transplantation.

1.2.1.3 Differentiation mechanism of P19EC/P19Cl6 cells

Both P19EC and P19Cl6 can be differentiated into different cell types using pharmacological agents such as Retinoic acid, DMSO or Oxytocin [100, 104, 105]. Initially P19EC cells were observed to efficiently differentiate into different cell types when cultured in non-adherent aggregates called Embryoid Bodies (EBs) [106, 107]. In addition, it was observed that adding retinoic acid on a teratocarcinoma stem cell-line called F9 cells in monolayer culture resulted into differentiation of these cells [108]. Taking together these findings, a combination of the EB formation and drug treatment was then used to induce P19EC cells to differentiate into different cell types. Treatment of the cells with retinoic acid led to formation of neuronal and glial tissue [104], whereas treatment with 0.5-1% DMSO differentiated these cells into both endo- and mesodermal cell lineages. Among the resulting mesodermal cell types, cardiac myocytes and skeletal muscles caught most attention from researchers [95, 109]. The mechanism by which DMSO induces differentiation of these cells is not fully uncovered. However, the induction of differentiation by DMSO seems not to be unique to P19EC cells. Other cell types such as Friend erythroleukemia (MEL) cells [110], lung cancer cells [111] and even mouse ES cells [112] have been reported to undergo differentiation by DMSO treatment. These findings suggest that the signaling pathway mediated by DMSO during differentiation could be a general one. It is known that the use of DMSO in P19 and various other cell types led to a transient increase in intracellular calcium due to their release from intracellular compartments. This release of calcium probably plays a vital

role in activating downstream signaling for inducing cardiac differentiation [113]. It has also been suggested that the DMSO differentiation pathway is linked to Oxytocin pathway. Interestingly, when P19EC were exposed to an inhibitor of Oxytocin, cell differentiation into cardiomyocytes was inhibited even in DMSO-treated cells, suggesting that DMSO acts by activation of the Oxytocin pathway [98]. However, a clear mechanism of DMSO action is still unclear.

1.2.1.4 Mesodermal differentiation characteristics of P19EC/Cl6 cells

The differentiation mechanism of P19EC cells is very similar to ES cell differentiation [99]. Compared to P19EC, P19Cl6 differentiate more efficiently into cardiac myocytes due to their long-term culture in mesoderm favouring media during their derivation (reviewed in [98]). Upon differentiation by DMSO, these cells express various mesoderm and muscle specific transcription factors. Mesoderm-specific Brachyury T is expressed on Day 2, followed by cardiac specific transcription factors Gata-4 on day 3. Expression of transcription factors Nkx2-5 and MEF2c followed Gata-4 expression on day 4 of differentiation [98, 114]. Several efforts have been made to understand the regulation of expression of the cardiac transcription factors mentioned above. Bone morphogenic proteins (BMPs) had been studied in chick embryo where the exposure of the embryo to BMP using soaked beads led to expression of Nkx2-5 and Gata-4 ectopically in the embryo [115]. From this observation, it was postulated that BMPs have a role in cardiac differentiation of P19 cells. However, studies showed that DMSO did not induce expression of BMP but DMSO-induced P19 cell differentiation into cardiomyocytes depended on BMP signalling [116]. Application of Noggin, a natural inhibitor of BMP, during induction of differentiation led to failure of P19 cells differentiation into cardiac myocytes [117].

1.2.1.5 Characteristics of P19 cell derived cardiac myocytes

Differentiation of P19 cells into cardiac myocytes leads to expression of many cardiac structural, contractile, ion channel and receptor proteins. An mRNA level analysis on day-6 beating myocytes revealed expression of cardiac actin. The cardiac myocytes co-expressed MLC1v, MLC2a, alpha-MHC and beta-MHC [118]. A contractile apparatus in P19 derived cardiomyocytes consists of both light and heavy chains, meaning components of both atria and ventricle. In addition they also expressed the skeletal form of actin, which showed another similarity with ESC derived cardiac myocytes [118]. In addition,

other cardiac structural proteins such as Cardiac Troponin C and Desmin have also been reported (reviewed in [98]). P19 derived cardiomyocytes demonstrate spontaneous beating, express calcium channels and limited amounts of sodium channels that are functional [119-121]. Their maximum diastolic potential is fairly low and the nature of their action potential resembles primary isolated embryonic cardiomyocytes (reviewed in [98]). Taken together, even though P19Cl6 are derived from teratocarcinoma, the cardiomycytes resulting from their differentiation resemble the myocytes derived from embryonic stem cells or embryonic cardiomyocytes, therefore appear to be a good candidate for a proof of principal for cell therapy.

1.2.2 The Gene: Insulin-like Growth Factor-1 (IGF-1)

A previous study from our laboratory suggested that one of the isoforms of IGF-1, IGF-1Ea, induces cardiac recovery with decreased scar formation and lower inflammatory response after myocardial infarction [77]. Furthermore, IGF-1Ea induced a gene expression profile related to decreased oxidative stress and increased cardiac-specific protective molecules, such as Adiponectin [77]. Similarly, Musaro et al. reported that in dystrophic muscle that underwent repetitive rounds of muscle damage and repair resulting in exhaustion of muscle regeneration and scar formation, IGF-1Ea transgene was able to attenuate this condition by reducing the extent of fibrotic tissue formation [122, 123]. Results from both Musaro and Santini indicated that expression of IGF-1Ea in a tissue-specific manner could be an effective and powerful approach to counter a number of life-threatening muscle damages [77, 122]**.** Direct gene therapy would be a possibility to deliver IGF-1Ea to the injured area, however gene therapy is yet to provide satisfactory clinical solutions due to its relatively inefficient delivery and possibly harmful ectopic expression. Therefore, a cell-based approach was utilized to deliver IGF-1Ea into injured hearts to improve both the active and the passive functions.

1.2.2.1 Insulin-like Growth Factor (IGF) system

The Insulin-like growth factor (IGF) system consists of Insulin (I), Insulin-like Growth Factor-1 (IGF-1) and Insulin-like Growth Factor-2 (IGF-2), cell surface receptors (IR, IGF-1R and IGF-2R) and six IGF binding proteins (IGFBP-1 to 6). In circulation and in the extracellular environment, IGFs can exist either in an unbound form or in bound complexes with IGF binding proteins (IGFBP). The IGFBPs serve as carrier molecules for IGFs, extend their half-life and modulate their actions and availability [124, 125].

1.2.2.2 Insulin-Like Growth Factor-1 isoforms

The rat Insulin-like Growth Factor-I gene used in this study spans more than 70kb of genomic DNA [126]. There are four different forms of IGF-1 that are synthesized from distinct mRNAs which are produced by alternative splicing, alternative promoter usage or post-translational modifications of the original IGF-1 transcript [18, 126, 127]. The IGF-1 gene consists of 6 exons separated by 5 introns. Transcripts initiated at exon 1 are spliced to produce mRNAs that contain exon 1 but lack exon 2 (class 1 IGF-1), whereas transcripts initiated at exon 2 produce mRNAs that lack exon 1 but contain exon 2 (class 2 IGF-1) [128, 129]. In addition, alternative splicing at the 3'-end of the IGF-1 gene adds further complexity to the IGF-1 transcripts and their resulting translated isoforms. When exon 4 is spliced to exon 6, 19 amino acids are added to the common 16 amino acids encoded by exon 4, thus generating a 35 amino acid long E-peptide, termed Ea-peptide. A second E-peptide, in rat known as the Eb-peptide, is translated when a 52 base fragment, derived from exon 5, is included and spliced to exon 6. This insertion encodes 17 codons and causes a frame shift in the reading frame, thereby introducing an earlier in-frame stop codon in the exon 6 sequence. The Eb-peptide contains 41 amino acids, with exon 4 coding for 16 amino acids, exon 5 for 17 amino acids, and exon 6 for eight amino acids [130]. Figure 2 shows the structure of the rodent IGF-1 gene and the isoforms that result from the several splicing events described above.

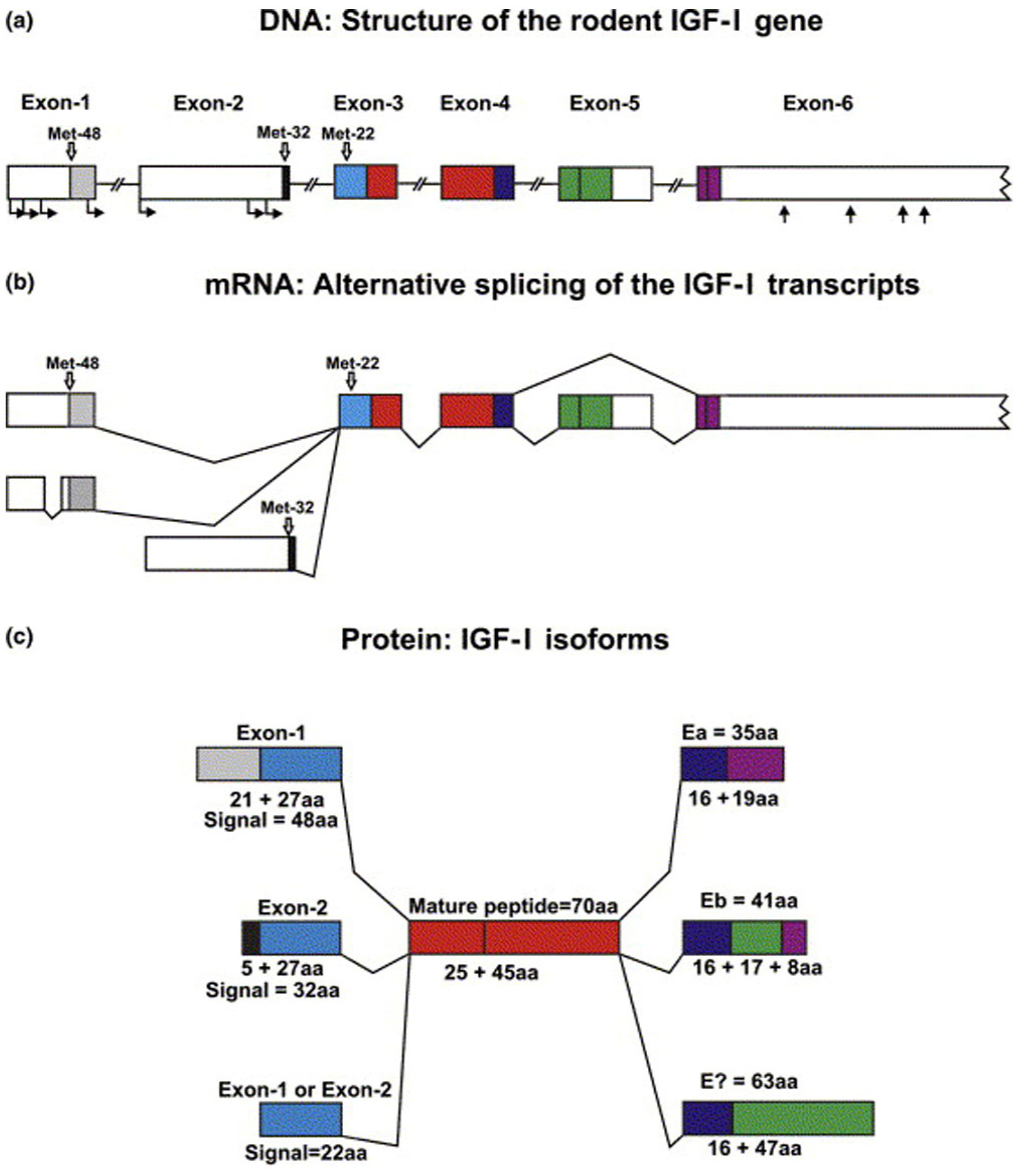

Figure 2. Structure of the Rat Insulin-like Growth Factor-1 Gene and Protein. (a) Shows multiple start sites indicated by the horizontal arrows at Exon 1, 2 and 3. The translation start codon AUG are located at positions -48, -32 and -22 with respect to the mature IGF-1 coding region (70 amino acid) marked by red boxes in exons 1, 2 and 3 respectively. Figure (b) shows alternative splicing events that occur at the 5' and 3' ends of the IGF-1 transcripts. Figure (c) shows IGF-1 protein isoforms resulting from the different splicing events. (Reprinted from Growth Hormone & IGF Research, Shavlakadze et al. Reconciling data from transgenic mice that over-express IGF-I specifically in skeletal muscle, Copyright (2005), with permission from Elsevier)

Different isoforms of IGF-1 exert different biological functions. IGF-1 is known to play an important role in growth, survival, differentiation and proliferation [18]. The rodent IGF-1 gene is very similar to human IGF-1 in its structure. Moreover, the nucleotide sequence and amino acids between the two species are highly conserved [126], therefore this study utilizes the rodent IGF-1 gene.

1.2.2.3 IGF-1 Function

IGF-1 is a multi-functional protein that plays a role in survival, growth, proliferation, differentiation and hypertrophy of various cell types. IGF-1 can induce both proliferation and differentiation, demonstrated very clearly by Musaro et al. in skeletal muscles [122, 131]. Studies on gene disruption of *IGF-1* or *IGF-2*, as well as the receptors IGF-1R and IGF-2R have led to important information on functions of IGF-1. Mice lacking either *IGF-1* or *IGF-2* exhibited growth retardation with weights approximately 60% of that of wild-type littermates [132]. More severe was the phenotype of mice lacking a functional IGF-1R. These mice were born with only 45% of normal weight and died soon after birth from respiratory failure [132]. IGF-2R null mice on the contrary exhibited a completely opposite phenotype, characterised by fetal overgrowth syndrome (135% compared to normal control), which also resulted in lethality due to lack of IGF-2 turnover. IGF-2R serves towards turnover of IGF-2 and in its absence IGF-2 over-stimulates IGF-1R that leads to lethality [133]. These studies clearly demonstrated the function of the IGFs on growth.

1.2.2.3.1 IGF-I in the *Brain*

In the brain, it has been noted that IGF-1 can be either transported through the blood-brain barrier or produced locally. Several studies showed that IGF-1R modulates neuronal activity, resulting in the regulation of food intake, energy metabolism, reproduction and possibly cognitive functions. Studies in the early 1990s showed that IGF-1 stimulates proliferation of neuron progenitors, induces differentiation of oligodendrocytes and increases the survival of neurons and oligodendrocytes *in vitro* [134-136]. In homozygous mice, disruption of IGF-1 or IGF-1R genes produced pathological abnormalities and impairment of brain growth [137]. On the other hand, in transgenic mice over-expressing IGF-1 in the brain, the size and the weight of the brain increased markedly [138].

1.2.2.3.2 IGF-1 in the Bone

IGF-1 has also been implicated in bone formation and growth. Genetic disruption of the IGF-1 gene led to a short bone phenotype and low bone mineral density [139]. A more striking phenotype was observed in mice with targeted deletion of the IGF-1 gene in osteoblasts. These mice showed a significant defect in bone formation with reduced osteoblastogenesis. Overall the mice presented a dramatic reduction in bone

mineralization by three weeks of age, suggesting a role of IGF-1 in bone matrix mineralization [140].

1.2.2.3.3 IGF-1 in the Skeletal Muscle

The role of IGF-1 in skeletal muscle has been studied extensively with various isoforms. In skeletal muscle, the predominant IGF-1 mRNA variant expressed is initiated at exon 1 (class1) with exon 4-6 spliced variant encoding the IGF-1 isoform containing Ea-peptide [122]. This isoform is often referred to as "local" isoform (IGF-1Ea) [122]. After exercise or muscle damage, an exon 4-5-6 splice variant is upregulated. This is called the Mechano Growth Factor (MGF), which presumably is the IGF-1Eb isoform (reviewed in [141]). The expression of MGF has also been detected in resting muscle although at a very low level compared to IGF-1Ea (reviewed in [141]). A study on a myogenic cell line, C2C12, suggested different roles of IGF-1Ea and MGF [142]. This study reported that MGF prolongs proliferation of these cells while IGF-1Ea promotes their fusion. MGF has also been reported to be involved in proliferation of myoblasts in humans [143] and rats [144].

In vivo, mice over-expressing IGF-1Ea isoform in skeletal muscles showed increased fiber size, protein content, and nuclei within myofibers [122]. These features were accompanied by activation of Gata2, a novel marker of myocytes hypertrophy [145]. Moreover, this isoform of IGF-1 conferred muscle mass and strength during aging, in neuromuscular disease, and after injury [122]. Over-expression of human IGF-1 exclusively in skeletal muscle prevented age-related decline in the number of dihydropyridine receptors [146]. Dihydropyridine receptors are coupled to ryanodine receptors to conduct excitation-contraction coupling mechanism in skeletal muscles. In ageing mammalian skeletal muscle weakness, a large number of ryanodine receptors are uncoupled to dihydropyride receptors. Expression of human IGF-1 transgene prevented age-related decreases in dihydropyridine receptor number and in muscle force [146].

1.2.2.3.4 IGF-1 in the Heart

IGF-1 has been known to play a role in cardiac growth, function, apoptosis and remodelling. IGF-1 expression increases DNA and protein synthesis of myocardium [147, 148] and it is required for entry into S-phase of the cell cycle. It has also been known to modulate the induction of genes that regulate the cell cycle [149, 150]. Transgenic mice over-expressing IGF-1 in cardiomyocytes have increased heart weight and number of

cardiomyocytes by 50% and 20-50% respectively [150]. On the contrary, loss of growth hormone or IGF-1 may lead to cardiac atrophy and decrease in cardiac function [151]. Cittadini et al. reported an improvement in cardiac function in normal adult rats by IGF-1 [152]. Similarly, IGF-1 has been shown to improve functions of infarcted rat heart [153], chronic heart failure patients [154] and healthy human [155]. However, the mechanism of action of IGF-1 on cardiac function remains largely unclear.

Studies show that IGF-1 may play a direct role in cardiac contractility [156, 157]. These studies noted that IGF-1 increases intracellular calcium ion concentration in parallel to its action on cardiomyocyte contractility. IGF-1 may enhance cardiac contractility by increasing synthesis of cardiac contractile proteins [158]. However various intracellular signalling pathways have been implicated which include the Phospho Inositol-3 (PI-3) kinase and Tyrosine kinase [158] that may be directly affecting the intracellular calcium ion elevation (reviewed in [159]). The cardiac contractility could be affected by IGF-1 also without affecting the calcium ion level by simply increasing the sensitivity of the ion by the cell. IGF-1 has been implicated in ion channel function [160]. In 1998, Solem and Thomas reported that IGF-1 doubled dihydropyridine (DHP) sensitive calcium ion channel activity in cardiac myocytes, which could contribute to attenuation of contraction. The study suggests that the increased activity of calcium channels might lead to increased cardiac muscle contractility and cytosolic calcium transients [160].

Cardiac myocytes are believed to be non-mitotic cells [161]. Upon prolonged ischemia, they suffer apoptotic death, after which the heart suffers from failure as there is no regeneration of the lost muscle mass [161]. IGF-1 being an anti-apoptotic factor was administered in a rat model of myocardial ischemic reperfusion where it was able to decrease myocardial death [162] by inhibiting leukocyte-induced cardiac necrosis and reperfusion-induced apoptosis of cardiac myocytes. In a myocardial infarction model caused by the occlusion of left descending coronary artery, transgenic mice over-expressing IGF-1 demonstrated decreased cell death and ventricular dilation [163]. Similarly work from our laboratory performed with transgenic mice over-expressing IGF-1Ea (IGF-1Ea) showed smaller scar size and better function after injury compared to wild type control animals [77]. Studies performed with higher mammals showed similar results. In higher organisms, IGF-1 plays a role in reducing the amount of apoptotic cells and increasing contractile function (reviewed in [159]). As a result of our previous findings

and known beneficial effects of IGF-1Ea expression on muscle cells reported by other groups outlined above, this study chose to study IGF-1Ea in the heart.

1.2.2.4 IGF-1 signaling

IGF-1 bio-availability is highly regulated by IGF1-binding proteins (IGFBPs) and its signal transduction occurs through the cell membrane by the IGF-1 receptor (IGFR), which forms dimers and shows tyrosine kinase activity upon ligand binding. There are two possibilities for the signaling event that follows the activation of the receptor. It can either lead to Mitogen Activated Protein (MAP) kinase pathway via Ras activation or to insulin receptor substrate (IRS) 1 and 2 leading to Akt. Both of these pathways eventually activate different genes in the nucleus. MAP-kinase pathway has been implicated in cell proliferation, differentiation, survival and hypertrophy.

Upon ligand binding, the intracellular kinase domain of the receptor becomes activated and in turn autophosphorylates the receptor. This autophosphorylation event leads to the recruitment of endogenous substrates, of which the IRS proteins-1 and the src-homology containing protein (SHC), an adaptor protein with src-homology 2 domains (SH2), play a major role [164, 165]. Binding of these proteins to the cytoplasmic domain of the IGF-1R phosphorylates the proteins, which then enable recruitment of other substrates that in turn activate different signal cascades [166]. Several other docking proteins that are recruited to an activated IGF-1R have been described (reviewed in [164]) and these provide a mechanism to activate distinct signaling cascades in a tissue- and cell-specific manner. Since the expression pattern of these proteins varies between tissues and throughout development, they might provide an explanation for the multiple functions of IGF-1. However, it is important to point out that most of the studies to unravel the intracellular signalling pathways induced by IGF-1 have been based on tissue culture. Therefore, the extent to which the information translates *in vivo* remains to be investigated. Figure below (Figure 3) gives an overview on IGF-1 signaling.

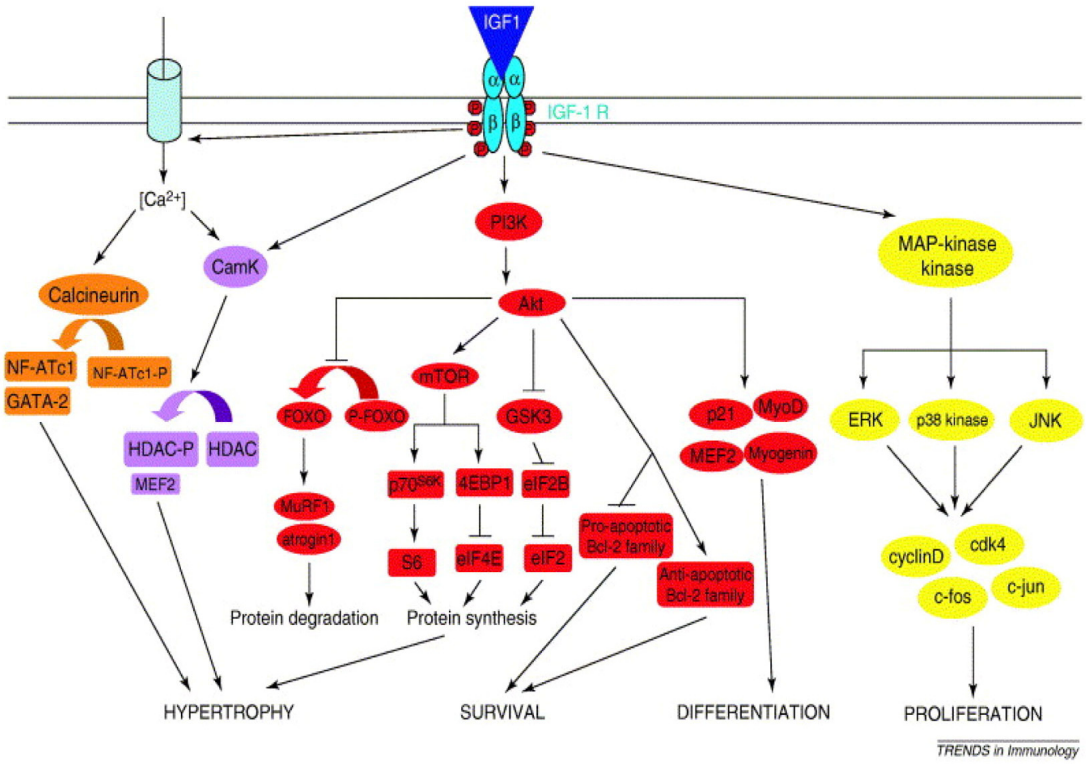

Figure 3. Overview of IGF-1/IGF1R Signaling Pathway. Binding of the ligand IGF-1 to the receptor IGF-1R leads to the downstream activation of MAP-kinase, PI3K, CamK and Calcineurin pathways, coded with different colours. (Reprinted from Trends in Immunology, Mourkioti et al., IGF-1, inflammation and stem cells: interactions during muscle regeneration, Copyright (2005), with permission from Elsevier)

1.2.2.4.1 MAP-kinase signaling

MAP-kinase signaling has been suggested to be one of the major pathways of IGF-1 for mediating cell proliferation [167]. The activated IGF-1R leads to recruitment of the docking protein SHC to the receptor. This leads to association of SHC with growth factor receptor-bound protein 2 (Grb2) via their SH2 domains. Grb2 is an adaptor protein, which recruits the GTP-exchange factor Sos (Sons of sevenless) via an additional SH3 domain. As a result of the interaction between Grb2 and Sos, the small G protein Ras is recruited. In addition this also leads to the transition of the inactive Ras-GDP to active Ras-GTP. Activated Ras induces sequential activation of Raf-1, MAP-kinase kinase (MAPKK), and a family of MAP-kinases, namely ERK1, ERK2 (extracellular regulated kinase), Jun kinase, and p38 MAP-kinase (reviewed in [158]). The MAPKs phosphorylate transcription factors, which increases their ability to induce expression of molecular markers of cell cycle progression, like c-jun, c-fos, cyclin D1, and cdk4 (reviewed in [158]). Cyclin D1 and cdk4 play a critical role in mediating the phosphorylation of the retinoblastoma protein (Rb). Upon phosphorylation, Rb releases E2F, a transcription factor essential for activating the transcription of many proteins involved in the cell cycle.

Also IRS-1 is able to recruit Grb2 and thereby activates the MAP-kinase pathway. Inactivation of the MAP-kinase pathways by using the specific inhibitor PD098059 in L6A1 myogenic cells induced a ~90% reduction of IGF-1 stimulated proliferation [167].

1.2.2.4.2 PI(3)-kinase signaling

The PI(3)-kinase has been linked to cell differentiation, survival and hypertrophy. Upon IGF-1R activation by ligand binding, IRS-1 interacts with the PI(3)-kinase, a heterodimer composed of a 110 kDa catalytic subunit and an 85 kDa regulatory subunit (p85) containing a SH2 domain. The p85 regulatory subunit directly binds to activated IRS-1 [168], phosphorylates and eventually triggers PI3-kinase activation. Activated PI3-kinase phosphorylates inositol phospholipids, which are required to induce several downstream targets, such as the serine/threonine kinase Akt, also known as protein kinase B. PI3-kinase plays a critical role on myogenic response to IGF-1 [167, 169-171]. PI(3)-kinase together with its downstream effector Akt had been implicated in activating factors involved in muscle differentiation and muscle cell survival. One of the most important effects of IGF-1 in stimulating myogenesis is its ability to activate expression of the myogenin gene via the PI(3)-kinase and direct translocation of Akt into the nucleus (reviewed [158, 172]. Myogenin is directly associated with terminal myogenic differentiation [173].

The PI(3)-kinase pathway has also been shown to induce the transcription of myocyte enhancer factor 2 (MEF2). MEF2 plays a role in activating muscle specific structural genes [174]. Activation of the PI(3)K/Akt pathway is crucial for regulation of protein synthesis in skeletal muscle cells as well as muscle hypertrophy [175, 176]. Muscle specific expression of constitutively active Akt in mice resulted in profound myofiber hypertrophy and decreased fat deposition [176]. Such muscle hypertrophy is observed in conditional transgenic mice, as well as when the transgene expression is induced in adult mice using tamoxifen-dependent recombination [176]. Activated Akt can lead to up-regulation of protein synthesis by regulating enzymes involved in carbohydrate metabolism. A recent report by Song et al. however suggested that hypertrophic pathway downstream of PI3-kinase can take place without involvement of Akt. They demonstrated this by showing activation of phosphoinositide-dependent protein kinase (PDK-1) and several other molecules without affecting Akt activity in the hypertrophic muscles of

transgenic animals over-expressing Class 1 IGF-1Ea (IGF-1Ea) specifically in skeletal muscle [177].

The PI(3)-kinase/Akt pathway also plays a role in inhibiting apoptosis by interacting with members of the Bcl-2 family of proteins [178] which have been shown to either inhibit or stimulate apoptosis. Following IGF-1 mediated stimulation, activated Akt can either lead to inhibition of pro-apoptotic Bcl-2 members and BAD at the earlier stage of apoptosis, and caspase 9 at later stages (reviewed in [172]), or to up-regulation of anti-apoptotic Bcl-2 members [179-181]. Although it is clear that the Akt pathway is the main pathway by which the activated IGF-1R exerts its anti-apoptotic affect, there is evidence that the IGF-1R has alternative pathways [182, 183]. Peruzzi et al. [183] showed a pathway which is dependent on mitochondrial translocation of Raf-1 and phosphorylation of BAD, which results in an anti-apoptotic event.

1.2.2.4.4 Calcineurin pathway

Calcineurin is activated by increased intracellular Ca^{2+} levels and causes dephosphorylation and nuclear translocation of cytoplasmic NF-ATc (nuclear factor of activated T cells) family members, which in combination with other transcription factors such as Gata2 activate transcription [184]. Two studies have linked the hypertrophic action of IGF-1 to calcineurin, although the calcineurin-mediated hypertrophy of skeletal muscle cells is not completely established. In one study, transfection of C2C12 myoblasts with plasmid encoding the IGF-1 gene induced mobilisation of Ca^{2+} within the cell, increased activation of calcineurin and resulted in nuclear translocation of the transcription factor NF-ATc1 [185]. This was associated with hypertrophy of the myotubes, a response that could be inhibited by addition of CsA or FK506, inhibitors of calcineurin [185]. However, the timing of IGF-1 addition mattered in driving the hypertrophy as hypertrophy occurred only when IGF-1 was added to proliferating culture or at the time of differentiation [185]. In a different study with L6E6 cells, which did not express endogenous IGF-1, transfecting the cells with IGF-1Ea led to hypertrophy of the cells associated with Gata2 and Calcineurin A accumulation [145]. However, the studies by Musaro et al. [145] and Semsarian et al. [185] were later questioned by Rommel et al. and Bodine et al. [175, 186]**.** They suggested that the reported inhibition of hypertrophy by addition of CsA could have been due to inhibition of fusion and differentiation of

myoblasts, as the inhibitor was applied to undifferentiated cells. These reports show discrepancies on the role of IGF-1 signaling on hypertrophy.

1.2.3 Tetracycline regulated expression of IGF-1Ea

The gene therapy fraction of this study was conducted via lentiviral transduction of rat IGF-1Ea gene into P19Cl6. The lentiviral expression vector carrying the IGF-1Ea gene (pLenti4/TO/V5-DEST) uses regulatory elements from the *E.coli* Tn10-encoded tetracycline (Tet) resistance operon. This allows tetracycline-regulated expression of *IGF-1Ea* from the expression construct. Expression of IGF-1Ea in the expression vector is under the control of human cytomegalovirus (CMV) promoter, into which 2 copies of tet operator 2 (TetO2) sequence have been inserted. The two operator sequences are binding sites for Tet Repressor (TetR) molecules [187]. The tetR molecules are generated through another lentiviral vector (pLenti/TR) that is transduced into the cells, prior to the IGF-1Ea expression vector. Upon transduction, TetR is generated constitutively. TetR molecules form homodimers, which then bind to TetO2 sequence in the IGF-1Ea construct with extremely high affinity. The two TetO2 sites get bound with 4 TetR molecules in total. The binding of the TetR to the TetO2 sequences represses transcription of IGF-1Ea. Upon addition, tetracycline binds with each of the TetR and causes a change in their conformation. The change in conformation then leads to dissociation of tetracycline:TetR from the TetO2 sequence, which then allows induction of gene expression [187]. Figure below demonstrates how tetracycline regulation of *IGF-1Ea* occurs in this study (Figure 4).

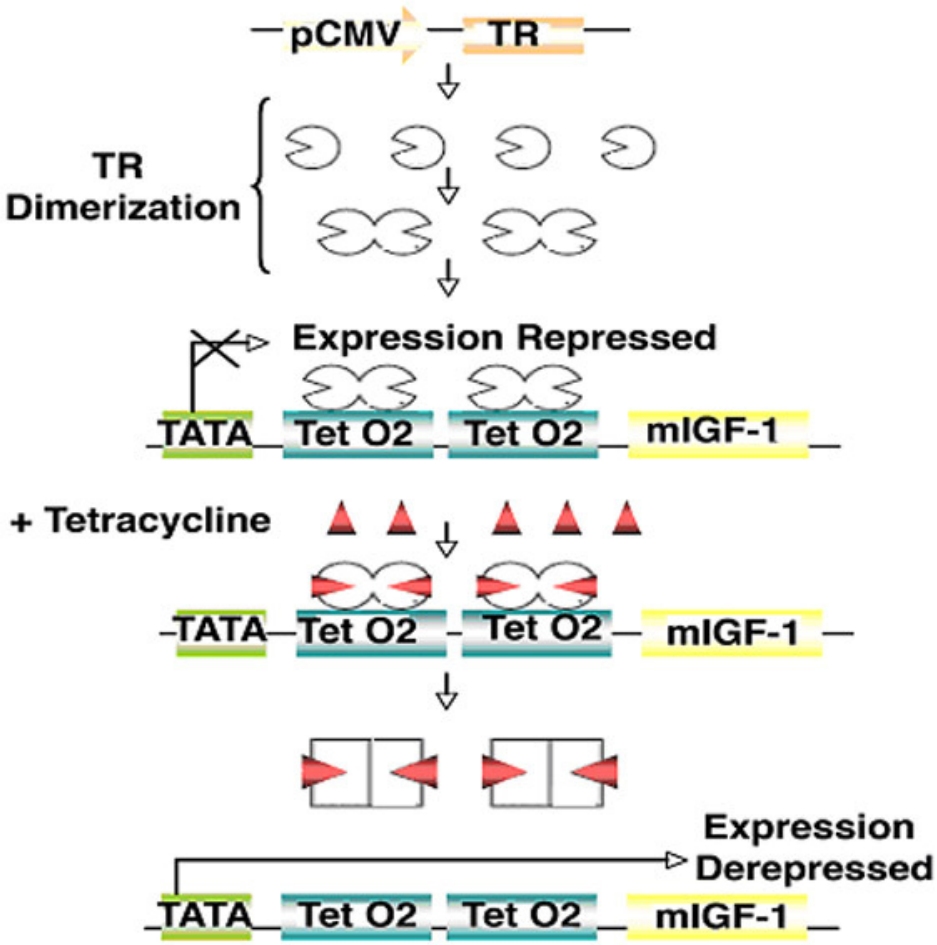

Figure 4. Mechanism of Tetracycline Regulated Expression of IGF-1Ea (mIGF-1) Gene. Expression of the tetracycline repressor (TetR) represses IGF-1Ea expression by tightly binding to the two tetracycline operator sequences (tetO2). Tetracycline treatment causes conformational change of the TetR homodimers causing the release of TetR from operator sequences and inducing transcription of IGF-1Ea. (Figure adapted from: ViraPower T-Rex Lentiviral Expression System, Invitrogen)

1.2.4 Objectives of this study

The objectives of this study were to (i) create tools to stably transduce pluripotent P19Cl6-MLC2v-GFP cells with *IGF-1Ea* and regulate the gene expression via tetracycline treatment, (ii) study the effects of *IGF-1Ea* transduction and expression on properties of the cell before and after differentiation, (iii) test feasibility of the *IGF-1Ea* transduced cells *in vitro* for subsequent *in vivo* cell therapy and (iv) test if function of impaired hearts caused by myocardial infarction could be preserved by transplantation of the engineered cells and whether or not IGF-1Ea transduced cells confer better cell survival, engraftment and preservation of function than the control cells.

1.2.5 Aims of this study

(i) Creating tools to stably transduce pluripotent P19Cl6-MLC2v-GFP cells with *IGF-1Ea* and regulate the gene expression via tetracycline treatment: The objective was met by cloning rat IGF-1Ea cDNA into lentiviral vectors of the Gateway system, where expression of the gene were driven by ubiquitous CMV promoter. For obtaining the tetracycline regulated expression of IGF-1Ea, P19Cl6-MLC2v-GFP cells were transduced with both IGF-1Ea and Tetracycline Repressor (TetR) lentiviruses, where TetR will bind to the IGF-1Ea operon sequences and repress expression of *IGF-1Ea* until activated. Expression of IGF-1Ea was induced upon tetracycline treatment.

(ii) Studying the effects of *IGF-1Ea* transduction and expression on properties of the cell before and after differentiation: Viral transduction as well as transduction of IGF-1Ea gene could theoretically affect the properties of the transduced cells. Therefore, following viral transductions, the P19Cl6-MLC2v-GFP cells were examined for their pluripotent feature, nature of cell cycle and their ability to form ventricular myocytes.

(iii) Testing feasibility of the *IGF-1Ea* transduced cells *in vitro* for subsequent *in vivo* cell therapy: After establishing the tools for cell-based gene therapy, *in vitro* analyses were conducted to test feasibility of the IGF-1Ea transduced cells for cell therapy. Firstly, the efficiency of differentiation into ventricular cardiomyocytes was analyzed in order to determine whether or not a reasonable amount of cells could be obtained for transplantation. Contractility of the differentiated cells was investigated to ensure that the cells are capable of contributing to mechanical function once transplanted into injured hearts. The myocytes obtained from differentiation were analyzed for cardiac structural proteins, to ensure their presence as well as to understand their organization. Finally, to test whether or not *IGF-1Ea* expression confers protection to the donor and the recipient cells, the *IGF-1Ea* transduced cells and neonatal cardiomyocytes treated with IGF-1Ea-cells conditioned media were assessed for cell viability following hypoxia exposure.

(iv) Testing if function of impaired hearts caused by myocardial infarction could be preserved by transplantation of the engineered cells and whether or not *IGF-1Ea* transduced cells conferred better cell survival, engraftment and preservation of function than the control cells: Following the *in vitro* assessments, the cells were transplanted into murine myocardial infarcted hearts. For transplantation, the *IGF-1Ea* expressing

ventricular cardiomyocytes were FACS sorted to select a pure cell population from all other cell lineages resulting from differentiation of the P19Cl6-MLC2v-GFP cells. The FACS sorting ensured that only differentiated ventricular myocytes were selected to avoid teratoma formation that might result from transplantation of undifferentiated cells. Myocardial Infarction was induced in C57BL6/J, 3-4 months old mice by permanent occlusion of the descending Left Coronary Artery. Immediately after induction of myocardial infarction, each heart received 1 million FACS sorted cells in five different spots surrounding the ligated area. Functional analyses were carried out before surgery, after 5 days and 2 months following induction of infarction and cell transplantation. Animals were sacrificed at 5 days or 2 months for molecular and histological analyses. Molecular analyses examined cytokines involved in inflammation, survival, vessel formation and homing of endogenous stem cells. Histological analyses studied scar size, cell engraftment and capillary densities.

With transplantation of IGF-1Ea expressing P19Cl6-MLC2v-GFP-derived cardiomyocytes, this study anticipated to achieve a lasting preservation of function of the infarcted hearts. The expression of IGF-1Ea was expected to confer better survival of the donor and the recipient cells, leading to reduced death of at-risk myocardium and better engraftment of the transplanted cells resulting in lasting maintenance of function of the injured hearts.

The following figure (Figure 5) outlines experimental plan, organized according to different chapters.

Figure 5. Outline of Experimental Plan

CHAPTER 2

2.1 MATERIALS AND METHODS

2.1.1 DNA preparation and quantification

DNA for all the experiments were isolated by using QIAGEN plasmid purification Kits (QIAprep Spin Miniprep ® Kit #27106; Endofree Plasmid Maxi Kit #12362) according to the manufacturer's instructions. Purified plasmids were eluted with sterile milliQ water and stored at -20°C. Concentration of the DNA was determined by spectrophotometric measurement of the absorbance (A) at 260 nm and 280 nm.

2.1.2 RNA isolation and quantification

2.1.2.1 Tissue Samples

Total RNA was isolated from frozen tissue following the standard TRIzol protocol (Invitrogen #15596-026)**.** All equipment used was pre-treated with RNAse ZAP (Ambion #9780;0782) to avoid damage of RNA by RNAse, which is ubiquitous. Tissues were homogenized with an electric homogenizer in the appropriate amount of TRIzol (50-100 mg of tissue per 1 ml of TRIzol). The homogenized samples were left at room temperature for 5 minutes for complete dissociation of nucleoprotein complexes. Following the incubation, RNA was separated using the appropriate amount of Chloroform (Merck #UN1888) (0.2mL/1mL Trizol) by mixing it vigorously and centrifuging at 11000 rpm for 15 minutes at 2-8^{o}C. With centrifugation samples formed three phases. The aqueous phase, the interphase and the red phenol phase. Aqueous phase was carefully pipetted out and RNA was precipitated with 0.5 mL Isopropanol/1 mL Trizol (BDH #102246L). The aqueous phase was left with Isopropanol at room temperature for 10 minutes and spun at 11000 rpm for 10 minutes at 2-8^{o}C. The precipitated RNA was washed once with 75% Ethanol (Merck #UN1170), using 1mL ethanol for 1mL Trizol. Following washing, samples were centrifuged at 8600 rpm and RNA was air dried before adding water to re-dissolve it. To ensure a clean preparation of RNA for quantitative Real Time PCR analyses, Trizol isolated RNAs were further purified using RNeasy mini-columns (Qiagen #74104). The RNA samples were made up to 100 µl with RNA grade water. 350 µl of lysis buffer containing recommended amount of B-mercaptoethanol and 250 µl of absolute ethanol were added sequentially. The content was mixed by pipetting and mixture was transferred to the mini-columns. The column was centrifuged at 13,000 rpm for a 15

seconds and RNA purification was performed by adding RNase-Free DNase solution as described by the manufacturer (QIAgen #79254). Finally the purified RNA was dissolved in 30-50µl of RNAse/DNAse free water and stored at -80°C until used.

Concentration of RNA was determined by spectrophotometeric measurement of the absorbance at A260 and A280 nm. A desired amount of RNA was diluted in TE buffer (10mM Tis, 1mM EDTA, pH 8.0) and the absorbance reading was taken using a double beam spectrophotometer which corrected for background absorbance by comparing the test cuvette with a reference cuvette containing the TE buffer. RNA concentration was determined using the formula that at 260nm, an OD of 1.0 represents 40 µg/ml RNA molecules. RNA purity was measured at 280nm OD. A pure RNA sample shows twice OD value at 280nm compared to 260nm and the ratio of absorbance 260 to absorbance 280 (A260/A280) is 2.0. Proteins absorb at 280nm therefore a ratio lower than 2.0 indicates contamination of RNA with protein.

2.1.2.2 Cultured cells

For RNA isolation from adherent cell cultures, plates were washed twice with sterile PBS and scraped in 1ml of TRIzol per 10 cm culture dish and followed the trizol extraction method described above for tissue samples. Alternatively for non fibrotic cells, RNA extraction kit was used (Qiagen #74104). The PBS washed cultured cells were lysed with 350 µl of lysis buffer. The cells were then scrapped off the plates and passed through a fine needle and syringe for homogenization. They were then added with 350 µl of 70% ethanol and mixed thoroughly before transferring to the mini-columns. The columns were then centrifuged at 13000 rpm for 15 minute to adsorb the RNA onto the silica membrane. Following this the DNA washing step was carried out by adding RNase-Free DNase solution as described by the manufacturer (QIAgen #79254) followed by RNA extraction and quantification as described above.

2.1.3 mRNA quantification by Real-Time Polymerase Chain Reaction (qRT-PCR)

Gene expression at transcript level was analyzed by using a real-time polymerase chain reaction. The analyses were performed using two separate systems for Reverse Transcription (RT) and PCR. RT was performed to generate cDNA and this was followed by a real-time PCR analysis to quantify gene expression levels. Sections 2.1.4 and 2.1.5 describe the methods for cDNA synthesis and real-time PCR analysis respectively.

2.1.4 cDNA synthesis

cDNA was synthesized using the Taqman reverse transcription kit supplied by Applied Biosystems (Applied Biosystems #N8080234). RNA samples for reverse transcription were thawed thoroughly. For cDNA synthesis, 100 ng/µl concentration RNA samples were prepared using RNA-grade water. Samples and the reagents were kept on ice at all times and handled with gloves to avoid contamination of RNases. The enzymes were left at -20°C until immediately before use. The reaction mix was prepared by combining all the reagents listed in table below (Table 2) and aliquoted into 0.5 ml microtubes. The RNA samples and RNA-grade water at appropriate volumes were added to each tube separately. For cDNA synthesis, the tubes were then transferred to a standard thermal cycler. They were incubated at 25°C for 10 minutes for primer binding, 48°C for 30 minutes for primer extension and 95°C for 5 minutes for enzyme inactivation. The synthesis was a single cycle. An aliquot of the synthesized cDNA was then diluted to 5x to get a concentration of 2 ng/µl for real-time PCR analysis.

Table 2. cDNA Synthesis

Reagent	Final Concentration	10 µl Rxn	20 µl Rxn	30 µl Rxn
10X RT buffer	1X	1.0	2.0	3.0
25mM MgCl2	5.5 mM	2.2	4.4	6.6
dNTPs	500µM each dNTP	2.0	4.0	6.0
Random hexamers	2.5 µM	0.5	1.0	1.5
Rnase inhibitor	0.4 U/µl	0.2	0.4	0.6
Multiscribe Reverse Transcriptase	1.25 U/µl	0.625	1.25	1.875
RNA-free water	-	3.475	6.95	10.425
RNA	10 ng/µl			

2.1.5 Quantitative Real Time PCR (qRT-PCR)

Following the cDNA synthesis, an aliquot of the 2ng/µl cDNA was thawed for real-time-PCR analysis. The off-the-shelf assays for all the genes of interest were obtained from Applied Biosystems, ready-to-use. The catalogue numbers for all the genes analyzed are listed in the table below (Table 4)**.** The reagents for real-time PCR, the 20X 18S assay (Applied Biosystems #4310893E), the 20X off-the-shelf assays (Applied Biosystems), and

the cDNA samples were thawed at room temperature. The assays were thawed protected from light. 2 X Taqman universal PCR master mix (Applied Biosystems #4604437) that consists all other components required for the PCR analysis was kept refrigerated until immediately before use. All the PCR tubes were optical grade (Applied Biosystems #403012). The PCR master mix was prepared by mixing all the reagents listed in (Table 3) in the required amount and aliquoted into the optical tubes. 3 µl of the 2ng/µl cDNA was pipetted into the optical tubes separately in duplicates. Real-time PCR was then performed in an ABI Prism 7700 Sequence Detection System (Applied Biosystems). The PCR cycle conditions are mentioned below. When the PCR run was over, data were collected and analyzed using Sequence Detection Software (Applied Biosystems, SDS). Data from SDS were exported into Excel and analyzed by using the comparative Ct method.

Table 3. Recipe for Real Time PCR

Reagent	**1 Rxn Total Volume = 25 µl**
2x Universal Master Mix	12.5 µl
20x off the shelf assay (primers and probes all mixed)	1.25 µl
20x 18S control	1.25 µl
cDNA	3 µl
Water	7 µl

Table 4: TaqMan off-the-shelf assays for Real Time PCR analyses

TaqMan® Gene Expression assay	**Gene name**	**Assay ID**
Mouse IL-10	Interleukin-10	Mm0043914_m1
Mouse Myl2	Myosin Light Chain 2	Mm000440384_m1
Mouse Nkx2-5	Nkx2-5	Mm00657783_m1
Rat IGF-1	Insulin-like Growth Factor-1	Rn00710306_m1
Mouse Gata4	Gata-binding Protein-4	Mm00484689_m1
Mouse VEGFa	Vascular Endothelial Growth Factor Alpha	Mm01281449_m1
Mouse IL-6	Interleukin-6	Mm00446190_m1
Mouse SDF/ Cxcl12	Chemokine (C-X-C motif) ligand 12	Mm00445552_m1
Mouse bMHC	Beta Myosin Heavy Chain	Mm00600555_m1
Mouse aSK	Alpha skeletal actin	Mm0080818_g1
Mouse Eln	Elastin	Mm00514670_m1

The comparative Ct method is a relative quantification technique which avoids use of standard curves and makes use of mathematical formulas [188]. This method relies on

approximately equal PCR efficiencies of the target and endogenous control genes. The formula used by this method to calculate abundance of a target mRNA by normalizing to an endogenous control and relative to a calibrator. The formula for relative expression is 2^-ddCt, where ddCt = dCt of test sample-dCt of calibrator sample and dCt = target gene Ct (eg. IGF-1) - endogenous control gene Ct (eg. 18S). The 2 in the formula as the base number is derived from the assumption that the PCR efficiencies of a well designed assay will be close to 100% and result in a doubling of amplicon with each cycle.

Stage 1: 50 ^{0}C for 2 min	UNG incubation
Stage 2: 95 ^{0}C for 10 min	Activate DNA Polymerase
Stage 3: 95 ^{0}C for 0.15 min	Denature
Stage 4: 60 ^{0}C for 1 min	Anneal and Extend

Stages 3 and 4 were run for 40 PCR cycles.

2.1.6 Cloning of IGF-1Ea cDNA into lentiviral backbone

IGF-1Ea rat cDNA was directionally cloned into a Gateway entry vector backbone pENTR Directional TOPO Cloning Kits (Invitrogen # K2400-20), using a blunt-end PCR product. The Gateway system allows cloning of the gene of interest into multiple vectors in a very efficient and rapid manner by recombination. Taking advantage of this property, after cloning into the entry vector, the gene of interest, IGF-1Ea, was cloned into a destination lentiviral backbone, p*Lenti4/TO/V5-DEST* (Invitrogen # K4965-00). The *IGF-1Ea* cloning from the entry vector into the destination vector was by site-specific recombination of attL and attR recombinant sites present on the entry and destination vectors respectively. The generated expression vector was transformed into One Shot Stbl3 Chemically Competent *E. coli* cells and plated on LB- plates with 30µg/ml Chloramphenicol, where a true clone with *IGF-1Ea* inserted will be Chloramphenicol sensitive. The expression clone was maintained and propagated in LB medium containing 100 µg /ml Ampicillin to select for resistant clones. The following are the vector maps for the IGF-1Ea and the TR genes (Figure 6).

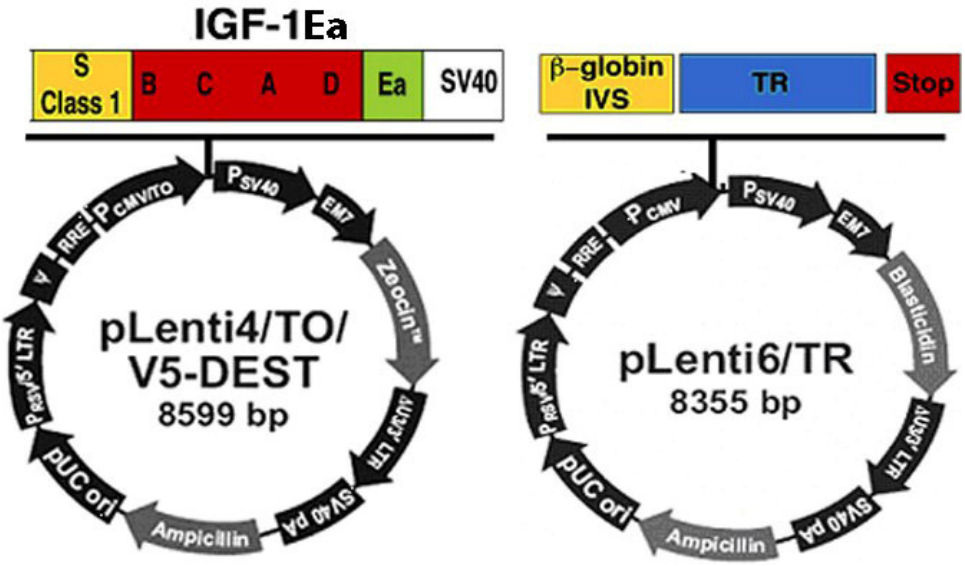

Figure 6. Maps of Lentiviral Constructs. The pLenti4/TO/V5-DEST consists of two tet operator sequences (TO) that serve as binding sites for the tetracycline repressor (TetR). Zeocin resistance allows selection of IGF-1Ea vector transduced cells and Blasticidin for TR vector transduced cells. The recombination sites attR1 and attR2 are downstream of the CMV-TO promoter. The pLent6/TR lentiviral construct consists of a TR gene under the control of the ubiquitous promoter CMV to allow its expression in different cell types. (Figure adapted from ViraPower T-Rex Lentiviral Expression System, Invitrogen)

2.1.7 Sequencing of IGF-1Ea

To confirm the presence and orientation of the IGF-1Ea insert, as well as the integrity of the lentiviral pLenti4/TO/V5-DEST, restriction analysis and sequencing of the expression vector was carried out. Table 5 below shows primers used for sequencing of IGF-1Ea gene. Below the table is the sequence for rat IGF-1Ea mRNA**.**

Table 5: IGF-1Ea sequencing Primers

Forward External Primer 1: 5'CACCACGACGGCCAGTGAATTGGATTTA 3'
Forward Internal Primer 2: 5' CCACAGGCTATGGCTCCAGCATT 3'
Reverse Internal Primer 3: 5' AATGCTGGAGCCATAGCCTGTGG 3'
Reverse External Primer 4: 5'GACTCACTATAGGGAGACAAGGTTG 3'

Rat IGF-1Ea mRNA sequence [189]

1 gaatgttccc ccagctgttt cctgtctaca gtgtctgtgt tttgtagata aatgtgagga

61 ttttctctaa atccctcttc tgcttgctaa atctcactgt cgctgctaaa ttcagagcag

121 atagagcctg cgcaatcgaa ataaagtcct caaaattgaa atgtgacttt gctctaacat

181 ctcccatctc tctggatttc tttttgcctc attattcctg cccaccaatt catttccaga

241 ctttgtactt cagaagcgat ggggaaaatc agcagtcttc caactcaatt atttaagatc
301 tgcctctgtg acttcttgaa gataaagata cacatcatgt cgtcttcaca tctcttctac
361 ctggcactct gcttgctcac ctttaccagc tcggccacag ccggaccaga gacccttgc
421 ggggctgagc tggtggacgc tcttcagttc gtgtgtggac caaggggctt ttacttcaac
481 aagcccacag gctatggctc cagcattcgg agggcaccac agacgggcat tgtggatgag
541 tgttgcttcc ggagctgtga tctgaggagg ctggagatgt actgtgctcc gctgaagcct
601 acaaagtcag ctcgttccat ccgggcccag cgccacactg acatgcccaa gactcagaag
661 tcccagcccc tatcgacaca caagaaaagg aagctgcaaa ggagaaggaa aggaagtaca
721 cttgaagaac acaagtagag gaagtgcagg aaacaagacc tacagaatgt aggaggagcc
781 tcccgaggaa cagaaaatgc cacgtcaccg caagatcctt tgctgcttga gcaacctgca
841 aaacatcgga acacctgcca aatatcaata atgagttcaa taccatttca gagatgggca
901 tttccctcaa tgaaatacac aagtaaacat tccgacattg tctttaggag tgtttgttaa
961 aaaaaaaaaa aaaaaaaaca aaaacaaaaa caaaaaaaaa aagctttgca ccttgcaaaa
1021 gtggtcctgg cgtgggtaga ttgctgttaa tcctttatca ataacgttct atagagaata
1081 tataaatata tatataatt

2.1.8 Virus production

Production of lentiviral stocks expressing IGF-1Ea, Tet repressor (TetR) and Empty vector (control virus without IGF-1Ea, with p*Lenti4/TO/V5-DEST* backbone only) were performed as instructed by the manufacturer [187]. In brief, human embryonic kidney (HEK) 293 cells were grown in adherent culture overnight to get 90% confluency the next day. For transfection, DNA-lipofectamine 2000 (Invitrogen #11668-027) complexes were prepared as follows. In a sterile tube, 9 µg of packaging mix and 3 µg IGF-1Ea expression vector (a total of 12 µg) were mixed in 1.5 mL of Opti-MEM I Medium without serum (Gibco #31985-070). An optimized mixture of pLP1, pLP2, and pLP/VSVG plasmids formed the Packaging/Envelope Mix (Invitrogen #K4975-00). The packaging/envelope mix was provided in the ViraPower T-Rex Lentiviral Expression System. In a separate tube, 36 µl (3:1 lipofectamine to DNA ratio) Lipofectamine 2000 was mixed with 1.5 mL of Opti-MEM I Medium without serum. The solution was mixed gently and incubated for 5 minutes at room temperature. Following the incubation, the DNA and lipofectamine dilutions were combined in one tube, mixed very gently and incubated for 20 minutes to form DNA-lipofectamine complexes. In the meantime, media was replenished for 293 cells with Opti-MEM I Media containing 10% serum. When the incubation was over, the

3 mL lipofectamine-DNA complex containing medium was added to the 293 cells. Cells were then incubated overnight at 37°C and 5% CO2. The next day, lipofectamine containing culture media was replaced with small volume of complete culture media. Virus containing supernatant was harvested 48 hours post-transfection and stored in 1ml aliquots at -80 ^{o}C.

2.1.9 Determining antibiotic sensitivity

As the stably transduced cells were selected using Zeocin (Invitrogen #R250-05) and Blasticidin (Invitrogen #R210-01) resistance, the minimum concentration of the antibiotics to select the cell of interest within 10-14 days was to be determined before transduction was carried out. Antibiotic sensitivity was examined with Zeocin concentrations ranging from 50-1000 µg/ml and Blasticidin from 2-10 µg/ ml in human connective tissue fibrosarcoma cell line (HT1080) (ATCC # CCL-121) and P19Cl6 cells (Gift from Prof. **C**. Mummery, Netherlands). Typically these concentrations are enough to kill most of untransduced mammalian cell lines [187]. Cells were plated in 25% confluency, 10 plates per cell type, and allowed to adhere overnight. The following day, normal growth medium was substituted with media supplemented with Zeocin and Blasticidin to respective plates. Two plates were used as negative control where normal media was continued. The selective media was replenished every 3-4 days and the percentage of surviving cells was carefully observed. Appropriate concentrations of antibiotics for each of the cells types were determined by finding the concentration that killed the cells within 10-14 days.

2.1.10 Lentiviral stock tittering

The expression vector *(Lenti4/TO/V5-DEST)* and the Tet repressor construct *(Lenti6/TR)* containing Zeocin and Blasticidin resistance genes respectively, are necessary to select stably transduced cell clones and for titration of the lentiviral stocks. To analyse the minimum concentrations of Zeocin and Blasticidin necessary to select the cells that integrated the lentiviral constructs, concentrations ranging from 50-1000 µg/ml of Zeocin and 2-10 µg/ml of Blasticidin were tested. The minimum concentration of the antibiotics required to induce death of untransduced cells was determined 10-14 days after the start of antibiotic treatment. Titering was performed with HT1080 (ATCC # CCL-121). The cells were transduced with lentiviral supernatant in a 10-fold serial dilution (10^0 to 10^5). A plate was left untransduced as a mock control. Forty-eight hours post-transduction, cells were

treated with 10µg/ml Blasticidin or 1000 µg/ml zeocin. After 10-14 days of selection, the transduced cells were stained with 5ml/10cm-dish crystal violet (Sigma # 10010-023 in 10% ethanol) for 10 minutes at room temperature and the titer of the virus was determined by counting Crystal violet-stained colonies as described in the instruction manual [187].

2.1.11 Transduction of viral vectors

Lentiviruses for the tetracycline operon system were transduced first into HT1080 followed by the cell of interest, P19Cl6. Transductions were performed following the protocol provided by the company. In summary, both the cell types were transduced with *Lenti6/TR* first, on cells growing on 10cm culture dishes. On the day of transduction, a 1ml vial of the TR virus was thawed and diluted with equal volume of culture media. The old culture media was replaced with 2 ml of virus containing media. Polybrene (Sigma #H9268) was added at 6 µg/ml concentration to the 2 ml media to maximize transduction. The transduced cells were incubated with TR virus for 24 hours until the next transduction of the *Lenti4/TO/V5-DEST-IGF-1Ea* constructs, to allow time for the Tet repressor protein to be expressed. *Lenti4/TO/V5-DEST-IGF-1Ea* virus was transduced the same way as TR virus except that the virus was diluted into 3 ml media instead of 2ml. This was to make sure that *Lenti6/TR* virus transduced at higher multiplicity of infection (MOI, i.e. number of virus particles per cell) than the *Lenti4/TO/V5-DEST-IGF-1Ea* virus to obtain Tetracycline regulated expression of the gene of interest. Media supplemented with Blasticidin (4 µg/ml for both HT1080 and P19Cl6) and zeocin (500 µg/ml for HT1080 and 200 µg/ml for P19Cl6) was changed regularly for 10-14 days to select for stably transduced cells.

2.1.12 Tetracycline regulated gene expression

Stably transduced, positively selected HT1080 and P19Cl6 cells were treated with/without tetracycline (Invitrogen #Q100-19) to induce gene expression. Tetracycline was added in culture media to a final concentration of 1 µg/ml. Cells were left with tetracycline for 48 hours to allow enough time for gene expression. Forty-eight hours after tetracycline treatment, RNA was extracted and qRT-PCR was carried out to determine *IGF-1Ea* transcript expression in the tetracycline treated versus untreated cells. From the remaining stably transduced P19Cl6 cells, 18 colonies were picked, expanded and stored for future analysis. The colonies were labelled clones 1-18.

2.1.13 Cell culture

2.1.13.1 HT1080

HT 1080 cells were obtained from ATCC and propagated in 10 cm plates with ATCC complete growth medium. The medium was ATCC-formulated Eagle's Minimum Essential Medium (EMEM) (# 30-2003). To make the complete growth medium, the EMEM was supplemented with 10% fetal bovine serum (Sigma #F7524). The cells became confluent every 2-3 days after which they were split into 1:4 ratio. They were incubated in a humidified chamber at 37°C and 5% CO2.

2.1.13.2 293T

293T cells were cultured for virus production purposes. They were plated in 10 cm tissue culture dishes without any coating. They were seeded at 2 * 10^6 cells per 10 cm tissue culture dishes and grown in media with high glucose DMEM (Gibco #D5546), supplemented with 10% FBS (Sigma #F7524), 1% Pen/Strep (Sigma #P0781), 1% MEM Non Essential Amino Acid (Gibco #11140) and 1% L-glutamine (Sigma #G7513). The cells became confluent after 2-3 days in culture after which they were trypsinized and split into 3 plates per confluent plate.

2.1.13.3 P19Cl6-MLC2v-GFP-IGF-1Ea Culture and Differentiation

The P19Cl6-MLC2v-GFP-IGF-1Ea cells were incubated in a humidified chamber at 37°C and 5% CO_2. For growth of adherent cells, culture dishes and flasks were prepared by coating with 0.1% gelatine (Sigma #G9391). They were grown on media consisting of 78% DMEM/F-12 (Ham) (1:1) (Gibco #31331-093), 10% Fetal Bovine Serum (Sigma #F7524), 1% Pen/Strep (Sigma #P0781), 1% MEM Non Essential Amino Acid (Gibco #11140) and 1% L-glutamine (Sigma #G7513). When they reached ~90% confluency they were washed with 1X PBS, trypsinized and re-plated. The remaining cells after trypsinization were frozen down in 10% DMSO (Sigma #D2650) containing culture media and stored in liquid nitrogen.

Cell differentiation was carried out by supplementing normal culture media with a new serum (ATCC #30-2020) and 1% DMSO. Cells for differentiation were trypsinized and re-suspended in differentiation medium in density of 400,000 cells/ml. Cell suspensions were transferred to bacteriological Petri dishes without gelatin for 4 days to facilitate Embryoid Bodies (EBs) formation. Media was replenished after 2 days. After 4 days in

suspension, the EBs were transferred to tissue culture dishes with normal growth medium to allow cell attachment. Media was changed every two days and cells were carefully monitored throughout.

2.1.13.4 Neonatal Rat Cardiomyocytes Isolation and Culture

Myocyte preparation was performed under a sterile tissue culture hood. Neonatal rat hearts were collected in 50 ml chilled 1x Ads (3,4g NaCl, 2,4g HEPES, 0,06g NaH_2PO_4, 0,5g glucose, 0,2g KCl, 0,05g $MgSO_4$, pH 7.35) solution and washed with the same buffer twice in a Petri dish to remove blood. The hearts were minced finely into mm^3 pieces and transferred into an upstanding 75 cm^2 culture flask. The minced tissue was then treated with 10ml enzyme solution (Pancreatin, GIBCO, and Collagenase, Worthington collagenase Type II, cls2) for 5 minutes at 37 ^{0}C. Supernatant was collected, and 10ml of fresh enzyme was added to the tissue and incubated for 20 min at 37°C. The steps for enzyme digestion and cell collection are outline in the table below (Table 6). The collected cell supernatant was added to pre-warmed FBS aliquots.

Each collection was resuspended in pre-warmed FBS and kept at 37^{0}C. Fibroblast contamination was minimized by cell pre-plating into 35mm culture dishes for 45 minutes. Myocytes were dislodged from the pre-plated dishes by tapping the dishes several times. Media containing the dislodged cardiomyocytes was collected into a falcon tube and added with 1xBrdu. Cells were then plated in 1% gelatinized dishes and kept in complete medium (Dulbecco's Modified Eagle Medium (DMEM) containing 4.5g/L glucose (65.5%), 199 medium containing 25 mM HEPES (20%), heat inactivated horse serum, heat inactivated foetal calf serum (10%), 1X HEPES (2.5%), 1X L-glutamine (1%), 1X penicillin streptomycin(1%)). They were left in culture for two days to recover before they were used for cell viability experiment upon hypoxia.

Table 6: Enzyme Digestion and Cell Collection

1	**2**	**3**	**4**	**5**
10 ml enzymes	8 ml enzymes	8 ml enzymes	6 ml enzymes	6 ml enzymes
20 mins	25 mins	25 mins	15 mins	20 mins
Collection #1	Collection #2	Collection #3	Collection #4	Collection #5

2.1.14 Immunofluorescence

For Immunofluorescence, cells were cultured overnight in either two or four-welled culture dishes in low density to get about 30-40% confluency the following day. The next day, they were washed with cold 1x PBS thrice, 3 minutes per wash and fixed with 4% PFA for 10 minutes at room temperature. Following fixation, they were washed with 1x PBS for three times and treated with 0.1% Triton X-100 to permeabilize the cell membrane for 5 minutes at room temperature. In the mean time 3-5% blocking solution was prepared with serum of the animal where the secondary antibody was raised. Cells were blocked with blocking solution for an hour. After the incubation with blocking solution, they were treated with primary antibody, in blocking solution, in appropriate dilutions recommended by the company for 2 hours at room temperature. Following the two hours incubation, they were washed thrice again with 1x PBS and treated with secondary antibody diluted in the blocking solution at the concentrations recommended by the company for an hour at room temperature. The slides were then washed with 1x PBS and treated with either 1:1000 Hoechst or 1:20000 DAPI in PBS for nuclei staining for 10 minutes. They were then washed with PBS and mounted in Mountant, PermaFlour (Thermo Scientific, #TA-030-FM) and analysed through a confocal or a fluorescence microscope.

2.1.15 Hypoxia and normoxia induction

To investigate the effect of IGF-1Ea constitutive expression on cells that undergo serum, glucose and oxygen deprivation, P19Cl6 cells transduced with empty vector or IGF-1Ea were exposed to either normoxia or hypoxia. Normoxia was obtained by treating cells with media without glucose and serum but normal oxygen (i.e. 20%) placed in an incubator at 37°C and 5% CO2. Hypoxia was induced by having the same conditions as normoxia except the cells were exposed to only 3% oxygen as opposed to 20% and placed in a special incubator (Sanyo #MCO-5M (UV)). The first experiment was carried out to determine the time when the cells start to die. Several treatment times were tested namely, 1 minute, 0.5 hour, 1 hour, 2 hours, 4 hours and 24 hours. After each time point Lactose Dehydrogenase (LDH) release was measured following the protocol described below.

2.1.15.1 LDH assay

Cell death can occur either by apoptosis or by necrosis. Necrosis is accompanied by mitochondrial swelling and increased plasma membrane permeability, whereas apoptosis

involves cell shrinkage, condensation of their chromatin and some times breakdown of cell into membrane-bound apoptotic bodies [190]. Unlike necrosis, apoptosis avoids involvement of scavenging inflammatory cells [190]. Lactate Dehydrogenase (LDH) is a stable cytosolic enzyme that gets released only upon cell lysis either by necrosis or apoptosis [191]. LDH is impermeable to cell membrane without damage. It is therefore a marker for cell membrane damage. With CytoTox96 Non-Radioactive Cytotoxicity Assay (Promega #G1782), necrotic cell death was determined upon hypoxia and normoxia exposure. The LDH activity is determined by enzymatic activity. Firstly, the NAD+ is reduced to NADH/H+ by the LDH catalyzed conversion of lactate to pyruvate. The second step involves the catalyst diaphorase, which transfers the H/H+ from NADH/H+ to the tetrazolium salt 2-(4-iodophenyl)-3-(4-nitrophenyl)-5-phenyltetrazolium chloride (INT), which gets reduced to red formazan [192-194].

96-welled plates were prepared for each time point; one for normoxia and one for hypoxia per time point. Twenty five thousand P19Cl6 cells, with or without IGF-1Ea were plated in triplicates in each of the plates and incubated overnight in normal media and culture conditions. The next day, using a multichannel pipette, the normal media was replaced by serum and glucose free media. Immediately after, the plates were placed either in normoxia or hypoxia. After 1 minute, the first set of plates was taken out and spun to sediment floating cells from the supernatant. An equal volume of supernatant was collected from both normoxia and hypoxia conditioned plates and stored in another 96-welled plate for further analysis. To the remaining cells and supernatant, lysis buffer was added at 1:10 dilution and incubated at 37 °C for 45 minutes. After the incubation, the plates were spun again, and the same volume of supernatant as above was collected into the new 96-welled plate where the supernatant without lysis was collected, and the plate was kept protected from light until the 4-hour time point supernatants were collected. The 24 hour samples were analyzed the next day when the incubation was over. To the rest of the samples**,** required volume of substrate solution was added, incubated for 30 minutes followed by addition of necessary amount of stop solution. When the reaction was stopped, the plates were read by a microplate reader at 490nm wavelength.

The percentage LDH Release was calculated relative to the 1 min exposure control (C1) for empty vector transduced cells, which was set to 0% LDH release.

In the subsequent experiments, which involved only 24 hour-exposure time, percentage LDH release was reported relative to the empty vector transduced cells with 24 hour-exposure, which was set to 100% LDH release

2.1.15.2 Hypoxia or normoxia treatment of neonatal rat cardiomyocytes with/without IGF-1Ea conditioned media

To replicate the effects of IGF-1Ea release in native heart cells *in vivo* when P19Cl6 with/without IGF-1Ea is transplanted following infarction, an *in vitro* model was setup where neonatal cardiomyocytes were treated with media from P19Cl6 cells lacking both glucose and serum under hypoxia. Neonatal cardiomyocyte cultures were prepared using the protocol described above in section 2.1.13.4 two days before the experiment. In the mean time, P19Cl6-IGF-1Ea or P19Cl6-empty cells were cultured and treated with serum and glucose free cardiomyocyte media for 24 hours to collect media with or without IGF-1Ea. Cardiomyocytes were treated with the media collected and subjected to either normoxia or hypoxia condition for 24 hours. The conditions for hypoxia and normoxia were same as mentioned above. After 24 hours incubation, media and cardiomyocytes were collected. Protein was extracted from the cardiomyocytes and western blot analysis was carried out for cleaved-Caspase-3 (Cell Signaling #9664) to investigate apoptotic signalling in IGF-1Ea media treated versus empty vector media treated myocytes. Results were normalized to total Caspase-3 (Cell Signaling #9662). Western blot was performed as described below. Primary and secondary antibodies were used at 1:500 and 1:1000 dilutions respectively and blocking was performed with 5% BSA.

2.1.16 Protein extraction

Cultured cells were washed twice in sterile PBS and scraped in the appropriate volume of lysis buffer (20mM Tris pH 7.5, 5mM MgCl , 150mM NaCl, 1% SDS, 1mM NaVO4 , 1mM NaF, 1mM PMSF; for 10ml of final lysis buffer, 1 tablet of cOmplete Mini EDTA-free Protease Inhibitors (Roche #11836170001) and 1 tablet of PhosSTOP (Roche #04906845001) were added. Lysates were homogenized and centrifuged for 20 min at 4°C and 13000 rpm, and protein concentration of the supernatant was determined by Bradford assay. Protein extracts were stored at -80°C until needed.

2.1.17 Western Blot analysis

For SDS-page, proteins were diluted in 2xSDS sample buffer (100mM Tris pH 6.8, 4% SDS, 20% glycerol, bromophenol blue), denatured by adding Beta-Mercaptoethanol and boiling for 5 min and subjected to gel-electrophoresis. Proteins were electrophoretically transferred onto a Trans-Blot Transfer Medium Pure Nitrocellulose Membrane (0.45um), (Bio-RAD Cat# 162-0115) and transfer was carried out in a wet transfer apparatus for 1.5 hours at 100V in transfer buffer (14.45g Glycin, 3g Tris-base, 0.75g SDS, 200 ml methanol and bringing the final volume to 1000 mL with water). After the transfer, membranes were incubated in blocking solution (5% non-fat powder milk or 5% BSA dissolved in 1X TBST buffer (20mM Tris pH 7.5, 140mM NaCl, 0.1% Tween20) for 1 hour at room temperature. Primary and secondary antibodies were diluted in blocking solution to the concentrations indicated by the suppliers. Membranes were washed 3 times, 10 minutes per wash in PBS-Tween buffer between primary and secondary antibodies were added. To detect specific bands the enhanced chemiluminescence system (ECL) Western Blotting Detection Reagent (Amersham #RPN2106) was used, followed by the exposure to Hyperfilm ECL films (Amersham #RPN3103K).

2.1.18 Confocal Calcium transient analysis

The Ca^{2+} sensitive fluorescent dye, Rhod2-AM (Molecular Probes #R1244), was used to monitor changes in cytoplasmic calcium concentrations. Differentiated P19EC cells were incubated with Rhod2-AM (10 μM) for 12 min and cells were allowed to de-esterify for at least 30 minutes prior to analysis by confocal microscopy. Experimental chamber was mounted on the stage of an Axioscope 2 Zeiss upright microscope with LSM 510 confocal attachment. Cardiomyocytes were observed through Zeiss water immersion Achroplan 10X lens. Rhod2-AM was excited using the 488 nm line of an argon laser. Line scans were collected and analyzed by Image J NIH software.

2.1.19 FACS Analysis

The percentage of GFP positive reporter cells were determined by FACS analysis using the FACS Aria (BD, Bekton Dickinson). For the analysis, confluent adherent differentiated (14 days post differentiation) and undifferentiated cells were washed with 1xPBS and trypsinized. Cells were collected and re-suspended in 3 mL 1x PBS and placed on ice. An aliquot with 10^6 cells was taken out, spun and re-suspended 300 μl 1xPBS. The cell suspension was filtered through 0.45 μm sieve to get rid of any lumps of cell and

added with 7AAD dye to discriminate any dead cells from analysis. Cells were left with the dye for 5 minutes and FACS analysis was carried out. 7AAD stained cells appear positive in pacific blue channel. They were discarded by gating for pacific blue negative cells. The gated population was then analyzed for width and height to discriminate any doublets. After discarding doublets, the final gated population was looked at FITC channel for GFP positive cells. Undifferentiated cells were used as negative control for deciding baseline for GFP positivity and the same gating was applied for differentiated cells to report percentage of GFP positive cells in differentiated population. For FACS sorting, the GFP positive population was gated and selected for sorting. The cells during sorting were released in 5 ml buffer for every 10^6. After every 10^6 cells were collected, the suspension was spun at 1300 rpm for 5 minutes, buffer discarded and the cells were re-suspended in 50 µl of 1x PBS for cell injection. At all times, cells were kept on ice to minimize cell death.

2.1.20 PI Staining for DNA analysis using FACS

PI intercalates between the bases in DNA by binding to the nucleotide pair of guanine and cytosine with a stoichiometry of one dye per 4–5 base pairs of DNA [195, 196]. Because it binds to guanine and cytosine that are also present in RNA molecule, PI also binds to double stranded RNA molecule therefore it is necessary to treat with RNAase to distinguish between RNA and DNA staining [195, 196]. PI is a fluorescent molecule. Once the dye is bound to nucleic acids, its fluorescence is enhanced 20- to 30-fold.

For PI staining, P19Cl6 cells transduced with empty vector or IGF-1Ea were harvested from adherent cultures by trypsinizing and centrifuging at 1000 rpm (400 xg) at 4°C. The cells were resuspended in 10-12 mL sample buffer (1g glucose in 1 Litre of PBS without Ca2+ and Mg2+, filter through a 0.22um filter, store at 4 degree*)*, washed twice with the buffer and counted. Following counting, the cell concentration was adjusted to 1-3 x 10^6 cells/ ml for each sample. 1 mL of the cell suspension was taken out, centrifuged and supernatant was poured off leaving only 0.1ml/ 10^6 cells. The tubes were vortexed very well in the remaining buffer. While vortexing, 1ml of the chilled 70% Ethanol solution was added drop by drop to the cell suspension for fixing. The samples were then left at 4°C to fix overnight.

The following day, the samples were vortexed very briefly and centrifuge at 3000 rpm for 5 minutes. Higher centrifugation is required after ethanol fixation as cells become lighter. After centrifugation, ethanol was poured off leaving approximately 0.2ml ethanol/ 10^6 cells. The cell pellet was gently vortexed in the remaining ethanol and added with 1 mL of PI staining solution (50µg/ml final concentration), drop by drop. RNAse A was added at a final concentration of 100U/ml to the PI solution. The samples were incubated at room temperature for at least 30 minutes, protected from light before FACS analysis. FACS analysis was performed for PI staining using PE-A channel, PI fluorescence at >/= 600nm wavelength**.**

2.1.21 General animal husbandry

Wild Type, male C57Bl6J mice at 12-16 weeks of age were obtained from Harlan. They were kept in IVC mouse racks at 22°C at a 12h/12h light-dark cycles. They were fed with pellet food and drinking water and beddings were changed every week. All the animal work was performed at European Molecular Biology Laboratory (EMBL), Monterotondo. The mouse procedures were approved by the EMBL Monterotondo Ethical Committee and were in accordance with national and European regulations.

2.1.22 LCA ligation and cell injection

2.1.22.1 Left-anterior Descending Coronary Artery (LCA) ligation

The LCA ligation was performed as previously described [197] and as carried out routinely in Prof Rosenthal's group at the EMBL. Half an hour prior to LCA ligation and cell injection immunosuppressive drug FK506 was administered at 5mg/kg/day concentration. The immunosuppressive was diluted 5% in absolute ethanol and further 95% diluted in Soybean oil (Sigma Life Science #S7381) to get the 5mg/kg/25µl concentration. The immunosuppressive drug administration was performed intraperitonealy with 25µl volume. Animals were anaesthetized with 3% isoflurane and intubated. An incision on the skin and the muscles was made to the left of the sternum. Following this, another incision was made in between the 4th and the 5th ribs to get access to the heart. Pericardium was opened completely and the left-anterior descending coronary artery (LCA) was visualized running from the left atrium towards the apex [197]. LCA was occluded by placing an 8-0 Ethilon Polyamide suture (Ethicon #W2808) 1-2mm from the atrium to achieve an infarction size of 40-50% of the left ventricle. Following permanent occlusion, cell injection was performed at the border zone using a fine micro

injection syringe as described in the following section**.** Occlusion was confirmed immediately after ligation by the pallor of the anterior wall of the left ventricle. However for certainty, echocardiography after a week was used to confirm occlusion. For closure, retractors were removed carefully and the incision between the ribs was closed by using a 6-0 Ethilon Polyamide suture (Ethicon #W1614T). The air in thorax cavity was squeezed out very gently during the closure. Muscle layers were then placed into their original position and the incised skin was closed also with the 6-0 Ethilon Polyamide suture. Mice were then moved to a different ventilator and a heat mat for recovery, where they were monitored carefully until awakening. Following their recovery, they were placed in cages individually.

2.1.22.2 Cell Injection

For cell injection, 10^6 ventricular cardiomyocytes per animal were collected by FACS sorting in 50µl 1XPBS and injected at the border zone of the animal after MI. A microliter syringe was used for delivering cells precisely in only 10µl volume of PBS per injection site (Hamilton Bonadus AG, #PB600-1). FACS selection of GFP positive ventricular myocytes was done in FITC channel. Sorted cells were injected into groups of animals, immediately after MI. This model was used to look at effects of cell transplantation on an acute model of MI. There were altogether three groups of animals. Nine animals received IGF-1Ea transduced cells, 11 animals received Empty vector transduced cells and 15 control animals received only PBS. However, all three groups received LCA ligation and immunosuppressive drug on a daily basis.

2.1.23 Functional analysis by Echocardiography

Following surgery, animals were left to recover for 5 days. At 5 days and 2 months post surgery; echocardiography was performed to analyze function of the cell transplanted injured hearts. For echocardiographic analyses, animals were prepared by shaving their Hemi-thorax region and anaesthetized with 2% Isoflurane. They were placed in a temperature and ECG controlled platform which kept in control the body temperature and heart rate throughout the measurement period. For all the animals the body temperature was kept at 34-38°C and the heart rate at 450-550 beats per minute. To obtain clear images, ultrasound transmission gel was applied at the Hemi-thorax region (Parker Laboratories Inc.) and images were obtained at parasternal short-axis view. Functional analyses were taken from B-Mode and M-Mode measurements. The functional analyses

were done using Vevo 2100 (Visual Sonics). Data analyses were performed using Vivo 2100 software (Visual Sonics). Ejection Fraction (EF), Fractional Area Change variable (FAC) and Fractional Shortening (FS) were taken as parameters for measuring left ventricular function.

2.1.24 Histological analyses

Following functional analyses, animals were sacrificed for both RNA/ protein extraction or for histological analysis. For histological analysis, samples were perfused and fixed with 4% Paraformaldehyde (PFA) and paraffin embedded as follows. PFA fixed samples were left overnight at 4°C. The following day, the fixative was replaced and washed twice 15min/wash with 1X PBS at 4°C. They were then dehydrated at 4°C by treating with 50% Ethanol (2x 30 min), 70% Ethanol (2x 30 min) and 95% Ethanol (1x 30 min). A complete rehydration was performed by treating the samples with absolute Ethanol (2x 1 hour) at room temperature. They were then placed in xylene (3x 30 min) followed by treatment with 1:1 mixture of xylene and wax at 56-58°C for 30 min- 1hour. After the incubation time, the mixture was replaced with wax and again incubated at 56-58°C for 30 min-1hour. The wax was changed once again before leaving it on wax overnight at the same temperature. The next day the samples were oriented in plastic molds and the wax was allowed to solidify at room temperature. When the wax had solidified, samples were cut into 5/10 µm thick sections using a microtome and plated on Polysine microscope slides (VWR-International #631-0107). Slides were left to dry overnight at 45°C overnight.

2.1.24.1 Masson's Tri-chrome Staining

Masson's trichrome staining was employed to selectively stain collagen fibres and muscle cells. The muscle is stained red and the collagen blue. Trichrome staining is generally combined with iron haematoxylin staining to stain the nuclei of cells (Sigma). Masson's Tri-chrome staining was performed to visualize and quantify scar size following infarction. Heart sections were deparaffinized by three 5 minutes washes in Xylene, followed by 3 minute ethanol washes of decreasing percentage (100%, 95%, 80% and 70%) and distilled water in chronological order. The sections were then fixed for 15 min at 56°C in Bouin's solution (Sigma-Aldrich #HT10-1-32). Nuclear staining was achieved by 5 min incubation in Weighert's Iron Haematoxilin solution (Sigma-Aldrich #HT 1079-1Set). Following hematoxylin treatment, slides were washed briefly in running tap water and rinsed in two changes of distilled water. The samples were then treated for 5 min in

Biebrich Scarlet-Acid Fucsin (Sigma-Aldrich #HT 1079-1Set) solution to stain for muscles and washed again thrice with distilled water. Slides were treated with Solution A for 10 min, which was composed of phosphotungstic/ phosphomolybdic acid solution. Sections were then stained for collagen for 5 min in Aniline blue (Sigma-Aldrich #HT 1079-1Set). Immediately after the incubation with aniline solution, slides were transferred to 1% acetic acid solution for 1 minute. They were then rinsed quickly with two changes of distilled water and dehydrated by 2 ethanol washes of increasing percentage (70%, 80%, 95%, and 100%), cleared in Xylene for 3min, and mounted using Aquatex (VWR International #363123S). They were left to dry overnight and afterwards visualized through a light microscope.

Scar size analysis was performed with samples from comparable region of the heart. Papillary muscles were taken as a reference for selecting the sections for the analysis. Scar size was calculated by taking into consideration the epicardial and the endocardial scarred surface as described in [198]. The following formula was used for calculating the scar size.

Scar Size (%) = ((Ratio Epicardial + Ratio Endocardial)/2) *100%

Where, Ratio Epicardial = Scarred Epicardial left ventricular circumference/ Total Epicardial left ventricular circumference

Ratio Endocardial = Scarred Endocardial left ventricular circumference/ Total Endocardial left ventricular circumference

2.1.24.2 Anti-GFP Staining

Anti-GFP staining was performed to trace the transplanted GFP positive ventricular myocytes**.** Paraffin embedded heart sections were deparaffinised in two washes of Xylene and rehydrated by treating with 2X 100 %, 1X 96 %, 1X 80%, 1X 70 % and 1X 50% Ethanol. Each treatment was done for 3 minutes. After the last ethanol treatment, the samples were washed twice with 1x PBS followed by antigen retrieval. Antigen retrieval was performed by treating the slides with Sodium Citrate (10mM, pH 6.0). Slides were dipped in Sodium Citrate solution and boiled in microwavable glass for a total of 5 minutes. Boiling was constantly monitored. The slides were let to cool down for 15-20 minutes. They were then washed once with 1xPBS followed by blocking. Blocking was performed with 5% serum in 1x PBS containing 0.1% Tween for 1 hour. After blocking, the samples were treated with 1:200 diluted, primary rabbit polyclonal anti-GFP antibody

(Abcam #ab290) in blocking solution. Following primary antibody treatment, slides were washed with TBS three times and treated with 1:1000 diluted biotin conjugated anti-rabbit secondary antibody. Streptavidin (BD, Bekton Dickinson) was added into the tissue samples and left to incubate for 30 minutes in humidified chamber. The Streptavidin solution was then decanted and the slides were washed again with TBS three times, 5 minutes each. In the mean time DAB solution (Sigma #D7679) was prepared by adding 1 drop Liquid Chrogen per ml buffer solution. DAB was applied to the samples very quickly and colour change was monitored very carefully. When the samples turned brown (1-2 minutes), DAB was decanted and slides were washed in distilled water for at least 5 minutes. Following this, slides were stained with hematoxylin for 30 seconds and immediately rinsed in running tap water for 5 minutes. The slides were then dehydrated with graded alcohol and finally treated with Xylene. They were then mounted with Permount (Fisher Scientific) and left to dry over night. The next day they were observed through a light microscope for brown stained, transplanted GFP expressing cells. Staining was analysed with a Leica microscope at 10X and 40X magnification.

2.1.24.3 Isolectin-B4 Immunohistological Labelling for Capillary Density Quantification

Isolectin B4 immunohistological labelling was performed to stain the endothelial cells. Isolectin B4 labelling is an excellent tool for quantifying vessel and capillary densities [199]. Paraffin sections were deparaffinised by treating them with Xylene (2X 5min/treatment) and rehydrated with alcohol as mentioned in section *2.1.24.1*. After the last 70% Ethanol, slides were treated with TBS buffer for 5 minutes before proceeding to antigen retrieval. Antigen retrieval was done with Sodium citrate 10mM (with 0.05% Tween) solution for 10-20 minutes boiling in a microwave. After the incubation, they were left to cool down for 20 minutes. The slides were then washed in 3 changes of distilled water for 5 minutes each. They were washed once with TBS for 5 minutes and treated with 3% hydrogen peroxide solution for 10 minutes to block endogenous peroxidases which could give false positive signal when incubated with DAB (3,3`-diaminobenzidine). After this, they were washed with TBS buffer thrice, 5 minutes per wash. Blocking was performed with solution containing TBS/Triton 0.02%, 1mM MgCl2, 1mM CaCl2 and 1mM MnCl2 for 1 hour followed by primary antibody treatment. Each tissue section was then circled with a Pan pen and biotinylated isolectin-B4 antibody (Sigma #L2140) was applied to the samples at 10 µg/ml concentration for 3 hours (or overnight) in humidified chamber. Slides were then washed with TBS three times as

mentioned above. Streptavidin was added into the tissue samples at the recommended amount by the company, BD Bekton Dickinson and left to incubate for 30 minutes in humidified chamber. The Streptavidin solution was then decanted and the slides were washed again with TBS three times 5 minutes each. In the mean time DAB solution was prepared and applied as described in section *2.1.24.2.* Slides were then stained with hematoxylin for 30 seconds and immediately rinsed in running tap water for 5 minutes. They were dehydrated with graded alcohol and finally treated with Xylene. They were then mounted with Permount and left to dry over night. The next day they were observed through a light microscope for brown stained vessels which were counted for analysis.

2.1.24.4 Wheat Germ Agglutinin (WGA) Staining for Assessing Cell Cross-sectional Area

The role of cell transplantation on LV remodelling was analyzed by measuring cardiac cross-sectional area at the infarct border zone**.** A WGA staining was performed to analyse the morphology of cells at the border zone of an infarct after LCA ligation and cell/PBS injection. WGA is a carbohydrate-binding protein of approximately 36 kDa. It selectively recognizes sialic acid and N-acetylglucosaminyl sugar residues that are mainly found on the plasma membrane (Product information Invitrogen, #W6748). Paraffin sections were deparaffinised by treating them with Xylene (3X 5min/treatment) and rehydrated with alcohol as mentioned in section *2.1.24.1.* After the last 70% Ethanol, slides were washed with running tap water for 5 minutes followed by antigen retrieval as described in section *2.1.24.3.* After the antigen retrieval, slides were washed with PBS/0.05%Tween solution for 5 minutes. Slides were then blocked with 3% BSA in PBS/0.05%Tween solution for 30 minutes. Following incubation with blocking solution, 5ug/ml WGA solution, prepared in 1.5% BSA/PBS 0.05% Tween was added to the samples. The samples were incubated with WGA for an hour, protected from light. After the incubation, slides were washed 3X with PBS and treated with DAPI (1:20000) for 5 minutes. The samples were then mounted in Perma-Flour and examined through fluorescent microscope for cell membranes emitting green fluorescence for measuring the cross-sectional areas of each cell.

2.1.25 Statistical analysis:

Statistical analyses were done using either Prism or Excel. For quantitative Real Time PCR, expression of gene was analyzed by normalizing with ribosomal 18S transcripts. To transfer Ct values to linear expression values, the following formula was used:

Relative Expression = 2^ -(ΔCt- Ct(constant))

Where, ΔCt = Ct(gene)-Ct(18S)

And Ct(constant) = Ct of one constant sample across all Cts for the same gene

For experiments with only two groups to compare, Mann-Whitney test (unpaired, 2-tailed) was applied whereas for experiments with more than three groups to compare, one way ANOVA was used (non-parametric, Kruskal-Wallis Test). Values are expressed as mean relative expression or mean fold induction ± standard error of the mean (SEM). $p<0.05$ was considered statistically significant and was given *, $p< 0.01$ ** and $p< 0.001$ ***.

CHAPTER 3

3.1 SECTION I: CREATING TOOLS FOR STABLE TRANSDUCTION OF IGF-1Ea INTO PLURIPOTENT P19CL6 CELLS AND TETRACYCLINE REGULATED EXPRESSION OF THE GENE

3.1.1 INTRODUCTION

The study aimed at a tetracycline controlled delivery of the IGF-1Ea gene through a cell-based therapy approach. The gene of interest was stably transduced into P19Cl6-MLC2v-GFP cells via a lentiviral system. Lentiviral vectors are at the forefront of gene delivery systems for research applications. This is mainly due to their ability to transduce dividing and non-dividing cells, to insert large genetic constructs into the host chromatin and to sustain stable long-term transgene expression [200]. A Gateway system was used to directionally clone rat IGF-1Ea cDNA into a lentiviral vector Lenti4/TO/V5-DEST at a specific site. Following cloning of the gene into the expression vector, restriction digest and sequencing analyses were carried out to confirm integrity of the vector and the gene, as well as to verify that cloning occurred at the correct site and orientation. A true expression clone with IGF-1Ea would be Chloramphenicol sensitive and Ampicilin- and Zeocin-resistant, therefore an antibiotic selection was performed to exclude any false positive clones. Prior to transduction of the viral vectors into HT1080 and P19Cl6 cells, an antibiotic sensitivity experiment was carried out to determine the minimum concentration of antibiotic required to select the transduced cells within 10-14 days of antibiotic treatment. The antibiotic sensitivity assessment was essential for a reliable selection of positively transduced cells as well as for obtaining an idea on toxicity of antibiotics, which could potentially kill even the positively transduced cells if used in excess amount. After determining the optimum antibiotic dose for positive selection, viral titre was investigated. Determination of viral titre was crucial as this study aimed at controlled expression of IGF-1Ea through tetracycline treatment, which is dependant on the TR-vector. Therefore, for transduction, it was imperative to obtain an optimal ratio of the Lenti4/TO/V5-DEST-IGF-1Ea and Lenti6/TR viruses that would deliver a tight regulation of the gene expression, generate reproducible expression and control the copy number of lentivirus integration into the genome. Experiments were performed to achieve this optimal ratio. Following these assessments, the viral vectors were transduced first into HT1080 human fibrosarcoma cells, as recommended by Invitrogen, to test whether the system was functional, followed by the P19Cl6-MLC2v-GFP cells. Control cells were transduced with

an empty vector consisting of only the Lenti4/TO/V5-DEST backbone (Lenti4/TO/V5-DEST-Empty) and Lenti6/TR. Gene expression was then induced by tetracycline treatment.

3.1.2 RESULTS

3.1.2.1 Cloning and Sequencing of IGF-1Ea

Restriction digest and sequencing analyses of IGF-1Ea lentiviral vector confirmed that IGF-1Ea was cloned into the vector in the correct site and orientation. The integrity of both the vector and the gene were conserved. Following these analyses, viruses were generated and their titres determined.

3.1.2.2 Determining Antibiotic Sensitivity

After successful cloning, Lenti4/TO/V5-DEST-IGF-1Ea, Lenti4/TO/V5-DEST (empty) and Lenti6/TR viruses were generated. Before proceeding to transduction of the viruses into P19Cl6 cells, an antibiotic sensitivity assessment was performed. The analysis was performed on HT1080 cells, provided by the supplier as a control cell, and P19Cl6 cells. The antibiotic sensitivity test examined how the cells responded to the antibiotics, Blasticidin and Zoecin, which would be used for their selection following transduction of the viruses. The responsiveness of HT1080 and P19Cl6 cells to the two antibiotics were different. The assessment on HT1080 cells revealed that 500 µg/ml of Zeocin and 4 µg/ml of Blasticidin were enough to induce death of untransduced HT1080 cells by 14 and 10 days of antibiotic treatment respectively. These amounts of antibiotics were then used to select for positively transduced cells in further experiments utilizing HT1080 cells. The P19Cl6 cells were however more sensitive to the antibiotics. Cell death of untransduced P19Cl6 cells could be induced with 200 µg/ml Zeocin and 4 µg/ml Blasticidin within 10-14 days of antibiotic treatment. These concentrations of antibiotics were then used for further experiments with P19Cl6 cells.

For both the cell types, the Zeocin method of killing was very different from that of Blasticidin. The Zeocin-killed cells increased in size with empty vesicles in the cytoplasm (Figure 7). In addition, the cells did not detach from the plates for a very long time and exhibited abnormal shape. Blasticidin treated cells on the other hand became round and detached from the plates immediately when they died (Figure 8).

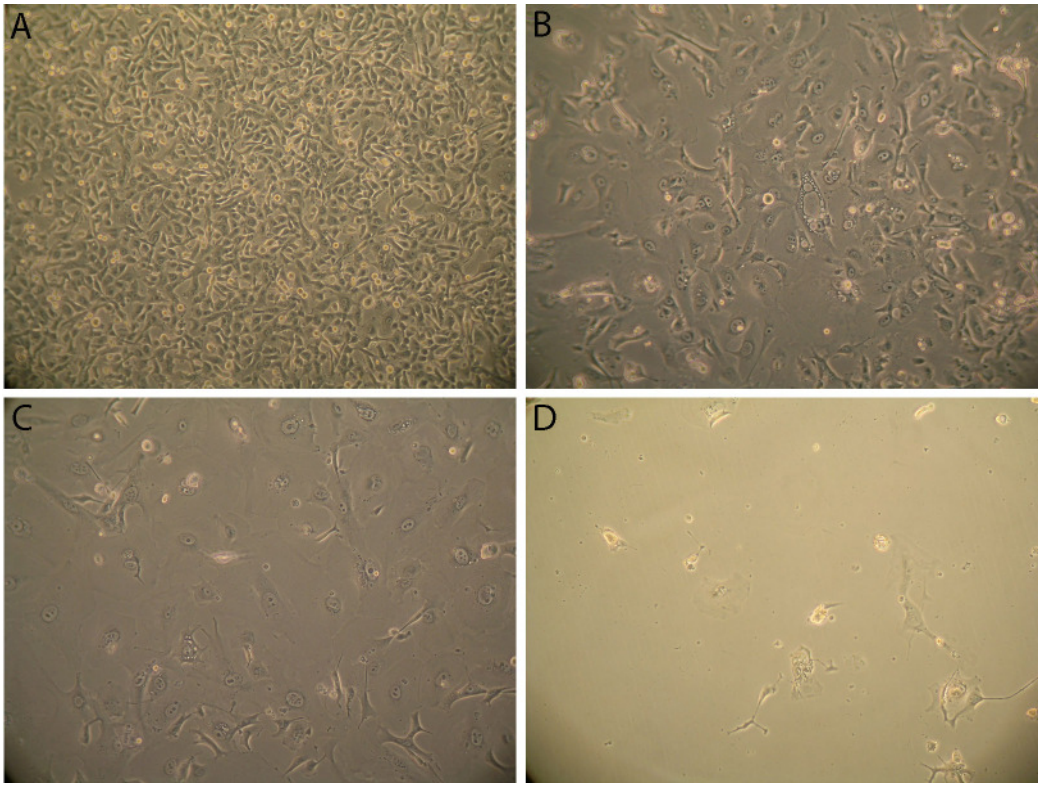

Figure 7. Antibiotic Sensitivity Assessment of HT1080 Cells treated with Zeocin. A) Control without antibiotic treatment B) Zeocin 50 µg/ml C) Zeocin 100 µg/ml D) Zeocin 500 µg/ml. Day 14 following antibiotic treatment. Zeocin killed cells showed vast increase in size, abnormal cell shape and large empty vesicles in the cytoplasm.

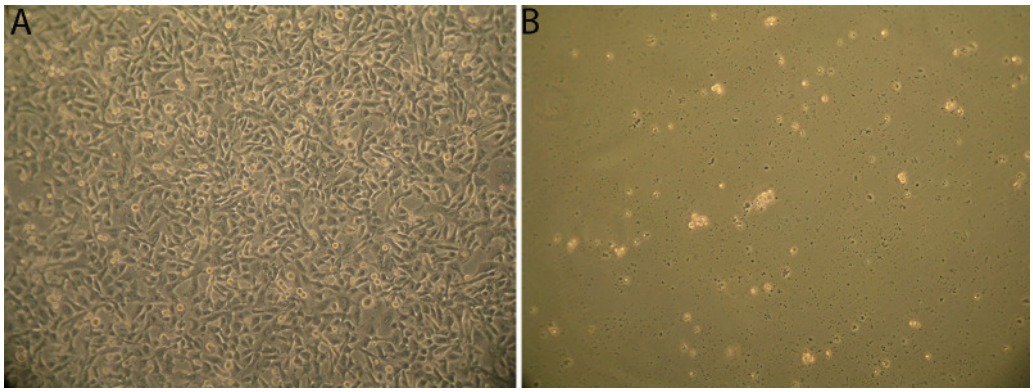

Figure 8. Antibiotic Sensitivity Assessment of HT1080 cells Treated with Blasticidin. A) Control without antibiotic treatment B) Blasticidin 4 µg/ml. Day 10 following antibiotic treatment. Blasticidin killed cells rounded up and detached from plates.

3.1.2.3 Viral Titre Determination

Viral titres for all the three viruses were determined by an average number of crystal violet positive colonies in plates of transduced HT1080 cells, which were treated with lentiviral supernatants at 10 fold serial dilutions. The titres were determined as transduction units

per ml (TU/ml). Lenti6/TR, Lenti4/TO/V5-DEST-empty and Lenti4/TO/V5-DEST-IGF-1Ea viral titres were 1.17*10^6 TU/ml, 1.0*10^6 and 3*10^5 respectively (Figure 9).

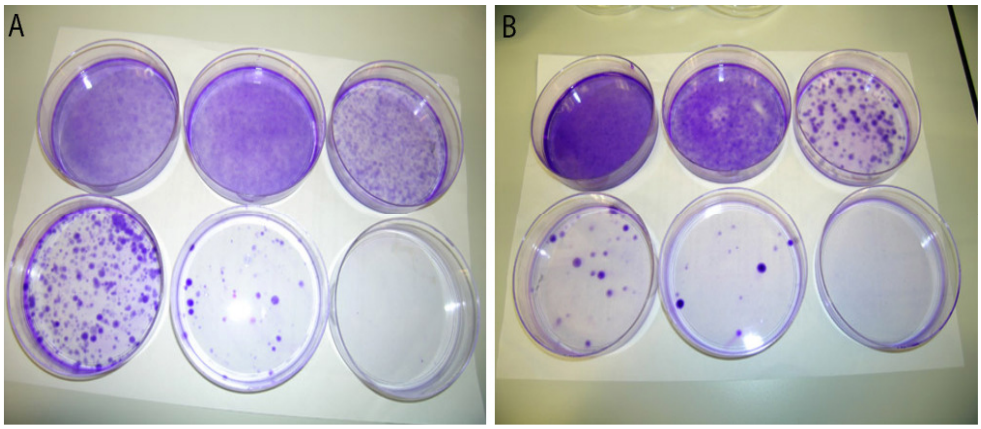

Figure 9. Determining Viral Titre. A) TR virus B) IGF-1Ea Virus. Top panels from left to right: Virus dilutions 10^-1, 10^-2, 10^-3. Bottom Panels from left to right: Virus dilutions 10^-4, 10^-5 and Mock without transduction.

3.1.2.4 Tetracycline Regulated Expression of IGF-1Ea

To test whether the tetracycline system employed in this study was effective, HT1080 cells were transduced with the Lenti6/TR and Lenti4/TO/V5-DEST-IGF-1Ea vectors. Real-time PCR analysis was performed to quantify the expression of IGF-1Ea. The analysis revealed that tetracycline treatment induced regulated expression of *IGF-1Ea* in the cells treated with tetracycline compared to control cells (4.5+/-0.13 *vs.* 0.60+/-0.03), demonstrating that the TetOn system was effective in the HT1080 cells (Figure 10).

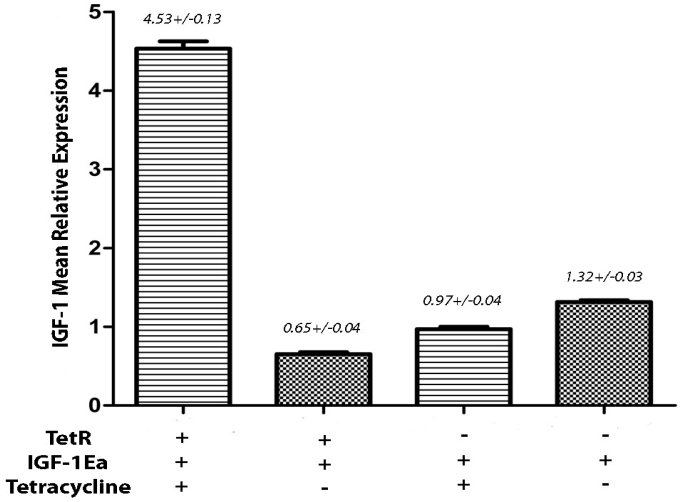

Figure 10. Tetracycline regulated IGF-1Ea expression on HT1080 cells. HT1080 cells showed tetracycline regulated expression of IGF-1Ea transcript (4.5+/-0.13 vs. 0.60+/-0.03 with or without tetracycline respectively). IGF-1Ea transcript expression was induced 24 hour post tetracycline treatment. 18S rRNA was used as internal reference gene. Values are presented as Mean +/- SEM. The values are average of 2 independent experiments.

However, experiments on P19Cl6 cells revealed that tetracycline treatment was ineffective in regulating expression of IGF-1Ea in this cell type. There was a very high constitutive expression of the gene (352.98+/-6.16 vs. 320.38+/-8.34), for both the tetracycline treated and untreated cells (Figure 11).

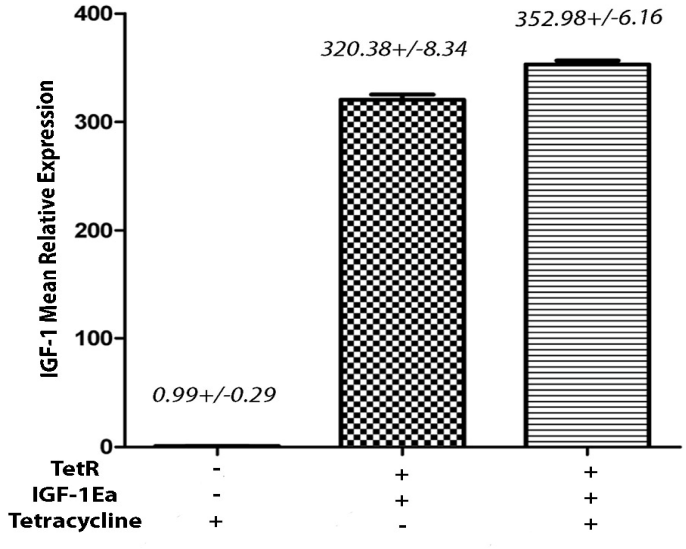

Figure 11. Loss of tetracycline regulated expression of IGF-1Ea in transduced P19Cl6 cells. Tetracycline treatment had no effect on regulation of IGF-1Ea transcript expression. Cells treated with/without tetracycline showed similar expression levels of IGF-1Ea transcript (352.98+/-6.16 vs. 320.38+/-8.34 with or without tetracycline respectively). 18S rRNA was used as internal reference gene. The results are mean relative expression with respect to the untransduced P19Cl6 cells. Values are presented as Mean +/- SEM.

As P19Cl6 cells showed no tetracycline regulated IGF-1Ea gene expression, insufficient repressor activity might be the cause. The integration event of lentivirus into the genome is random therefore depending upon the influence of surrounding genomic sequence at the site of integration and varying amount of TR virus transduction, different levels of Tet repressor expression might be obtained. Tetracycline regulated IGF-1Ea gene expression is controlled by the availability of the TR protein in the selected cells. Therefore, 18 TR and IGF-1Ea virus transduced P19Cl6 clones (named clones 1-18) were picked and a number of them analyzed for IGF-1Ea expression. None of the analyzed clones numbered 5, 6, 11, 12, 15 and 16 showed Tet repressor activity that was sufficient to repress IGF-1Ea expression in the absence of tetracycline. All the clones expressed in a constitutive manner high levels of IGF-1Ea transcripts compared to the untransduced P19Cl6 cells (ranging from 200-800 fold) (Figure 12).

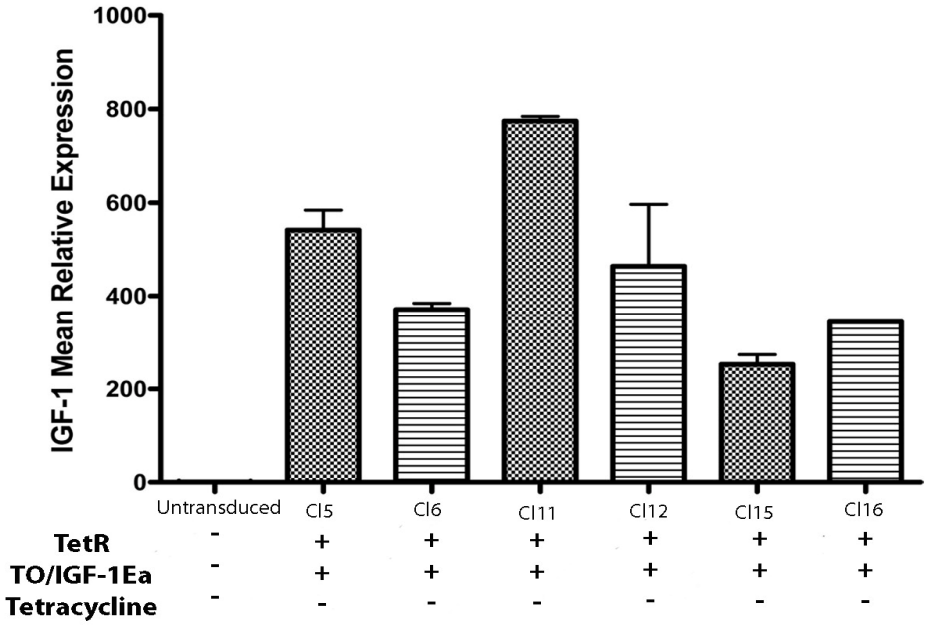

Figure 12. Constitutive IGF-1Ea expression. Stably transduced P19Cl6-IGF-1Ea/TR clones contitutively expressed IGF-1Ea transcripts. Tet repression was not sufficient to repress IGF-1Ea expression in the absence of tetracycline. 18S rRNA was used as internal reference gene for normalization. Values are Mean +/- SEM.

3.1.3 DISCUSSION

The Lenti4/TO/V5-DEST-IGF-1Ea Lenti4/TO/V5-DEST-empty and Lenti6/TR viruses were produced and transduced successfully into mammalian cell lines. When transduced into HT1080 cells, the expression of the IGF-1Ea gene occurred in a tetracycline-regulated manner. In the absence of tetracycline, cells that were transduced with both Lenti4/TO/V5-DEST-IGF-1Ea and Lenti4/TR showed minimal basal expression of the gene, suggesting effective repression of the transgene by TetR. However, in P19Cl6 cells although the transduction conditions were maintained identical to the one used for HT1080 cells, the result obtained was completely different. The transduced P19Cl6 cells showed a very high constitutive IGF-1Ea expression, suggesting that Tet repression in P19Cl6 cells was not effective as in the HT1080 cells. This could arise either from lack of or insufficient Tet Repressor activity in this cell type. The integration event of lentivirus into the genome is random and depending upon the influence of surrounding genomic sequence at the site of integration, varying levels of Tet repressor expression might be obtained. Although several P19Cl6 clones were further analysed, the Tet repressor activity in the absence of tetracycline was insufficient to repress IGF-1Ea expression in all the analyzed clones. A possible explanation for this observation could be that P19Cl6 cells

have an endogenous mechanism, such as a molecule that resembles tetracycline, which is capable of binding to the Tet repressor molecule. It has been recently reported that Gata transcription factors, which are expressed in embryonic and many adult cell types, compete with TR in binding the tetracycline operator repeats (TO) present on the lentiviral vectors. The Gata motif is located within the central core of the tetO, therefore Gata transcription factors have the potential to compete with TetR binding. The endogenous Gata factors may therefore influence the degree of gene regulation by the tetracycline system between different cell types [201]. Future analyses could be conducted at examining the Gata factor expression in HT1080 and the P19Cl6 cells to understand if these factors conferred this outcome. In addition, it would be interesting to investigate if the tetracycline system works on other pluripotent cells and if the failure of the system is unique to P19Cl6 cells.

Although a controlled expression of *IGF-1Ea* could not be achieved on P19Cl6 cells, the objective to stably transduce P19Cl6 with IGF-1Ea vector was achieved. Moreover, the *IGF-1Ea* expression by the transduced cells was highly efficient, making it possible to utilize these cells for analyzing *IGF-1Ea* signaling. Most importantly, the *IGF-1Ea* transduced cells could be utilized for *in vivo* cell transplantation, which was the prime objective of this study, to analyse the effects of *IGF-1Ea* over-expression on donor cell engraftment and its role on modulating function and morphology of infarcted hearts.

3.2 SECTION II: EFFECTS OF IGF-1Ea TRANSDUCTION AND CONSTITUTIVE EXPRESSION ON PROPERTIES OF P19CL6 CELLS BEFORE AND AFTER DIFFERENTIATION

3.2.1 INTRODUCTION

P19Cl6 cells transduced with the (i) Lenti4/TO/V5-DEST-IGF-1Ea Lenti6/TR and (ii) Lenti4/TO/V5-DEST-empty Lenti6/TR viruses were cultured and expanded. Following the examination of *IGF-1Ea* expression, the cells were analysed for their pluripotent status by Oct3-4 staining before proceeding to their differentiation. Oct3-4 is a POU-domain transcription factor encoded by the POU5F1 gene that lies in the centre of a gene regulatory network which maintains pluripotency and self renewal in embryonic stem cells. An alteration in the expression of Oct3-4 leads to loss of pluripotency and initiation of differentiation [202]. IGF-1 has been reported to play a role in proliferation and differentiation of skeletal and neuronal cells [131, 203, 204] and induction of differentiation of adipose-derived mesenchymal stem cells into chondrocytes-like cells [205]. Moreover, a study on the role of IGF-1Ea-mediated muscle regeneration following injury, Musaro et al. reported that expression of IGF-1Ea (mIGF-1) improved muscle regeneration by increasing the Sca-1^+ bone marrow stem cell population at the injury site and by promoting their differentiation towards a myogenic lineage [131]. Likewise, cell culture experiments by An et al. revealed that the IGF-1Ea isoform promoted myogenic differentiation and cell hypertrophy, resulting in enlarged myofibers [206].

A study on embryonic stem cells by Klinz et al. [207] showed a role of phosphatidylinositol-3-kinase (PI3-kinase) on development of embryonic cardiomyocytes. Treating early Embryoid Bodies (EBs) with an inhibitor of PI3-kinase, LY294002, blocked the growth and induced apoptosis as well as necrosis of D3 ES cells. Treatment of the EBs in the later stage from day 3 to day 7 with the inhibitor on the other hand resulted in a massive loss of alpha-actinin-positive cardiomyocytes after plating the EBs for additional 7 days. In addition, they observed a strong decrease in the number of beating cardiomyocytes in the EBs, whereas the formation of endothelial cells was unaffected, suggesting that the PI3-kinase inhibitor was cardiomyocyte development specific. The role of PI3-kinase on cardiomyocyte development was later supported by Sauer et al. [208] who observed that treatment of EBs with LY294002 and wortmannin abolished cardiac

commitment and down-regulated Reactive Oxygen Species (ROS). They suggested that cardiotypic development might be regulated by ROS and PI3-kinase might be involved in regulating intracellular redox state [208]. As PI3-kinase is one of the downstream molecules involved in IGF-1 mediated signaling (refer to section 1.2.2.4 for IGF-1 signaling), it is possible that IGF-1 plays a role in cardiac commitment and development. As the Lenti4/TO/V5-DEST-IGF-1Ea Lenti6/TR transduced P19Cl6 cells produced IGF-1Ea in a constitutive manner, it was vital to examine proliferative and differentiation characteristics of these cells.

A study by Laflamme et al. showed that cardiomyocytes derived from human ES cells proliferate via IGF/PI3K/Akt pathway [209]. Therefore, to check if IGF-1Ea transduction and constitutive expression caused changes in cell cycle of the transduced P19Cl6, a cell cycle analysis was performed by propidium iodide (PI) staining. Cell cycle analysis can be achieved by labelling the nuclei of cells in suspension with fluorescent dye like the PI and then analyzing the fluorescence properties of each cell in the population. PI intercalates between the bases of the DNA by binding to the nucleotide pair of guanine and cytosine with a stoichiometry of one dye per 4–5 base pairs of DNA [195, 196]. Cells at quiescent (Go) and G1 stages of the cell cycle will have one copy of DNA and will therefore have 1X fluorescence intensity. Cells in G2/M phase of the cell cycle will have two copies of DNA (just before mitosis has occurred) and accordingly will have 2X intensity. The cells at S phase, which refers to the synthesis phase as the cells are synthesizing new strands of DNA, will have fluorescence values between the 1X and 2X populations [196]. Depending on the amount of DNA present at a particular stage of the cell cycle, different amount of PI molecules bind with DNA, giving rise to emission of specific fluorescence intensity, enabling analysis of the cell cycle.

Oct3-4 and PI staining were performed with both the IGF-1Ea and empty vector transduced cells. These analyses were followed by cell differentiation, which was performed by supplementing the culture media with 1% DMSO and forming embryoid bodies (EBs). Upon differentiation into cardiogenic lineage, the differentiated cells were microscopically analysed for occurrence of GFP positive cardiomyocyte clusters. Also, a quantitative Real Time PCR was carried out with the differentiated cells to verify and quantify the expression of cardiac specific markers namely, Nkx2-5, MLC2v and Gata4.

Following analysis of the cardiac marker expression and the pluripotency features of the transduced cells, the efficiency of differentiation into ventricular myocytes was determined for both IGF-1Ea and empty vector transduced cells using FACS analysis. Percentage of GFP positive ventricular cells derived from the *IGF-1Ea* transduced cells were compared with the empty vector transduced P19Cl6 cells to determine if *IGF-1Ea* constitutive expression led to enhanced cardiac lineage differentiation.

In addition to the qualitative and quantitative analyses on expression of cardiac markers, differentiated cells were stained for sarcomeric alpha-actinin (Sigma, Cat# A7811) to investigate the organization of the sarcomeric apparatus that is central for contractile function. Alpha-actinin is an actin-binding protein present in both muscle and non-muscle cells [210]. However, the sarcomeric alpha-actinin is specific for only alpha skeletal and alpha cardiac muscle actinins. It stains the Z lines in the muscles [211]. For a successful cell therapy, upon delivery into infarcted tissue, the cells for transplantation must improve overall mechanical functions. Therefore, expression of structural protein responsible for mechanical function such as the sarcomeric alpha-actinin is vital. Furthermore, an additional IGF-1Ea transcript expression was examined by quantitative real time PCR (qRT-PCR) to ensure that the transgene over-expression was not lost during differentiation.

From all the IGF-1Ea and empty vector transduced P19Cl6 clones (described in Section I), only clone 6 was chosen for the following analyses as some of the other clones failed to form EBs that seemed important for their efficient cardiac lineage differentiation. The failure in EB formation could be resulting from the site of integration of the viral vector or due to the level of *IGF-1Ea* expression.

3.2.2 RESULTS

3.2.2.1 Staining for Pluripotency Marker Oct3-4

P19Cl6 cells transduced with IGF-1Ea- or empty-vectors were cultured for a day and stained for Oct3-4, to verify that the pluripotency was retained following transduction of the viral vectors. Both the cell types stained positive for Oct3-4 antibody. Oct3-4 being a transcription factor, staining was observed mainly localized in the nucleus and moderately in the cytoplasm marked by the red staining in Panels A and C in the figure below (Figure

13). The staining was specific for Oct3-4, which was verified by absence of staining in the control cells in Panels B and D. Control cells were treated with only the secondary antibody. No difference was observed in Oct3-4 expression and localization between the IGF-1Ea- and the empty-vector transduced cells. The analysis illustrated that transduction of viral vectors and the IGF-1Ea gene maintained undifferentiated state of P19Cl6 cells.

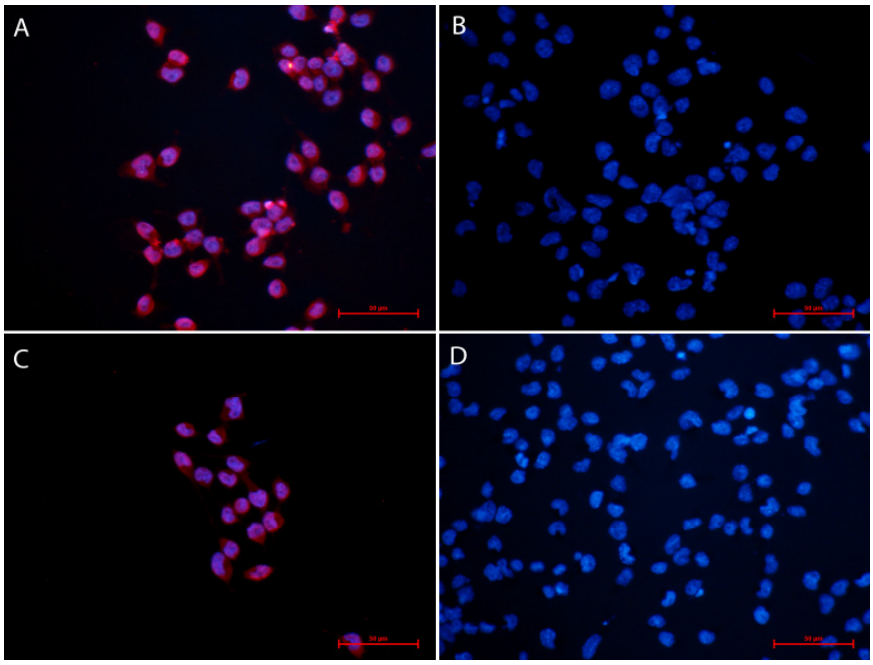

Figure 13. Staining for Pluripotency Marker Oct3-4. (A) empty-cells (B) Antibody control for empty-cells (C) IGF-1Ea-cells D) Antibody control for IGF-1Ea-cells. Nuclei were stained with DAPI. Scale bars are 50µm.

3.2.2.2 Cell cycle analysis by Propidium Iodide (PI) Staining

PI staining was conducted to understand the cell cycle characteristics of IGF-1Ea- and empty-vectors transduced cells. Clone 6 P19Cl6 cells were fixed with 70% ethanol, permeabilized and stained with 50 µg/mL Propidium Iodide solution followed by FACS analysis. The analysis resulted in a histogram consisting of three populations: two Gaussian curves for Go/G1 and G2/M phases (1X and 2X peaks) and the S-phase population. Before obtaining the final results, any doublet and cell debris were excluded from the analysis. The three cell populations obtained in the histogram overlapped each other, therefore a modeling program (Flow Jo) was utilized to seclude the individual populations and to assign percentage values to each population. Clone 6 P19Cl6 transduced with IGF-1Ea- and the empty-vector showed similar percentages of cells in their S phases (12.8% vs. 15.1%), indicating similar proliferation profiles between the two cell types. The analysis showed that viral transduction as well as transduction of IGF-1Ea

gene did not alter proliferation of the P19Cl6 cells. Figure below shows the FACS plots for the IGF-1Ea and empty transduced clone 6 P19Cl6 cells (Figure 14).

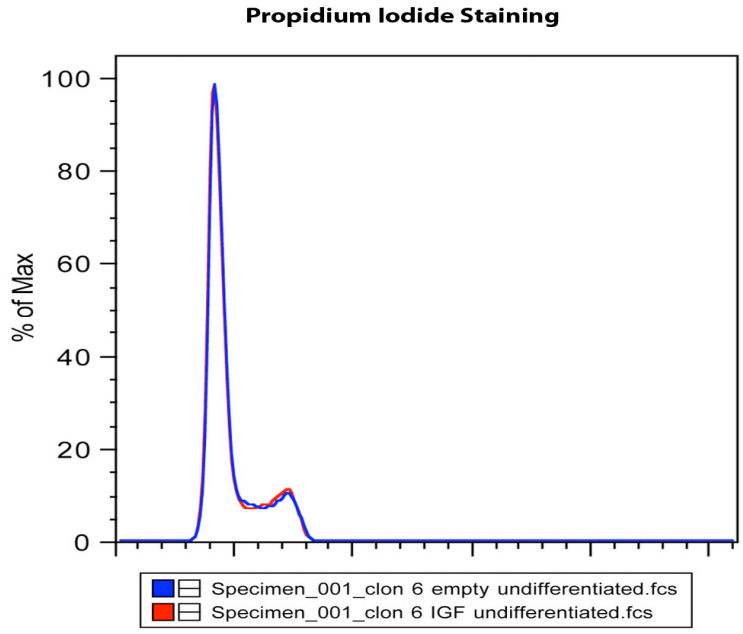

Figure 14. Cell Cycle analysis by Propidium Iodide Staining. Cell Cycle analysis of undifferentiated Clone 6 P19Cl6 cells, transduced with either empty (Blue) or IGF-1Ea (Red) viral vectors. Percentage of cells in S phase for Clone 6 for both IGF-1Ea and the empty vector transduced were similar (12.8 vs. 15.1). PI was used at 50 µg/mL concentration, samples were treated with RNAase A to exclude double stranded RNA from analysis. FACS analysis was performed at PE-A channel and results obtained using Flow Jo. The X-axis represents percentage of cells and y-axis, fluorescence intensity.

3.2.2.3 Differentiation of P19Cl6 Cells into Cardiomyocytes

Clone 6 P19Cl6 cells transduced with both IGF-1Ea and empty vectors were successfully differentiated into spontaneously beating cardiomyocytes. The differentiation into GFP positive ventricular myocytes was very efficient, which was demonstrated by appearance of abundant GFP positive clusters and quantitatively revealed by the FACS analysis in Section 3.2.2.4. The GFP positive cells appeared in clusters of different morphologies and exhibited spontaneous beating. The spontaneously beating colonies appeared in cultures from day 9 after induction of differentiation. The beating was recorded up to day 21, after which the cultures were terminated for molecular analyses. From the day of their differentiation, the intensity of GFP expressed by the clusters improved gradually up to 15-16 days after which the expression became stabilized (data not shown). The figure below (Figure 15) shows the differentiated clone 6 P19Cl6 cells.

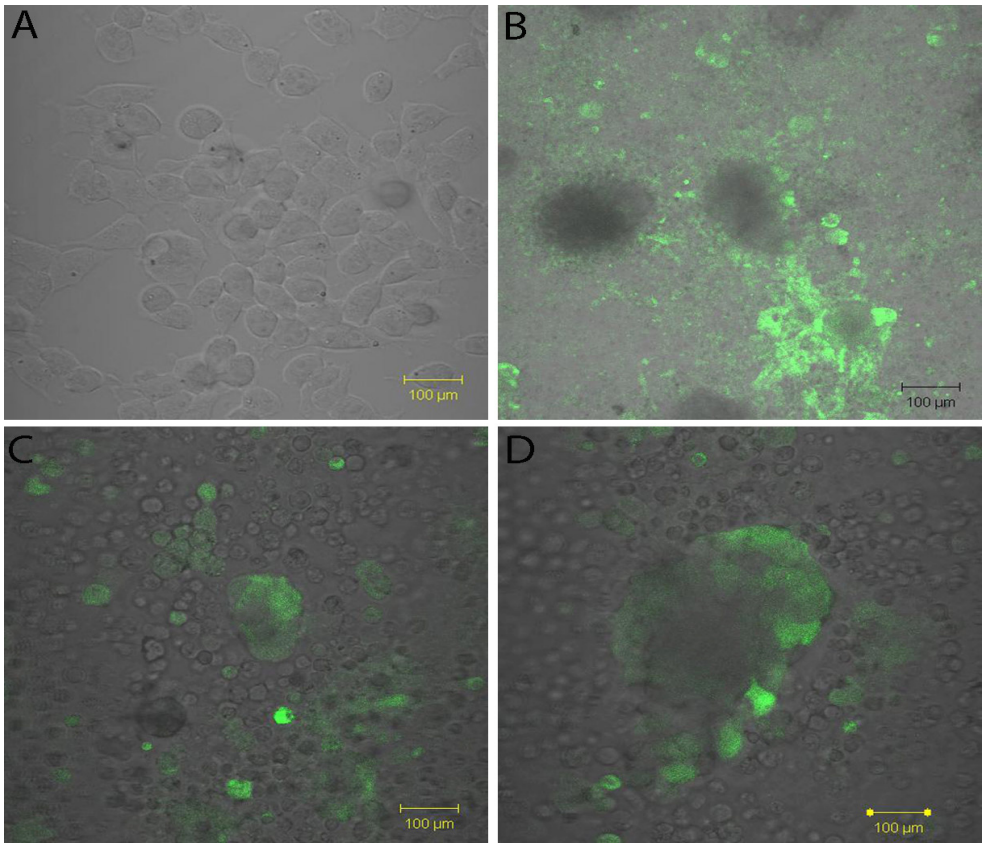

Figure 15. Representative Confocal Images of Differentiated P19Cl6-MLC2v-GFP Cells. (A) Undifferentiated, (B) (C) (D) Differentiated. The GFP positive spontaneously beating cluster of cells appeared in different morphologies for both IGF-1Ea and empty vector transduced cells. The images above are representative images from clone 6 P19Cl6 IGF-1Ea-cells showing morphologically different clusters. Images were taken at day 16 after differentiation. Scale bars are 100 µm.

Furthermore, analysis of the expression of cardiac specific protein was performed using qRT-PCR. Nkx2-5 (a cardiac transcription factor), MLC2v (a cardiac structural protein) and Gata4 (a mesodermal transcription factor) expressions were analyzed. The analyses were performed as relative expression compared to the undifferentiated control P19Cl6 cells. Nkx2-5 and MLC2v transcripts increased in IGF-1Ea vector transduced, differentiated P19Cl6 cells (Figure 16) compared to control differentiated cells. Gata4 expression however seemed to be higher for control differentiated P19Cl6 cells than IGF-1Ea transduced P19Cl6 cells. At undifferentiated state, the IGF-1Ea transduced cells expressed similar levels of Nkx2-5, MLC2v and Gata4 to the control cells. The analysis further proved differentiation of the cells into cardiomyocytes. The expression levels of both Nkx2-5 and MLC2v were higher in IGF-1Ea transduced cells, suggesting that IGF-1Ea together with DMSO could trigger differentiation towards cardiac lineage.

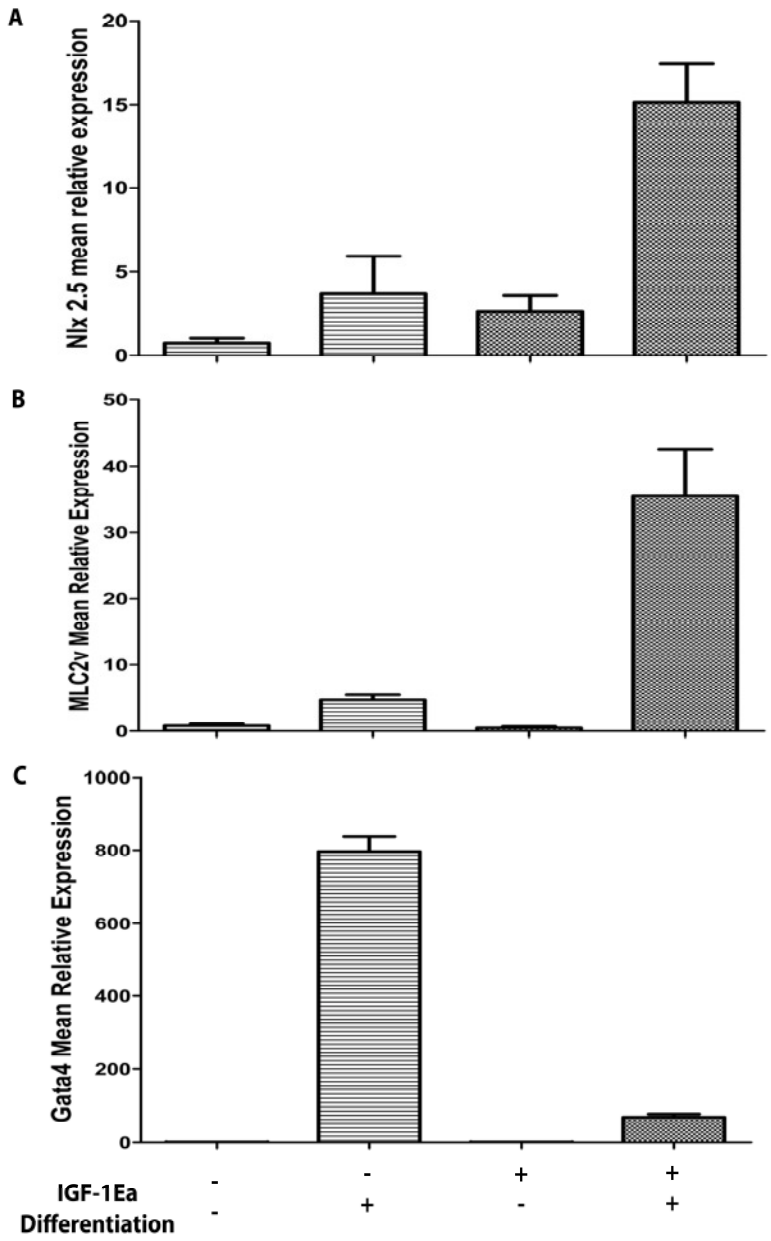

Figure 16. A quantitative Real Time PCR analysis for cardiac specific marker expression by IGF-1Ea untransduced and IGF-1Ea transduced P19Cl6 cells with or without differentiation. A) Nkx2-5 expression B) MLC2v expression C) Gata4 expression. Differentiation led to higher expression of Nkx2-5, MLC2v and Gata4 compared to undifferentiated cells. Upon differentiation, IGF-1Ea transduced cells expressed higher levels of Nkx2-5 and MLC2v compared to the IGF-1Ea untransduced differentiated cells. Gata4 expression was higher for IGF-1Ea untransduced differentiated cells compared to IGF-1Ea transduced differentiated cells. RNA was obtained on day 22 following differentiation of cells. 18S ribosomal RNA was used as an internal reference gene.

3.2.2.4 FACS Analysis to Quantify GFP Positive Ventricular Cardiomyocytes

Clone 6 P19Cl6-IGF-1Ea or clone 6 empty vector transduced cells were differentiated and FACS analyzed at day 19 to determine their efficiency of differentiation into ventricular cardiac myocytes. Ventricular cardiac myocytes were marked by GFP expression, which was under the control of ventricular cardiomyocyte-specific marker MLC2v. The GFP

expression was utilized as a tool to quantify the ventricular myocytes. FACS analyses showed remarkably high efficiency of differentiation into ventricular myocytes for both IGF-1Ea and empty vector transduced P19Cl6 cells (29.60+/- 4.87 vs. 35.16+/- 6.66 respectively, where n=5). There was however no significant difference in the amount of GFP positive cells between the IGF-1Ea and empty vector transduced groups, p= 0.55. In the figures below (Figure 17), panels (A) and (B) show FACS plots for Clone 6 P19Cl6 IGF-1Ea transduced cells with or without differentiation. In panels (A) and (B), population 5 (P5) represents the parent population from where the viable cell population (P1), the single cell population (P3) and GFP positive population (P2) were obtained by gating out the dead cells, the doublets and the non-GFP positive cells respectively. The GFP positive cells (P2) were sorted for cell transplantation. Panel (C) shows quantitative measurement of the GFP positive ventricular cardiomyocytes obtained from differentiation of clone 6 P19Cl6 IGF-1Ea or empty vector transduced cells. The analysis revealed no significant difference in the amount of GFP positive ventricular cardiac myocytes between the IGF-1Ea and empty vector transduced cells suggesting that IGF-1Ea gene over-expression did not trigger ventricular cardiac lineage differentiation. Nevertheless, the very high efficiency of differentiation into ventricular cardiomyocytes was optimal for obtaining large quantities of cells for cell transplantation experiments that followed.

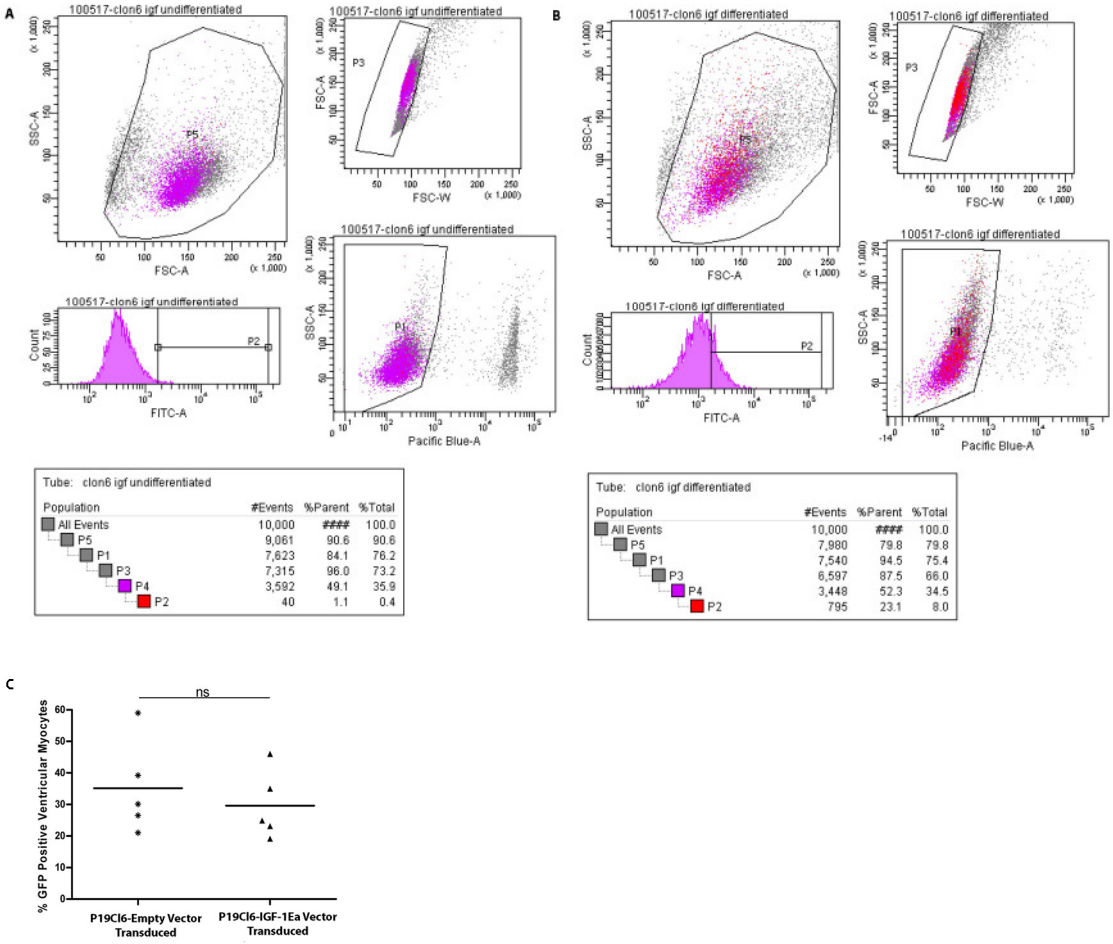

Figure 17. Quantification of GFP Positive Ventricular Myocytes by FACS Analysis. Representative FACS plots for A) Undifferentiated Clone 6 P19Cl6 IGF-1Ea-cells B) Differentiated Clone 6 P19Cl6 IGF-1Ea-cells. Panels A and B show gating of the GFP positive population for sorting. Populations P2 in the two cell types represent the GFP positive cells. The tables show the percentage of GFP positive P2 population with respect to the parent population. P5 are the parent population from which P1, P2 and P3 were gated out. P3 represent the single cells, P1 are the cells that are viable. C) Percentage of GFP positive cells derived from IGF-1Ea-cells versus empty-cells (29.20+/- 3.82 vs. 35.12+/- 5.91) respectively, where n=5, p = 0.55. FACS analysis performed on day 19 after differentiation. Values are Mean +/- SEM.

3.2.2.5 Sarcomeric alpha-actinin Staining

As the quantitative FACS analysis on GFP positive cells revealed no difference in the amount of GFP positive cells even though the molecular analyses on Nkx2-5 and MLC2v showed higher transcript expression for IGF-1 transduced cells, a protein level analysis was performed to visualize structural protein alpha-actinin in the differentiated cardiomyocytes. Analysis of cardiomyocyte specific sarcomeric alpha-actinin was necessary to understand if (i) cardiomyocytes resulting from IGF-1Ea transduced cells

possessed higher amount of structural protein than the control cells and (ii) whether the cardiomyocytes were structurally mature and possessed structural machinery for mechanical function. Nineteen days after induction of differentiation, IGF-1Ea and empty-vector transduced cell-derived cardiomyocytes were stained for sarcomeric alpha-actinin and analyzed using a confocal microscope. As a positive control, neonatal rat cardiomyocytes, maintained in culture for five days, were used. The negative control was treated with the secondary antibody only. All the samples, the positive control neonatal cardiomyocytes, the IGF-1Ea-cell-derived cardiomyocytes and the empty-vector cell-derived cardiomyocytes stained positive for alpha-actinin. The Z lines in the muscles were clearly stained by the antibody marked by red striations, seen in Panels A, C and D. The secondary antibody was specific for primary alpha-actinin antibody as shown by the lack of staining in the negative control that received only the secondary antibody (Panel B, (Figure 18). The alpha-actinin positive clusters were positive also for GFP indicating that the clusters were ventricular cardiomyocytes. The analysis illustrated that cardiomyocytes obtained from differentiation of both IGF-1Ea and empty vector transduced P19Cl6 cells expressed cardiac structural protein alpha-actinin that is necessary for their mechanical function and vital for cell therapy approach.

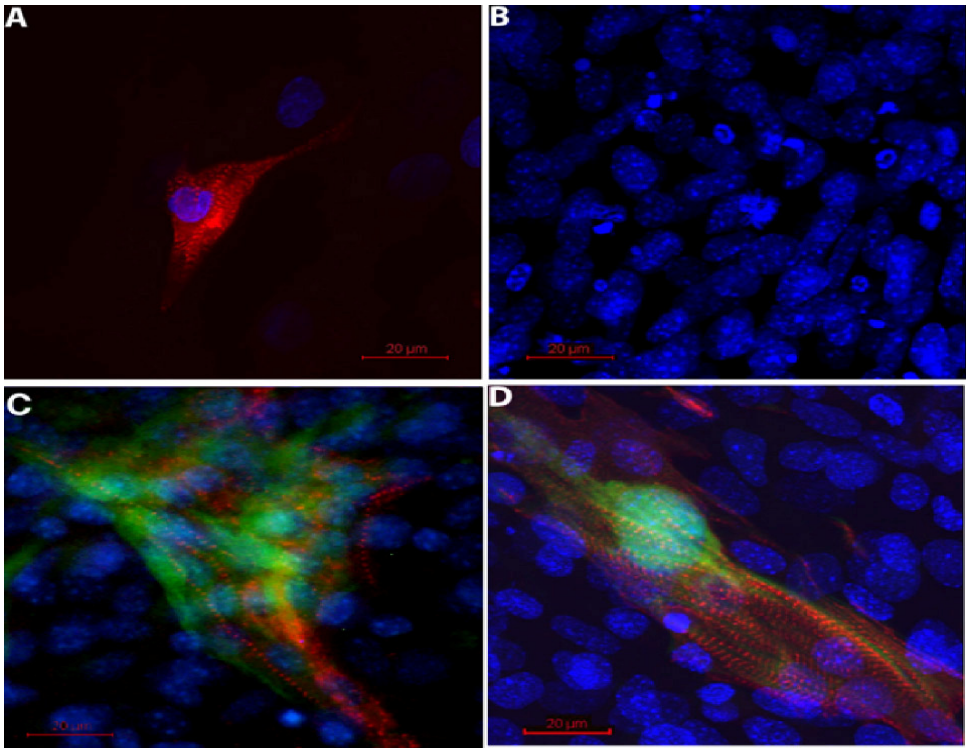

Figure 18. Sarcomeric alpha-actinin Staining. Differentiated cells were stained for sarcomeric alpha actinin to confirm presence of the cardiac structural protein and investigate its organization. Panel (A) is a representative image of the positive control neonatal cardiac myocyte, maintained 5 days in culture. Panel (B) is a representative image of the negative control that received only the secondary antibody. Panel (C) shows a cluster of empty-cells derived cardiomyocyte cluster and Panel (D) represents IGF-1Ea-cells derived cardiomyocyte cluster. GFP expression verifies that the cluster were ventricular cardiomyocytes. Images were acquired using confocal microscope at day 19 following differentiation. n=1 and scale bars are 20µm.

3.2.2.6 IGF-1Ea Expression Following Differentiation

Before proceeding to further *in vitro* analyses and cell transplantation studies, *IGF-1Ea* expression was analyzed at mRNA level to understand if differentiation of the transduced cells affected IGF-1Ea over-expression. The analysis showed that IGF-1Ea expression was retained in the gene transduced cells even after differentiation. However, also the control P19Cl6 cells expressed IGF-1 upon differentiation. When compared to the undifferentiated IGF-1Ea over-expressing cells, the differentiated IGF-1Ea cells expressed double the amount of IGF-1Ea, suggesting that induction of differentiation of P19Cl6 cells caused expression of the endogenous IGF-1. Indeed, IGF-1 levels increased significantly in control cells upon differentiation. The analysis revealed that differentiation of P19Cl6 cells with DMSO alone led to expression of IGF-1. Although the IGF-1Ea transduced cells expressed higher amount of IGF-1 than the control cells after differentiation, both the cell types expressed high amount of the gene. Figure below shows the mean relative

expression of the gene with or without differentiation by IGF-1Ea transduced or untransduced cells (Figure 19).

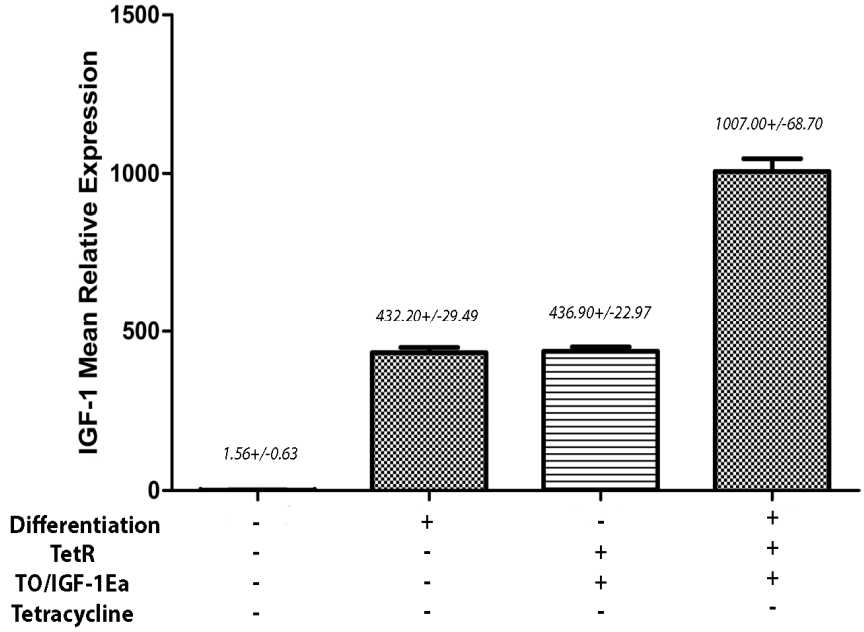

Figure 19. IGF-1Ea Transcript Expression in Differentiated Cells with/without IGF-1Ea Transduction. IGF-1Ea is expressed by both IGF-1Ea transduced and untransduced cells following differentiation. Results are expressed as Mean +/- SEM. 18S rRNA was used as internal reference gene.

3.2.3 DISCUSSION

Expression of Oct3-4 by both the IGF-1Ea and empty vector transduced cells illustrated that transduction of viral vectors and the IGF-1Ea maintained undifferentiated state of P19Cl6 cells. When differentiated, both the cell types efficiently formed GFP positive ventricular myocytes illustrated by the confocal and the FACS analyses. The efficient differentiation into ventricular cardiomyocytes even after *in vitro* manipulations of the cells was a remarkable finding for the cell therapy objective of this study. Large quantities of cells could be readily obtained for cell transplantation, which remains a challenge with many candidate cell types that are being studied to date [33, 65]. The molecular analysis on the cardiac-specific markers, Nkx2-5, MLC2v and Gata4 expression further proved differentiation of the cells into cardiomyocytes. The expression levels of both Nkx2-5 and MLC2v were higher in IGF-1Ea transduced cells, suggesting the possible role of IGF-1Ea over-expression on driving differentiation towards cardiac lineage. However, as the expression levels of cardiac markers were not enhanced in the IGF-1Ea-cells at undifferentiated state, the enhanced cardiac marker expression was not dependant on IGF-

1Ea alone, but may be triggered by the action of IGF-1Ea and DMSO together. The quantitative analyses performed using FACS however was unable to show a significant difference in the amount of GFP positive cells obtained from IGF-1Ea- and empty-cells, indicating that IGF-1Ea over-expression did not enhance differentiation of P19Cl6 cells into cardiomyocytes. The molecular and FACS analyses together indicated that *IGF-1Ea* over-expression either enhanced expression of cardiac proteins without increasing their differentiation efficiency (as it occurs during hypertrophy) or accelerated cardiac differentiation of P19Cl6 cells. A time-course analysis on cardiac marker expression following differentiation of IGF-1Ea transduced and untransduced control cells would be able to show whether IGF-1Ea expression caused acceleration of cardiac lineage differentiation of P19Cl6 cells.

Klinz et al. [207] treated EBs with PI3-kinase inhibitor and observed a massive loss of alpha-actinin-stained cardiomyocytes. The PI3-kinase pathway has been shown to induce the transcription of myocyte enhancer factor 2 (MEF2) and MEF2 plays a role in activating muscle specific structural genes [174]. Also, activation of the PI(3)K/Akt pathway is crucial for regulation of protein synthesis in skeletal muscle cells as well as in muscle hypertrophy [175, 176] and IGF-1 is one of the activators of the PI3-kinase pathway. Considering the observations of these studies, it is likely that over-expression of IGF-1Ea leads to increased PI3-kinase and MEF2 activities resulting into increased protein synthesis. To test this, an alpha-actinin staining was performed on the cardiomyocytes derived from empty- and IGF-1Ea-cells. There was no apparent difference in the amount of sarcomeric protein expression between the *IGF-1Ea* transduced compared to the untransduced cells. However, the sarcomeric apparatus appeared to be better organized in the cardiomyocytes derived from the *IGF-1Ea* transduced cells compared to the untransduced cells suggesting that the over-expression of IGF-1Ea might be involved in organization of the alpha-actinin protein structure rather than increasing their amount. However, more analysis is required to verify this observation as this examination was based on one analysis. The positive staining for the alpha-actinin nonetheless demonstrated that the differentiated cells resulting from the IGF-1Ea and empty vector transduced cells were structurally mature and suitable for transplantation studies.

Interestingly, differentiation of P19Cl6 cells by DMSO alone led to induction of endogenous IGF-1 expression. Upon differentiation, also the control cells expressed high amount of IGF-1 to the levels comparable to the undifferentiated IGF-1Ea transduced cells. This indicated that differentiation of P19Cl6 cells into cardiomyocytes is associated with IGF-1 expression. As observed previously, treatment of embryonic stem-cell aggregates with PI3-Kinase inhibitor LY294002 abolished cardiac commitment in ES cells [208] without affecting endothelial cell formation [207] indicating that activation of PI3-K signaling by specific growth factors such as IGF-1, FGF or TGFβ promote development of cardiomyocytes in a selective manner [207]. This could be investigated further by inhibiting IGF-1Ea action on the transduced cells by blocking IGF-1R by IGF-1R inhibitors.

The proliferation analyses of clone 6 P19Cl6-IGF-1Ea or -empty vector transduced cells showed similar proliferation profiles for both the cell types, indicating that an excess of *IGF-1Ea* isoform did not affect proliferation of the transduced P19Cl6 cells.

3.3 SECTION III: TESTING FEASIBILITY OF THE IGF-1Ea TRANSDUCED CELLS *IN VITRO* FOR *IN VIVO* CELL THERAPY

3.3.1 INTRODUCTION

The previous sections focused on engineering P19Cl6 cells for cell-based gene therapy. The first part outlined the tools and methods that were applied to create a stable clone of P19Cl6 cells that over-expressed the IGF-1Ea gene. The second section analyzed the effects of IGF-1Ea stable transduction on properties of the P19Cl6 cells. Following successful completion of the above two objectives, the focus of this section was to conduct tests for examining feasibility of the transduced cells for cell transplantation therapy in an *in vitro* system. To do so, the donor cells for transplantation were tested *in vitro* for their cardiogenic potential. The functionality of the IGF-1Ea over-expressing transduced cells were investigated by electrophysiological analyses, followed by the examination of the role of IGF-1Ea over-expression on cell viability and protection.

Electrophysiological analyses were carried out to examine calcium handling by the differentiated transduced cells. Calcium handling is fundamental to the function of heart, as excitation - contraction coupling of the muscle cell is mediated by changes in cytoplasmic calcium [212-214]. In a cardiac myocyte, arrival of an action potential leads to membrane depolarization. The depolarization causes activation of voltage-dependant L-type Ca channels, which leads to influx of Ca2+ into the cytosol. Ca2+ influx then triggers the release of Ca2+ from sarcoplasmic reticulum (SR) via Ca2+ release channels such as the ryanodine receptors. This mechanism by which influx of calcium ions through the L-type receptor triggers release of more calcium ions into the cytosol from the SR is commonly known as calcium-induced calcium-release (CICR) mechanism. Calcium ions released via the CICR mechanism diffuse through the cytosolic space. In the cytosol there are the sarcomeric proteins, which are the contractile proteins of a myocytes [214]. A sarcomere is a region of a myofilament between the two Z lines, composed of a thin (Actin, tropomyosin and troponin) and a thick (Myosin) filament. Interactions between the actin and myosin cause the sarcomere length to shorten causing the myocyte to contract during the process of excitation-contraction coupling. This interaction is dependent on chemical and physical interactions between calcium ions and the thin and the thick filament proteins such as the myosin, troponin C and troponin I. Troponin C serves as a

binding site for Ca^{2+} and troponin-I inhibits the myosin binding site on the actin. Upon binding of Ca^{2+} to troponin C, a conformational change occurs in the troponin complex. This causes exposure of a site on the actin molecule that is able to bind to the myosin ATPase located on the myosin head. This binding results in hydrolysis of ATP that supplies energy for a conformational change to occur in the actin-myosin complex, that triggers the sliding of thin and thick filaments causing cell shortening and force generation. The troponin complex recommences its inactivated state, inhibiting myosin-actin binding, when Ca^{2+} is removed from the Troponin-C. Recovery occurs as Ca^{2+} is pumped out of the cell by the Na^{+}/ Ca^{2+} exchanger (NCX) or is returned to the sarcoplasmic reticulum (SR) by sarco(endo)plasmic Ca^{2+} -ATPase (SERCA) pumps [214].

Calcium-Induced-Calcium Release mechanism can be visualized by performing a confocal Ca^{2+} analysis by treating cardiac myocytes with fluorescence conjugated calcium indicator dye such as Rhod-2AM. Rhod-2 AM is a rhodamine-based (Rhod) dye with acetoxymethyl (AM) ester, which is cell permeable. The dyes bind to the calcium ions in the cytosol. Binding of the calcium ion leads to release of the fluorescence. Therefore, the fluorescent intensity depends on the amount of dye that binds to the calcium ions [215]. The increase of cytoplasmic [Ca^{2+}] leads to contraction and extrusion from the cell brings relaxation [216]. Therefore right before contraction, the cells express the highest amount of fluorescence and when it relaxes, the lowest. This analysis not only verifies the presence of CICR mechanism in the cells but also sheds idea on the frequency of contraction.

The next objective of this section was to study the role of IGF-1Ea over-expression on survival signaling. When IGF-1 was administered in a murine model of myocardial ischemic reperfusion it was able to decrease myocardial apoptosis [162]. In a myocardial infarction model caused by the occlusion of left descending coronary artery, transgenic mice over-expressing IGF-1 demonstrated decreased cell death and ventricular dilation [163]. Similarly work from our laboratory performed with transgenic mice over-expressing IGF-1Ea (IGF-1Ea) showed smaller scar size and better function after injury compared to the wild type control animals [77]. This study engineered IGF-1Ea transduced P19Cl6 cells for cell therapy to be utilized in myocardial infarction model. As the cells were transplanted into infarcted hearts, it was essential to engineer cells that were

capable of surviving the hostile environment upon injection. Therefore, the next analysis was performed on cell survival signaling upon hypoxia and normoxia treatment by Lactose Dehydrogenase (LDH) release assay.

Lactate Dehydrogenase (LDH) is a stable cytosolic enzyme that is released upon damage to cell membrane as a result of necrosis and some times apoptosis [191]. Cell death can occur by apoptosis or necrosis. Apoptosis is referred to as a programmed cell death, which involves cell shrinkage, condensation of cellular chromatin and some times breakdown of cells into membrane-bound apoptotic bodies [190]. Unlike apoptosis, necrosis is un-programmed death and is accompanied by mitochondrial swelling and increased plasma membrane permeability. Apoptosis avoids involvement of scavenging inflammatory cells [190] to protect tissues from damaging events that result from the inflammatory cells whereas homing of inflammatory cells is one of the components of necrotic cell death. For LDH release assay, the IGF-1Ea and empty vector transduced P19Cl6 cells were exposed to either normoxia or hypoxia. In normoxia, the cells were deprived of glucose and serum but given normal amounts of carbondioxide (5%) and oxygen (20%), whereas in hypoxia they were deprived of both nutrients and oxygen, which was reduced to only 3%. This study was performed to investigate whether over-expression of the survival factor IGF-1Ea could provide the transduced cells with better protection from cell death. In addition, to investigate whether or not IGF-1Ea release could protect native cardiomyocytes from cell death in the context of cell therapy *in vivo*, neonatal rat cardiomyocytes were treated with normoxia and hypoxia conditions in the presence of conditioned media from empty- or IGF-1Ea transduced cells.

3.3.2 RESULTS

3.3.2.1 Confocal [Ca^{2+}] Transient Analysis

IGF-1Ea transduced and untransduced cells were differentiated and analyzed for their calcium handling through confocal microscopy. Cytoplasmic calcium ion changes were measured during contraction/relaxation. The [Ca^{2+}] changes were examined using the Ca^{2+} sensitive fluorescent indicator Rhod-2AM. Upon binding to the cytoplasmic calcium ions, Rhod-2AM fluorescence intensity showed an oscillation that corresponded with the spontaneous rhythmic contraction of cardiomyocyte clusters. In the figure below (Figure 20), panel (A) demonstrates representative confocal images of a beating cluster derived

from empty vector transduced P19Cl6 cells, showing the oscillations of Rhod-2AM fluorescence intensity during relaxation and (B) contraction (light red image vs. bright red image). Panel (C) shows that the contracting cells were also GFP positive. Panel (D) shows a bright field image of the beating cluster. Below the confocal images are the fluorescent oscillations recorded at a certain plain of the cluster where panels (E and F) show Rhod-2AM fluorescence intensity (Y-axis) at a particular time in seconds (X-axis) during contraction and relaxation. IGF-1Ea-cells derived beating clusters showed similar CICR mechanism (data not shown). The calcium transient analysis illustrated that the cardiomyocytes derived from P19Cl6 cells transduced with both IGF-1Ea and empty vectors exhibited CICR mechanism proving that they are functionally active and capable of contributing to functional improvement upon their transplantation.

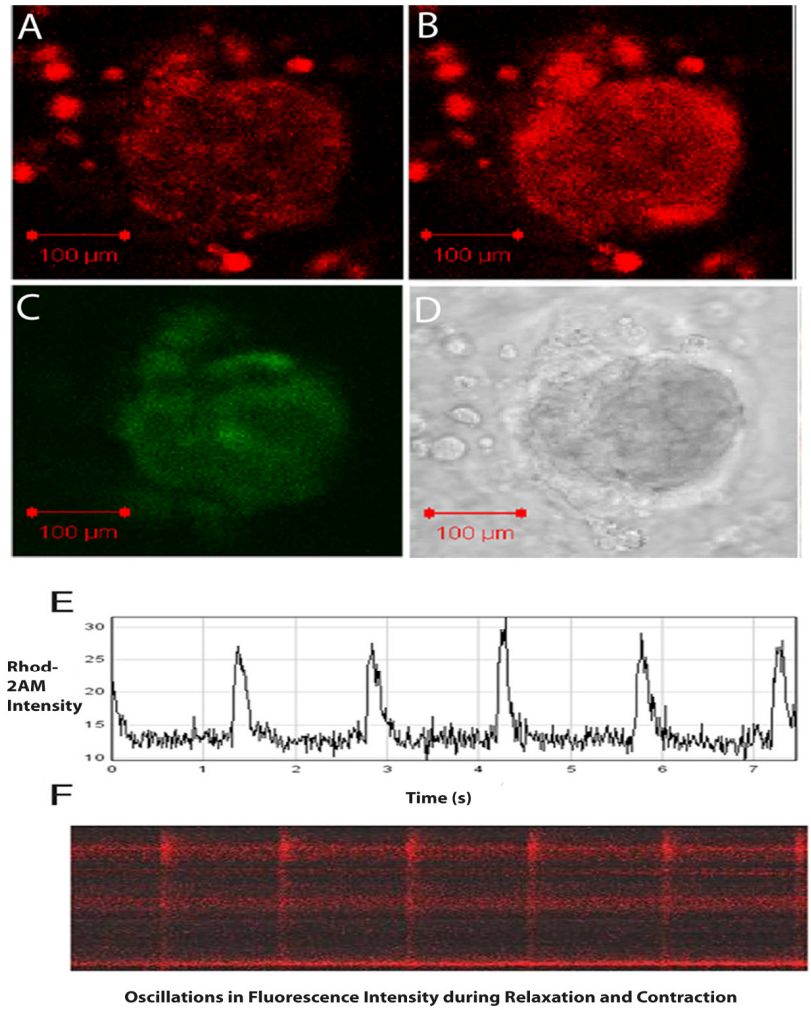

Figure 20. Confocal Ca2+ Transient Analysis. Representative confocal images of a beating cluster derived from P19Cl6 untransduced cells. The images show the oscillations of Rhod-2AM fluorescence intensity during relaxation (A) (light red) and contraction (B) (bright red). The beating cluster expressed GFP (C). Image (D) shows a bright field image of the beating cluster. Figures (E and F) show the amplitude of fluorescent intensity and oscillations in fluorescence intensity during relaxation and contraction respectively. The oscillations in fluorescence intensity were recorded at a certain plain of the beating cluster.

3.3.2.2 Cytotoxicity Assessment

The normoxia-hypoxia exposure study began with a cytotoxicity assessment. The cytotoxicity determination was essential to confirm occurrence of hypoxia. It was conducted by exposing cells to hypoxia or normoxia for varying amounts of time as described in materials and methods**.** After each treatment time, LDH release was measured and cytotoxicity was determined by comparing the amounts of LDH released by empty-cells with the IGF-1Ea-cells. Percentage LDH release (% LDH release) was obtained as a relative expression, achieved by comparing to the LDH released at 1 minute normoxia exposure. At 1 minute normoxia, %LDH release was set as 0% as there would be no/minimal cell death at this time point. Both the normoxia and hypoxia treatments resulted in no cell death up to 4 hour (240 min) exposure time-point, illustrated by no difference in the %LDH release in the empty (blue curve) and IGF-1Ea (pink curve) vector transduced cells. At 24 hour however, in both the treatments, very high levels of LDH release were detected, confirming occurrence of cell death. There was higher LDH release in the samples that were exposed to hypoxia than normoxia as expected, which confirmed occurrence of hypoxia. As LDH release was observed at 24 hour exposure time, subsequent experiments were conducted at 24 hour time-point. The figure below shows the results obtained for normoxia (A) and hypoxia (B) treatments (Figure 21). The X-axis shows exposure time in minutes and the Y-axis, %LDH release.

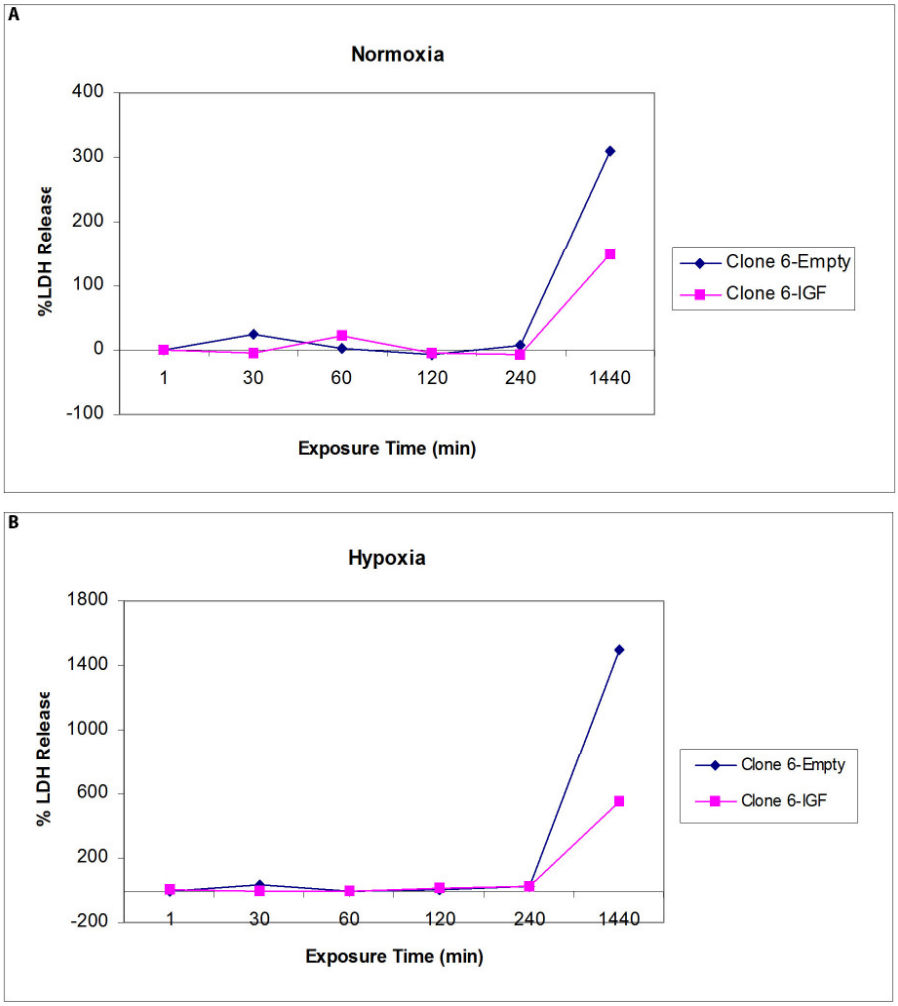

Figure 21. Determining Cytotoxicity following Normoxia or Hypoxia Treatment. Cytotoxity determination of IGF-1Ea and empty vector transduced cells following exposure to normoxia or hypoxia. Both the IGF-1Ea and empty vector transduced cells showed no LDH release at exposure time below 240 minutes (4 hours). Upon 24 hour exposure, there was a massive induction of LDH release. IGF-1Ea transduced cells showed lower LDH release at 24 hour compared to the empty vector transduced cells in both normoxia and hypoxia treatments.

3.3.2.3 Effect of IGF-1Ea over-expression on cell survival

After determining the exposure time to achieve cytotoxicity from the hypoxia and normoxia treatments, the transduced P19Cl6 were exposed to 24-hour treatment for subsequent experiments. After 24 hours hypoxia and normoxia, percentage LDH release was measured relative to the LDH released by the empty-cells, for which the value was set as 100%. Below are the bar graphs showing LDH release for normoxia (A) and hypoxia treatments (B) (Figure 22). Upon normoxia treatment, the IGF-1Ea transduced cell cultures released approximately 25% less LDH (99% +/- 9% empty-cells vs. 74% +/- 2.7% IGF-1Ea-cells), indicating 25% higher cell viability for IGF-1Ea transduced cells compared to the empty vector transduced cells in normoxia treatment. In the hypoxia treatment (shown in panel B), IGF-1Ea provided even higher protection (100% +/- 7.8%

LDH release for empty-cells vs. 41% +/- 5.5% LDH release for IGF-1Ea-cells) than the normoxia treatment. Transduction of IGF-1Ea vector therefore conferred higher cell viability to the transduced cells exposed to 24 hour hypoxia and normoxia. The higher survival capability of the transduced cells would be beneficial for their transplantation into ischemic tissue.

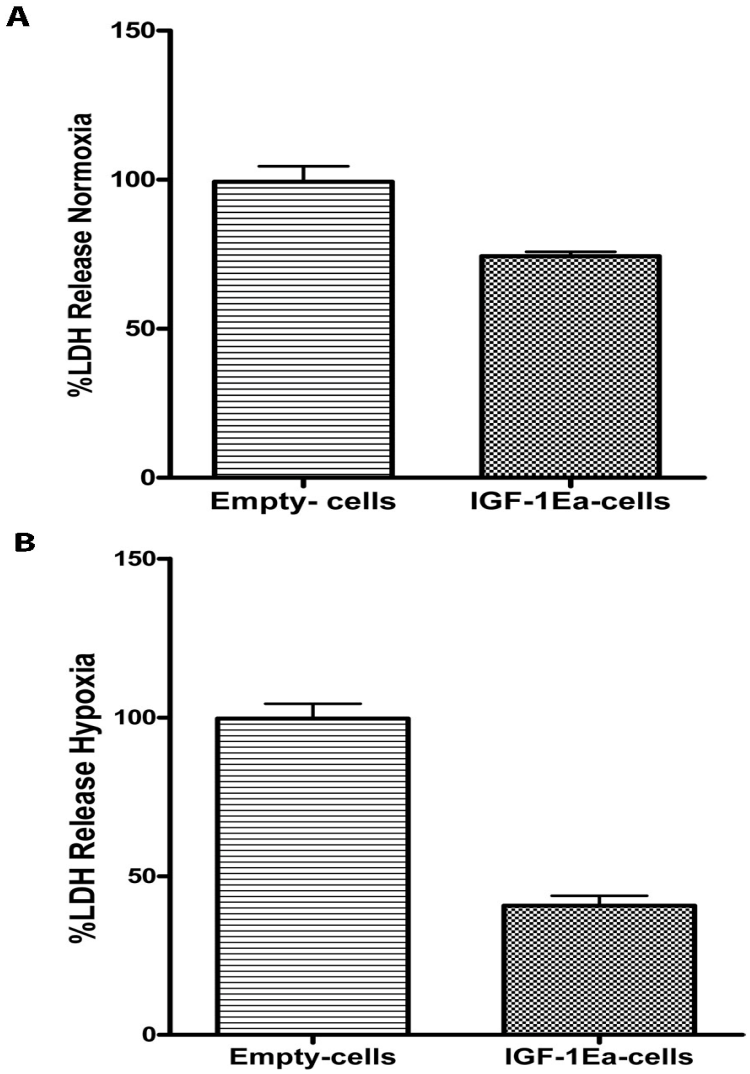

Figure 22. Effect of IGF-1Ea Over-expression on Cell Survival in vitro. P19Cl6 transduced with IGF-1Ea or empty vector were exposed to normoxia (A) or hypoxia (B) to investigate the effects of IGF-1Ea over-expression on cell survival. Upon normoxia, IGF-1Ea transduced cell cultures released 25% less LDH (99% +/- 9% empty vs. 74% +/- 2.7% IGF-1Ea). In the hypoxia treatment, IGF-1Ea conferred even higher cell survival (100% +/- 7.8% LDH release for empty vs. 41% +/- 5.5% for IGF-1Ea transduced). Percentage LDH release was determined relative to the LDH released from empty vector transduced cultures at 24-hour as 100%.

3.3.2.4 Effect of IGF-1Ea conditioned media on cardiomyocyte survival

IGF-1Ea over-expression showed enhanced survival of transduced P19Cl6 cells. To analyse whether release of IGF-1Ea may affect survival of cardiomyocytes exposed to

hypoxia and normoxia, the conditioned media of IGF-1Ea-cells and control cells was used to treat neonatal cardiomyocytes. Hypoxia or normoxia were induced for 24 hours as performed with P19Cl6 cells. The following day, protein was extracted from the cultures and western blot analysis was performed for the apoptotic marker cleaved-caspase 3. The western blot analysis revealed higher expression of cleaved-caspase 3 (3 fold to 1.5 fold), for neonatal cardiomyocytes treated with empty- conditioned media compared to IGF-1Ea-condioned media (Figure 23). As a control, protein from untransduced P19Cl6 was loaded, which showed minimal cleaved-caspase 3 expression.

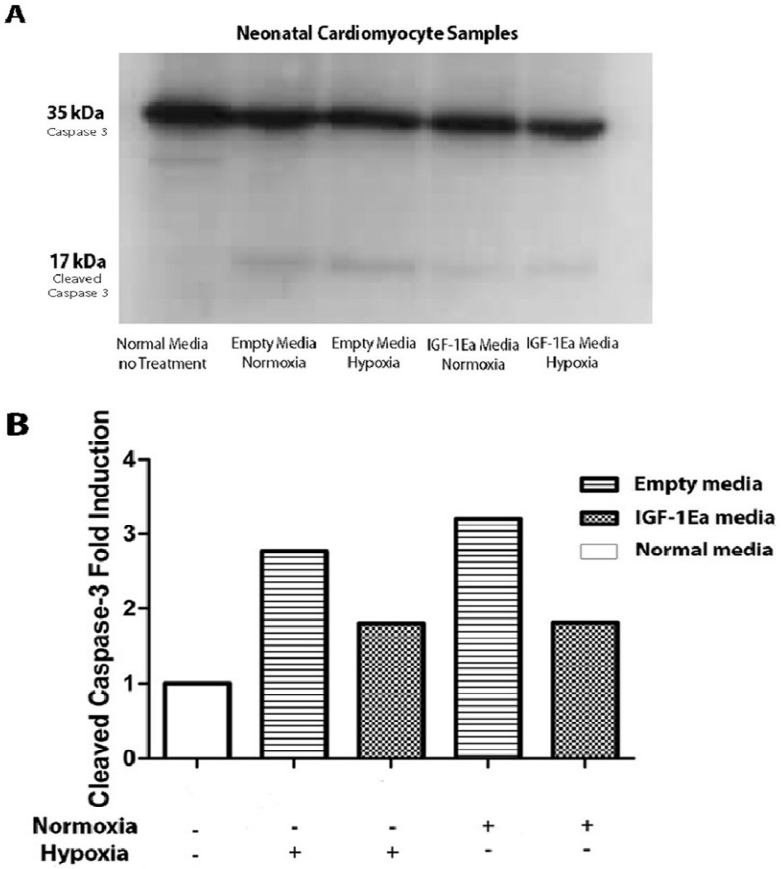

Figure 23. Effects of IGF-1Ea Conditioned Media on Cardiomyocyte Survival. (A) Western blot analysis on cleaved caspase-3 expression for hypoxia and normoxia exposed neonatal rat cardiomyocytes (CM) treated with conditioned media from IGF-1Ea and empty vector transduced P19Cl6 cells. (B) Cleaved caspase-3 expression was higher in CM treated with empty-conditioned media (approximately 3 fold induction in both the treatments) compared to IGF-1Ea treated media (approximately 1.5 fold induction in both the treatments). The relative expression was obtained by comparing with normally grown CM, n=1.

3.3.3 DISCUSSION

The aims of this section were to test the functionality of transduced differentiated cells by studying calcium transients and to analyze the practicability of using the transduced cells

for cell transplantation therapy, in an *in vitro* system. Calcium transients were in the differentiated cells derived from both transduced cell types, confirming that transduced P19Cl6-derived cardiomyocytes would make a suitable candidate for cell transplantation therapy, to potentially achieve an improvement of the mechanical function of the injured region.

The most imperative goal of this project was to engineer pluripotent P19Cl6 capable of surviving better upon exposure to an injury. To accomplish this, P19Cl6 cells were transduced with the IGF-1Ea gene. Upon successful transduction of the gene, an *in vivo* ischemic injury model was mimicked *in vitro* whereby the transduced cells were exposed to nutrient and oxygen deprivation (hypoxia). The objective was to analyze the robustness of the transduced cells to survive the hostile host environment. Cytotoxity determination showed that in general, the P19Cl6 cells were very robust cells, showing LDH release only after a prolonged exposure (24 hour) to both the treatments. Interestingly, IGF-1Ea cells survived the treatments better compared to their controls, which was marked by lower LDH release in the IGF-1Ea transduced versus the control cells. Considering the outcome of the cytotoxicity assay and the robustness of these cells, the 24-hour time point was taken as the choice of exposure time for further analyses. Even at the prolonged exposure to hypoxia or normoxia, IGF-1Ea over-expressing cells showed approximately 25% (normoxia) and 50% (hypoxia) higher cell viability when compared to the control cells. The control cells were more susceptible to hypoxia induced injury than the IGF-1Ea transduced cells. As the cell viability analysis was a relative analysis to the control cells and because higher amount of control cells died at hypoxia than normoxia exposure, relatively higher number of IGF-1Ea-cells survived hypoxia injury than the control cells. This robust nature of the IGF-1Ea over-expressing cells was a valuable property that the P19Cl6 cells acquired through the transduction of the gene, which made them an excellent candidate for cell therapy.

Following the cytotoxicity analyses, transduced P19Cl6 cells were examined for their possible role in maintaining cultured cardiomyocyte viability, to determine whether upon transplantation into infarcted hearts, they would confer protective signaling to the at-risk myocardium. Indeed neonatal rat cardiomyocytes treated with IGF-1Ea conditioned media demonstrated tendency for higher cell viability upon hypoxia and normoxia treatments. However, whether the observed effect was a direct effect of IGF-1Ea expression or an

indirect effect of IGF-1Ea transduction was not tested. Functional analyses are being carried out in the laboratory to analyze whether the treatment of IGF-1Ea conditioned media led to expression of IGF-1 signalling mediators such as Akt, PDK1 and MAPkinases. Directly or indirectly, IGF-1Ea transduction conferred higher survival upon hypoxia and normoxia exposure, suggesting that the transduced cells make suitable candidate for transplantation into ischemic tissue that suffers from similar deleterious conditions.

Taken together, these data showed that deprivation of nutrients and oxygen as normally occurs after coronary occlusion, leads to both necrotic and apoptotic cell death and that transduction of IGF-1Ea vector has the potential to protect P19Cl6 cells and cardiomyocytes from both the deleterious events.

CHAPTER 4

4.1 TO TEST IF FUNCTION OF IMPAIRED HEARTS COULD BE IMPROVED BY TRANSPLANTATION OF THE IGF-1Ea TRANSDUCED P19CL6 CELLS

4.1.1 INTRODUCTION

Despite significant advancements in gene therapy and stem cell biology, treatment for myocardial infarction remains unresolved, although optimism persists. Exciting new strategies for endogenous and exogenous regeneration of the damaged myocardium have evolved. However, whether these strategies can provide enough contractile cell mass to adequately restore the lost mechanical function remains unanswered [217]. During myocardial infarction and heart failure the mechanical function is affected due to loss of contractile cells and introduction of stiff scar. A successful therapy targeted at improving the impaired mechanical function must target both of these components in order to repair the total function [27].

Realizing the importance of the two components, this project aimed at conducting a cell therapy exploiting a combinatorial approach whereby pluripotent P19Cl6 were transduced with IGF-1Ea gene and the ventricular cardiomyocytes derived from the transduced cells, transplanted into infarcted murine hearts. IGF-1Ea has been shown by our laboratory to restore cardiac function by reducing scar size, modulating inflammatory response and increasing anti-apoptotic signaling [77]. With the transplantation of IGF-1Ea over-expressing cells, the project anticipated to maintain functions of injured hearts. The IGF-1Ea component was expected to enhance survival of the donor and the at-risk native myocardial cells. With increased cell survival of both the donor and the recipient cells, tissue regeneration, reduction of scar size and consequently preservation of function were anticipated.

In the earlier chapters, the P19Cl6 cells over-expressing IGF-1Ea were generated successfully. The engineered cells continued to produce large quantities of cardiomyocytes, which were mechanically active and possessed structural properties resembling mature cardiac myocytes. The IGF-1Ea over-expressing cells showed increased resistance against cell death upon hypoxia and normoxia treatments compared to the control cells, proving that they would make excellent candidates for transplantation studies.

For cell transplantation, purification of cardiomyocytes is required to avoid cancer formation. Therefore, P19Cl6 cells, expressing GFP under the control of the MLC2v promoter [100], were purified by fluorescence-activated cell sorting (FACS). Following cell sorting, GFP positive ventricular myocytes transduced with IGF-1Ea or empty vector were injected into wild type C57BL6-J mice to exploit an allogeneic transplantation. The use of allogeneic transplantation, which required immune suppression, was to emulate clinical set-up. Cell transplantation was performed in an acute model of myocardial infarction induced by permanent occlusion of the left-anterior descending coronary artery. Following transplantation, functional analyses were carried out at 5 days- and 2 month-time points to account for both the short and the long-term effects of cell transplantation.

Functional analyses were performed using Echocardiography by means of the B-and M-Mode measurements at 5-days and 2-months time points. Ejection Fraction (EF), Fractional Shortening (FS) and Fractional Area Change (FAC) parameters were used for measuring the left ventricular regional functions. Following the functional analyses, animals were sacrificed for various histological and molecular analyses. The 5-day samples were collected for molecular analyses only, whereas the 2- month samples were collected also for the histological analyses.

The 5-day and 2-month samples were used for molecular analysis of some paracrine factors implicated previously in stem cell transplantation studies. Paracrine factors are generally released from endogenous cells of the heart locally in response to injury. These may include growth/ survival factors and cytokines that support neovascularisation (eg. VEGF, SDF-1), cell protection (eg. IGF-1), modulate inflammation (eg. IL10, IL6), reduce fibrosis (eg. IGF-1) [218] or modulate contractility. Elastin is one of the extracellular matrix components that offers compliance to the contracting myocardium [29]. These factors (eg. SDF-1) may also signal via the circulation, bone marrow or tissue to the site of injury, thus aiding in tissue repair [218, 219]. In addition to the endogenous cells, exogenously transplanted cells have also been reported to secrete paracrine factors [218]. Paracrine factors resulting from either of the cell types may contribute to an improvement of function, therefore their expression profiles were analyzed.

The molecular analyses on the 5-day samples were followed by histological and molecular analyses of the 2 months samples. The histological analyses included scar size, cell

engraftment and capillary density measurements of the injured hearts using the masson's trichrome, anti-GFP staining and Isolectin B4 labelling respectively on paraffinized tissue sections. Additionally, the role of cell transplantation on LV remodelling was briefly analyzed by measuring cardiac cross-sectional area at the infarct border zone and molecular analysis of alpha skeletal actin (aSK) and beta myosin heavy chain (bMHC).

4.1.2 RESULTS

4.1.2.1 Survival Analysis of Surgical Animals

Twelve to 16 weeks old C57BL6-J mice were subjected to permanent occlusion of the descending left coronary artery. The animals were divided into four groups that were named 1) non-ligated, wild type control (WT), 2) ligated, saline injected (Saline), 3) ligated, empty vector transduced cells transplanted (empty-cells) and 4) ligated, IGF-1Ea vector transduced cells transplanted (IGF-1Ea-cells). Groups received cells or saline injections immediately after the occlusion of the left coronary artery. All groups, except the WT, received immunosuppressive an hour before the occlusion of the left coronary artery. The total intra- and early post myocardial mortality (between 0-3 days) was 34.92% (22 out of 63). The survival percentage to surgical procedure was determined by considering deaths that occurred up to 5 days post-myocardial infarction induction. The total number of animals that survived the surgical procedure for 5 days was 41 giving the surgical procedure 65% survival rate (41 out of 63). However, six animals died between 5-7 days, leading to only 35 survivors. A 55.56% final surgery survival rate was accomplished.

4.1.2.2 Functional Analyses

Following induction of myocardial infarction and cell transplantation, animals were left to recover for 5 days. At 5 days and 2 months, functional analyses were performed using echocardiogram to examine the short- and the long-term effects of cell injection on function of the injured hearts. Echocardiographic analyses were performed under anaesthesia obtained with 2% Isoflurane by constantly monitoring the body temperature and ECG of the subjects. Images were obtained at parasternal short-axis view. Functional analyses were taken from B- and M-Mode measurements using the Vevo 2100 (Visual Sonics) and data analyses performed with Vivo 2100 software (Visual Sonics). Ejection Fraction (EF), Fractional Area Change variable (FAC) and Fractional Shortening (FS)

were taken as parameters for measuring left ventricular function. Figure below (Figure 24) shows the parasternal short axis view for M-Mode and B-Mode measurements.

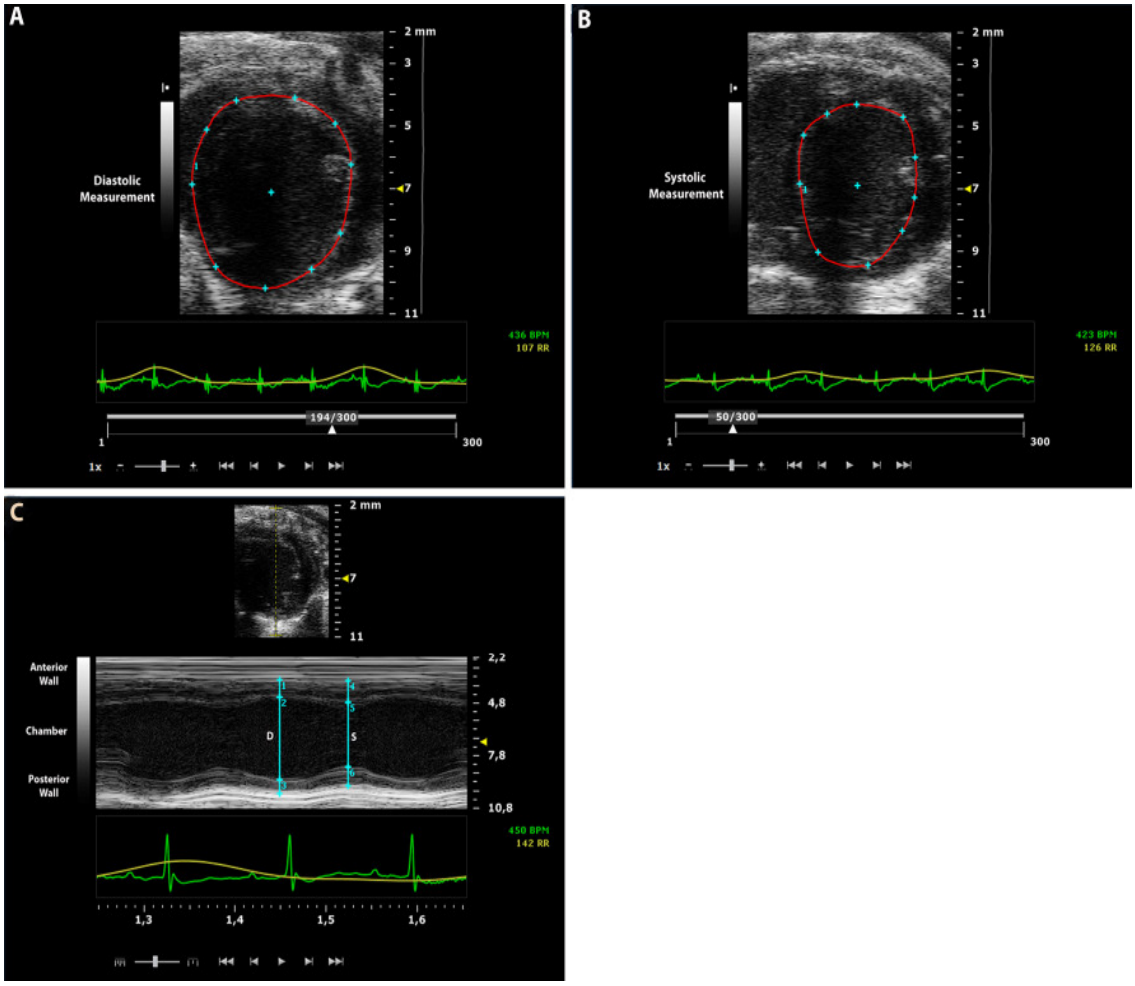

Figure 24. Echocardiographic Images of M-Mode and B-Mode. (A) A representative image for B-Mode analysis where diastolic endocardial wall circumference is marked for FAC measuement. (B) A representative image for B-Mode analysis where systolic endocardial wall circumference is marked for FAC measurement. (C) A representative image of M-Mode, where the anterior wall, the LV chamber and the posterior wall are labelled. In panel C, label D marks for anterior and posterior wall thickness and chamber dimension at diastole and S the systolic wall and chamber dimension measurements. Images were acquired with Vivo2100 and data analyses performed with Vivo 2100 software (Visual Sonics).

4.1.2.2.1 Ejection Fraction (EF)

The Ejection Fraction (EF) analyses at 5 days revealed a significant difference in the function of WT animals compared to the saline injected animals. The following table summarizes functional data for EF, FS and FAC (Table 7). The saline treated animals showed significantly reduced EF, p= 0.0098, suggesting induction of substantial myocardial infarction. Interestingly, both the IGF-1Ea- and empty- cells transplanted hearts showed no significant reduction of EF compared to the non-ligated WT controls,

although there was decrease in function in both of these groups compared to the wild type controls. Similarly, both the IGF-1Ea- and empty- cells treated animals did not show significantly higher EF compared to the saline only treated animals.

At two months, the saline injected animals continued to show a significantly reduced EF compared to the WT. There was still no significant difference in the EFs between the saline-treated and empty- and IGF-1Ea- cells transplanted animals. However, at 2 months, also the empty- and IGF-1Ea-cell treated groups showed significantly reduced EF compared to the WT animals. Taking together the 5 day and 2 months EF data, EF was mildly preserved, although for short time, in cell transplanted hearts compared to the saline treated hearts. No significant difference was observed in ejection fraction between the IGF-1Ea- and the empty- cells transplanted animals, suggesting that IGF-1Ea expression did not have any effect in the EF of the IGF-1Ea-cells transplanted hearts. One-way ANOVA was utilized for statistical analysis between the different groups. Panels A and B (Figure 25) demonstrate the results described for both the 5 days and 2 months EF analyses.

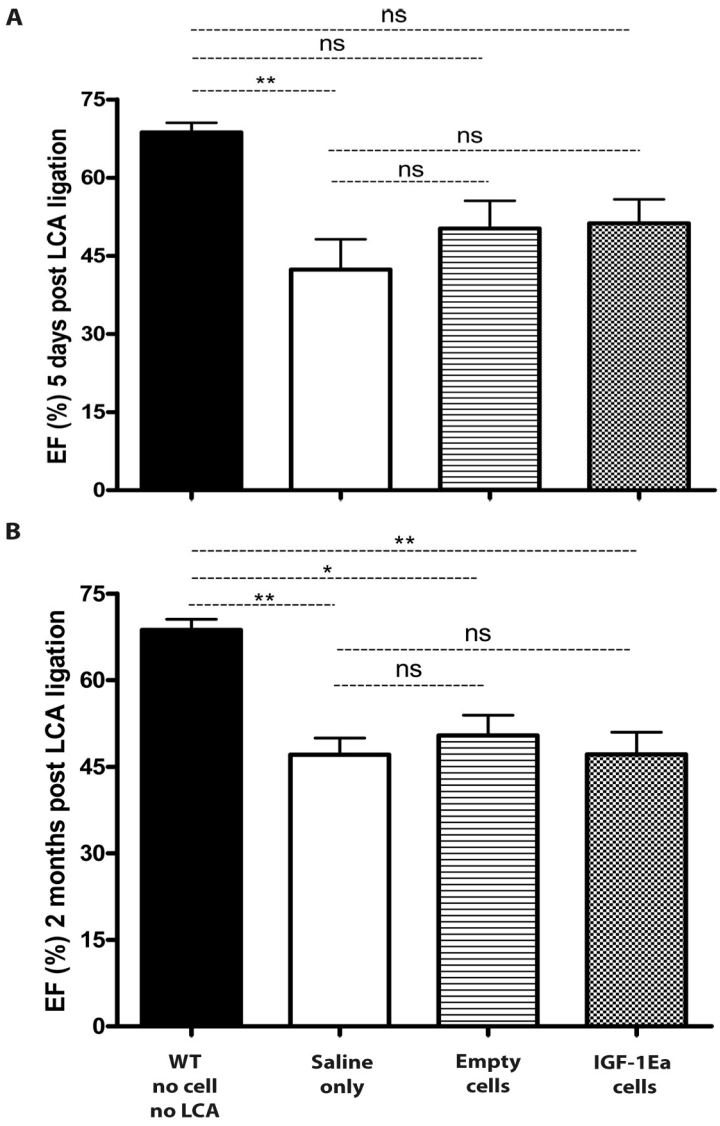

Figure 25. Ejection Fraction (EF) Analyses upon Myocardial Infarction Induction and Cell Transplantation. Panel (A) EF at 5 days. EF was significantly reduced in the saline injected animals, p= 0.0098 compared to the wild type animals. EF of animals that received cell transplantation was also reduced but not significantly compared to the WT control, p>0.05. Similarly, there was no significant difference between the cells and saline injected hearts and IGF-1Ea- and empty- cells injected hearts. The n values for WT, Saline and IGF-1Ea-cells injected are 4, and empty-cells injected 3, for the 5 day EF analysis. (B) EF at 2 months. At 2 months, there was significant difference between the WT and the saline injected hearts (p= 0.0010), the WT and the IGF-1Ea-cell injected hearts (p= 0.0010), and the WT and the empty-cells injected animals, p< 0.05. There was no significant difference between the saline treated to the cells-injected hearts and the IGF-1Ea- and the empty- cells injected animals p>0.05. One-way ANOVA was used for statistical analysis. The n values for the 2 months analyses were: n=4 WT, n=7 Saline, n=5 IGF-1Ea-cells, n=4 empty-cells.

Table 7: Functional Analyses of Infarcted Cell/Saline Injected Hearts

	EF (%) Mean +/-SEM		**FS (%) Mean +/-SEM**		**FAC (%) Mean +/-SEM**	
	5 days	***2 months***	***5 days***	***2 months***	***5 days***	***2 months***
WT no ligation	68.70 +/- 1.83	68.70 +/- 1.83	38.00+/- 1.41	38.00+/- 1.41	48.40 +/- 2.86	48.40 +/- 2.86
Saline ligated	42.35 +/- 5.79	48.12 +/- 2.89	20.95 +/- 3.33	23.65 +/- 1.69	27.40 +/- 1.27	28.24 +/- 1.35
empty-cells ligated	50.23 +/- 5.34	50.4+/- 3.55	27.90 +/- 3.62	25.45 +/- 2.23	31.40 +/- 6.23	36.50 +/- 2.72
IGF-1Ea-cells ligated	51.25 +/- 4.56	44.15 +/- 3.85	25.77 +/- 2.94	23.76 +/- 2.27	35.55 +/- 5.05	37.38+/- 1.09

4.1.2.2.2.Fractional Shortening (FS)

Fractional Shortening (FS) analyses were also carried out at 5 day and 2 month time points, using the M-Mode analysis as the EF analysis. The analysis showed that FS of saline treated animals was significantly lower compared to the WT control animals, p= 0.01. No significant difference was observed in the FS between the cells-treated and the WT or cell-treated and the saline-treated animals, p>0.05. The results for 5-day analysis are shown in panel (A) below. Panel (B) illustrates FS at 2 months. The numerical data is presented in table 7 together with EF and FAC. At 2 months, FS of saline-treated animals was significantly lower than the WT control, p= 0.0004. Interestingly, FS of the cell-injected hearts decreased significantly compared to the WT control at 2 months, with p<0.01 for WT compared to empty-cell treated hearts and p<0.01 for WT and IGF-1Ea-cells transplanted hearts, suggesting that cell transplantation did not preserve function of infarcted hearts at long-term. There was no significant difference in fractional shortening between the IGF-1Ea- and empty-cells treated groups suggesting no effect of IGF-1Ea on function at long-term. One-way ANOVA was used for statistical analysis. The figure below (Figure 26) illustrates the results described above.

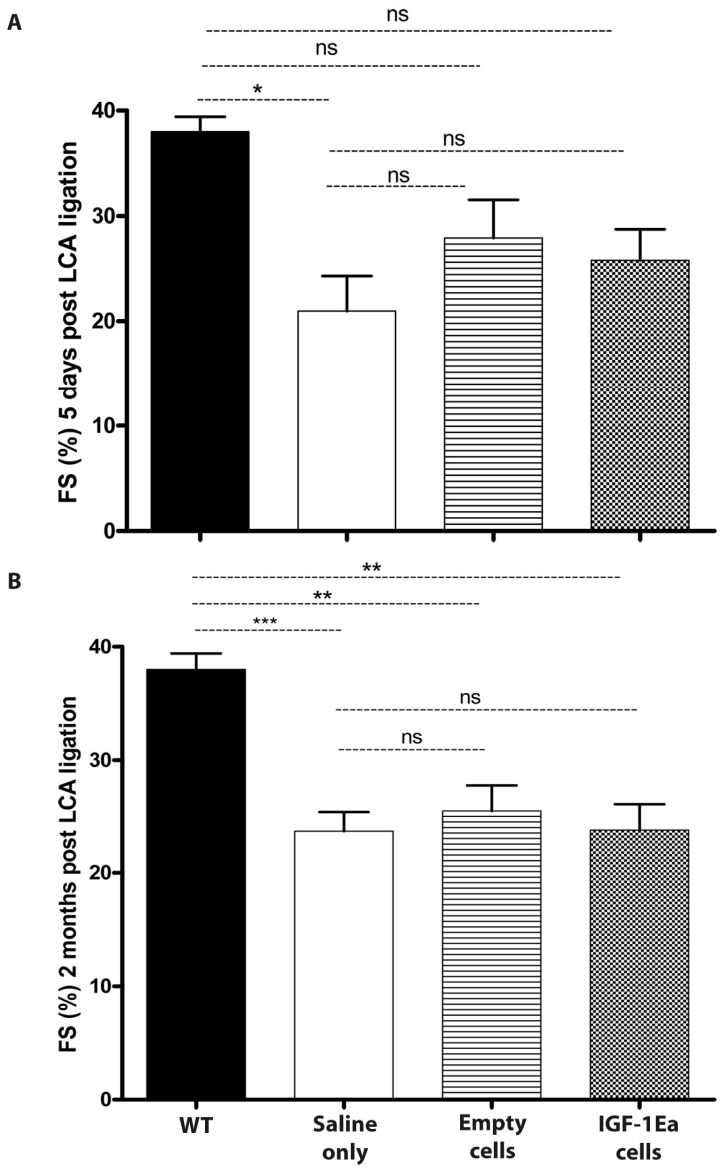

Figure 26. Fractional Shortening (FS) Analyses upon Myocardial Infarction Induction and Cell Transplantation. (A) FS at 5 days post treatment. FS of saline-injected animals was significantly lower than the WT control, p= 0.01. There was no significant difference between the cell injected and the WT or the saline-injected animals, p>0.05. (B) FS at 2 months. FS of saline -injected was significantly lower compared to WT control, p= 0.0004. FS of the cell-injected was significantly lower than the WT, p<0.01. There was still no significant difference between the saline treated and the cell transplanted groups. One-way ANOVA was used for statistical analysis. The n for 5 days analyses was equal to 4 for all groups. The n values for the 2 months analyses were: n=4 WT, n=7 saline no cells, n=5 IGF-1Ea cells, n=4 empty cells.

4.1.2.2.3 Fractional Area Change (FAC)

Unlike EF and FS, FAC was analyzed using the B-Mode echocardiography. FAC measurements were obtained at 5 days and 2 month after infarct induction and cell/saline injection as the EF and the FS. Panel (A) below illustrates the FAC results obtained for the 5-day analysis and Panel (B) illustrates the 2-month analysis. The saline-treated group showed significantly lower FAC compared to the WT control animals, p= 0.02. No

significant difference was observed between the WT and cell-injected groups as well as the saline-injected and the cell-transplanted groups, $p>0.05$.

At the 2-month analysis, FAC of saline treated group remained significantly lower than the WT group, $p= 0.0006$. The FACs of the cell-treated groups were also significantly lower than the WT controls, $p< 0.01$. As EF and FS, FACs of cell-injected hearts were not statistically different from the saline-injected group, $p>0.05$. There was also no significant difference in the FACs between the IGF-1Ea- and empty-cells transplanted hearts, $p> 0.05$. Statistical analysis was performed using the One-way ANOVA test. Table 7 summarizes the numerical data for FAC. The figure below shows the results summarized above (Figure 27).

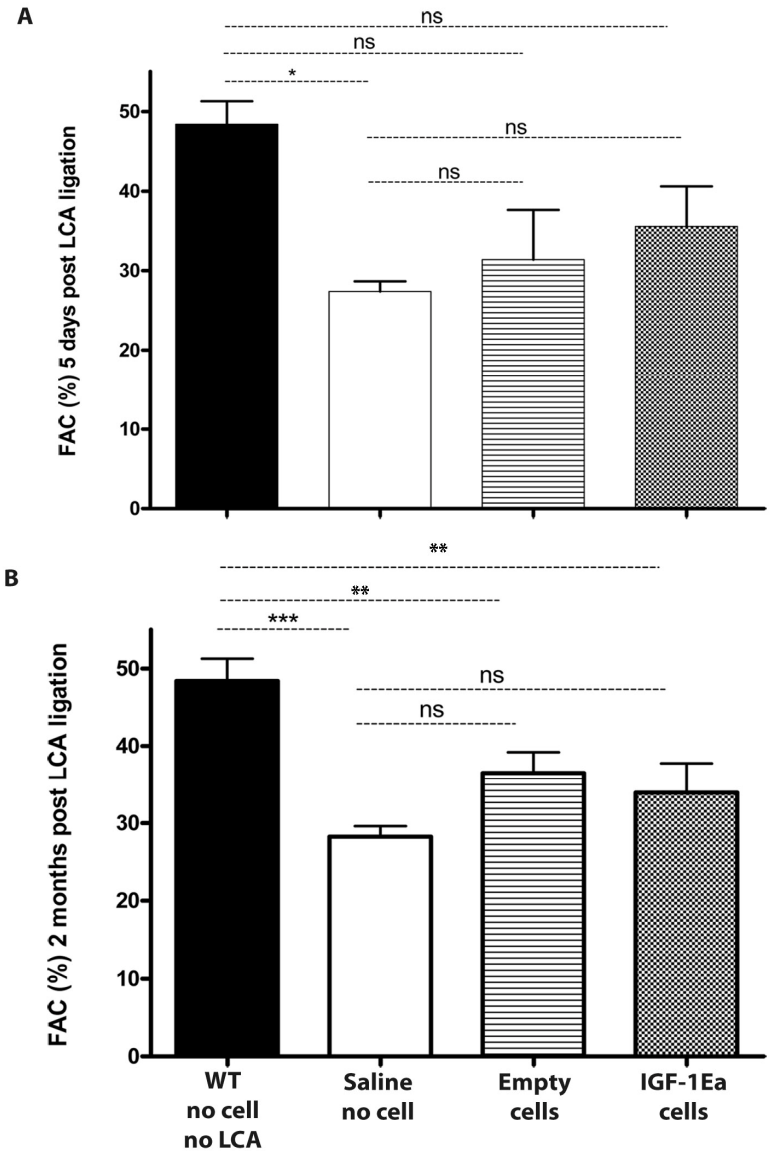

Figure 27. Fractional Area Change (FAC) Analysis upon Induction of Myocardial Infarction and Cell Transplantation. (A) FAC analysis at 5 days post treatment. The saline only treated group demonstrated significantly lower FAC compared to the WT control animals p= 0.02. No significant difference was observed between the other groups, p>0.05. (B) FAC analysis at 2 months post treatment. FAC of saline-injected hearts remained significantly lower than the WT group, p= 0.0006. The FACs of IGF-1Ea- and empty-cell treated groups also went down to give a significantly lower value than the WT, p<0.01. FAC of the cells-injected groups were not significantly higher than the saline-injected group, p>0.05. Statistical analysis was performed using the One-way ANOVA test. The n for 5 days analyses was equal to 4 for all groups. The n values for the 2 months analyses were: n=3 WT, n=7 saline, n=4 IGF-1Ea cells, n=4 Empty cells. Values are Mean +/- SEM

Taking together the EF, FS and FAC data at 5-day time point, cell transplantation conferred a tendency for maintenance of function of the infarcted hearts. A significant decrease in function was observed in the saline treated hearts compared to the WT controls whereas there was no significant decrease in the cells treated hearts compared to the WT. In long-term analyses, the cell-transplanted hearts showed significant decline in EF, FS

and FAC compared to the WT control and there was no significant difference between the saline-injected compared to the cell-transplanted hearts. The short- and long-term functional analyses data for all three variables together suggested that cell transplantation mildly protected hearts from decline of function at short-term, although it was not statistically significant. At long-term however, cell transplantation did not confer any beneficial effects on function.

To investigate the factors that could have contributed to this differential functional response at the short and the long term analyses, survival, inflammatory and angiogenic factor expression levels were analysed by quantitative real time PCR.

4.1.2.3 Molecular Analyses of Short-term Samples

IGF-1, Elastin, VEGF, SDF-1, IL6 and IL10 have been implicated as paracrine factors to conduct different functions during myocardial injury and cell transplantation. Real time quantitative PCR analyses were carried out to analyse at mRNA level the expression of the above mentioned paracrine factors. The mRNA analyses on all of these genes revealed no significant difference between any of the 4 experimental groups $p>0.05$. There was a tendency for higher IGF-1, Elastin, IL6 and IL10 expression in the infarction induced groups (both cells and saline treated) compared to the wild type uninjured group. In addition, no significant difference was observed between the IGF-1Ea- and empty-cells transplanted hearts $p>0.05$, suggesting no role of IGF-1Ea on expression of the examined paracrine factors. The IGF-1 mRNA was detected in all the injured hearts treated with both the cells and saline, suggesting induction of endogenous IGF-1 production upon injury. There was no significant difference in the expression of VEGFa and SDF-1 between any of the four experimental groups. The figure below summarizes the outcome of the gene expression analyses for all 6 genes (Figure 28). Values are represented as Mean +/- SEM and statistical analyses were performed using the non-parametric one-way ANOVA (Kruskal Wallis Test).

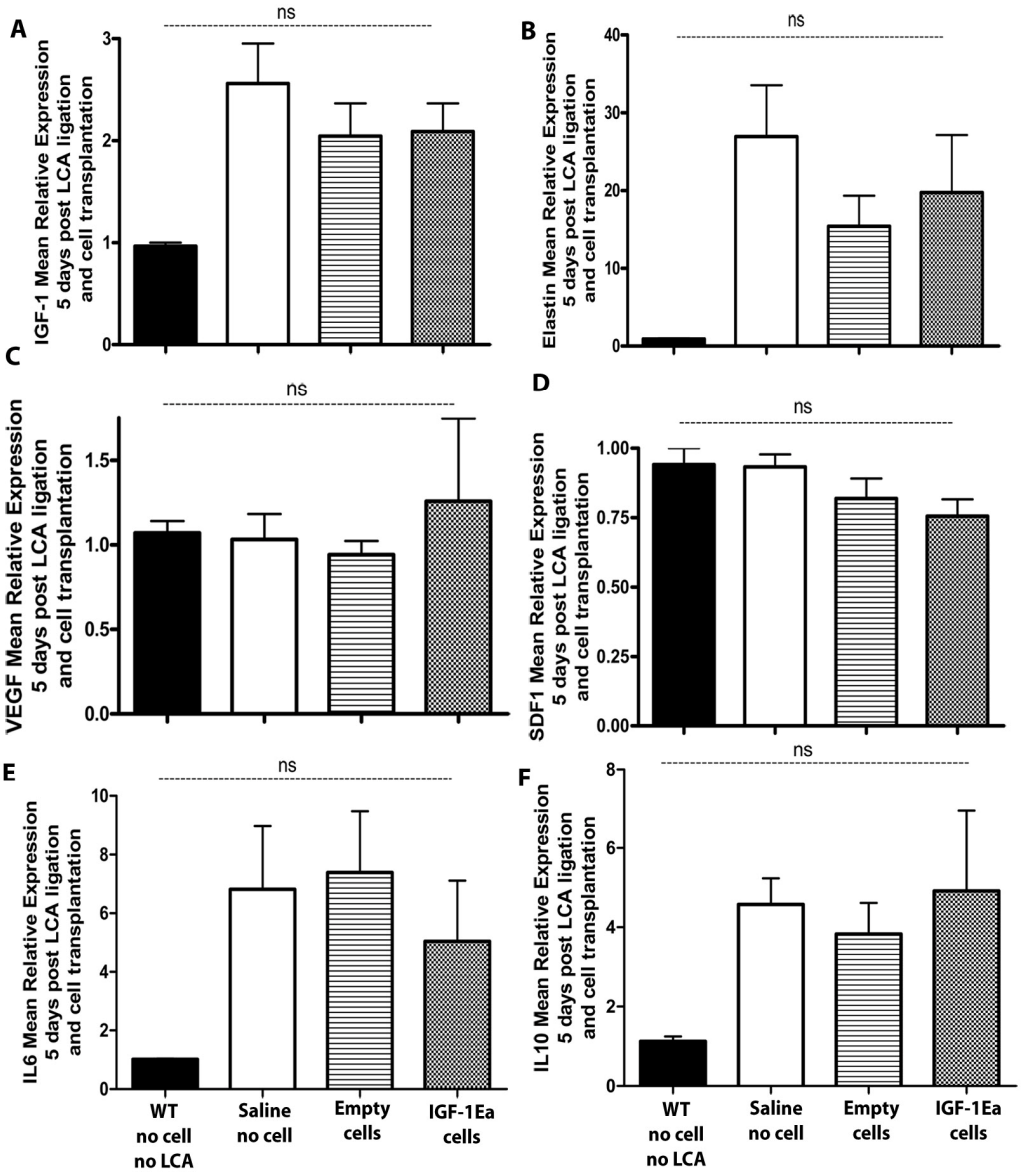

Figure 28. Mean Relative Paracrine Factor Expression. Real time PCR analyses were performed with 5 day infarcted, cells/saline treated left ventricle samples. For all the treatment groups n=3. (A) IGF-1, (B) Elastin, (C) VEGF, (D) SDF-1, (E) IL6 and (F) IL10 mean relative expressions. No significant difference was observed between the WT control versus the infarcted cell/saline treated groups; IGF-1: p=0.09, Elastin: p=0.07, VEGF: p=0.7, SDF-1: p=0.18, IL6: p=0.15 and IL10: p=0.06. There was a tendency for increased IGF-1, Elastin, IL6 and IL10 expressions in the infarcted hearts. Statistical analyses were performed using the non-parametric One-way ANOVA (Kruskal-Wallis Test) in Prism. Values are Mean +/- SEM.

Taken together, these data showed that the paracrine molecules normally implicated in cardiac recovery that are released either by the donor or the native cells after injury and cell transplantation, were not significantly modulated at 5 days after myocardial infarction. However, the lack of statistically significant difference in the expression profiles of IGF-1, Elastin, IL6 and IL10 between the injury induced and WT animals indicated that possibly the high variations in animals within groups might be accountable for such outcome.

4.1.2.4 Histological Analyses of Long-term Samples

Following the functional analyses at 2 months, animals were sacrificed for histological and molecular analyses. The histological analyses were performed (i) to examine the morphology of the scar, (ii) to assess engraftment of the transplanted cells, (iii) to analyze capillary density and (v) to examine morphology of the native cells at the border zone after injury induction and cell/saline injection.

4.1.2.4.1 Scar Size Analysis

Scar size analysis was performed using the Masson's Trichrome Staining. Trichrome allowed visualization of cardiac muscle fibers (red) and fibrotic scar tissue (blue) by staining the collagen. Representative pictures are shown in the figure below (Figure 29) panels A-C. Scar size assessment revealed that the myocardial infarction model produced scar size of approximately 35-50% of the left ventricle (panel D). There was no significant difference in the scar size between the saline –treated and the empty- and IGF-1Ea-cells transplanted groups (45.42 +/-9.74% saline vs. 47.30 +/- 3.64% empty-cells transplanted and 45.42 +/-9.74% saline vs. 41.59 +/- 1.50% IGF-Ea-cells transplanted, $p>0.05$, $n = 3$ per group). Similarly, the scar sizes of the IGF-1Ea- and the empty-cells injected hearts were not significantly different (47.30 +/- 3.64% empty-cells vs. 41.59 +/- 1.50% IGF-Ea-cells transplanted, $p>0.05$, $n = 3$ per group).

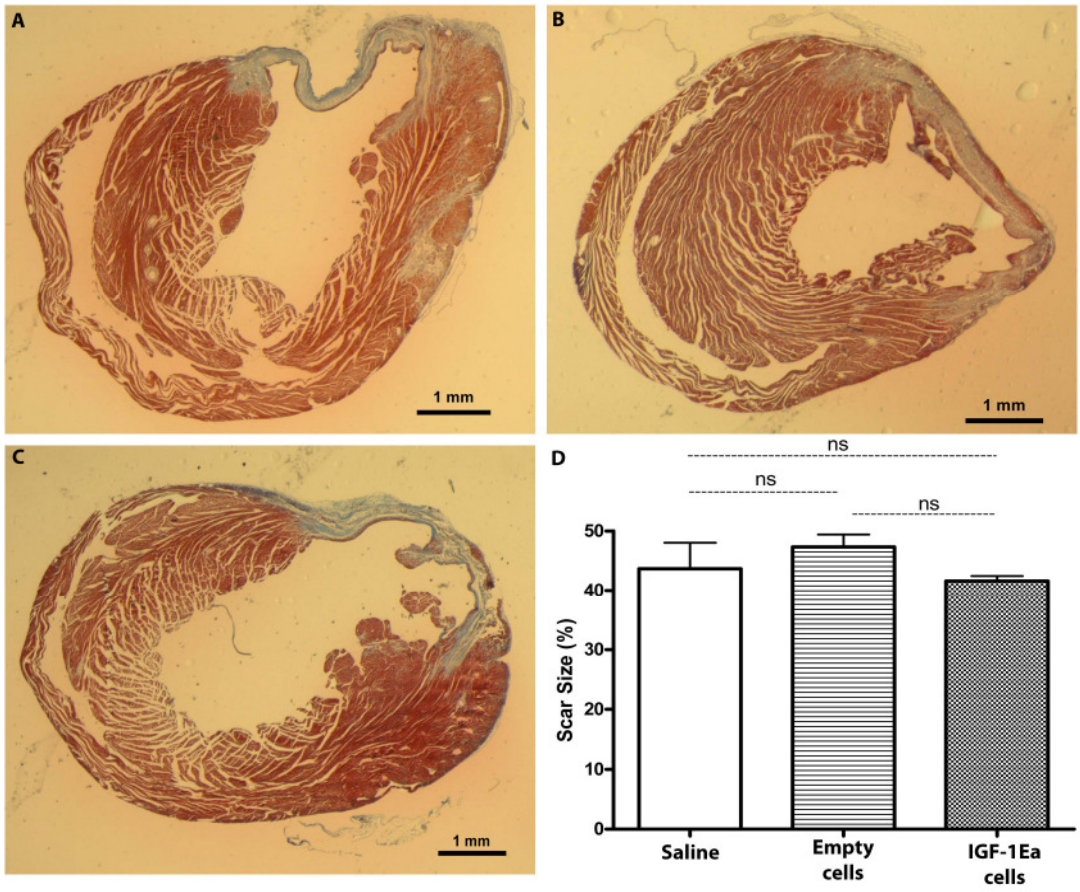

Figure 29. Scar Size Analysis by Trichrome Staining. 3-4 months old WT C57BL6-J mice were subjected to myocardial infarction and saline/cell transplantation. 2 months after the treatments, samples were collected for histological analysis. 10µm transverse sections were cut and trichrome staining was performed. Representative images of saline (A), empty-cells (B) and IGF-1Ea-cells treated infarcted hearts. Image (D) illustrates quantitative analysis of the scar size. Three hearts were analyzed per group (n=3) and scar size is presented in percentage. The analysis revealed no significant difference in the scar size between the cell transplanted and the saline treated hearts, p>0.05. Similarly, there was no significant difference between the IGF-1Ea-cells treated hearts compared to the empty-cells treated hearts, p>0.05. Images were captured using LEICA MZFLIII microscope at 1.25X magnification. Statistical analysis was conducted using the non-parametric one-way ANOVA test (Kruskal-Wallis Test). Values are Mean +/- SEM.

In summary, the findings suggested that MI caused induction of 35-50% left ventricular scar. The size of the scar could not be reduced by transplantation of cells, possibly due to lack of/ insufficient engraftment of the transplanted or native stem cell population at the site of injury. The following analyses were conducted to trace the transplanted cell by anti-GFP staining.

4.1.2.4.2 Cell-engraftment Assessment

The heart samples were examined for engraftment of the GFP positive donor cells. This was conducted through both immunofluorescence and immunohistochemistry with anti-GFP staining. 10µm transverse sections of the hearts were de-paraffinized and subjected to

antigen retrieval as described in materials and methods. The immunofluorescence examination showed that the saline-injected samples ((Figure 30), panels A and B), which did not receive GFP cell-injection, were highly positive for the staining due to auto-fluorescence resulting from the samples. Autofluorescence can result from artefacts introduced during injury induction and inflammation of the tissue, immune activation and cell death (reviewed in [220])**.** Van Laake et al. [220]have reported a method based on examining emission wavelength spectra of GFP (peak at 515nm) and autofluorescent dead cells (peak at 550nm). The method successfully eliminates autofluorescence resulting from the dead cell artefacts. As it was not possible to conduct cell-engraftment assessment on paraffin embedded tissue sections using traditional fluorescence technique, future analysis should utilize the technique described above for eliminating background fluorescence, on cryo-sections instead of paraffin sections. Due to lack of technical success, immunofluorescence was then replaced by immunohistochemical analysis for tracing the transplanted cells.

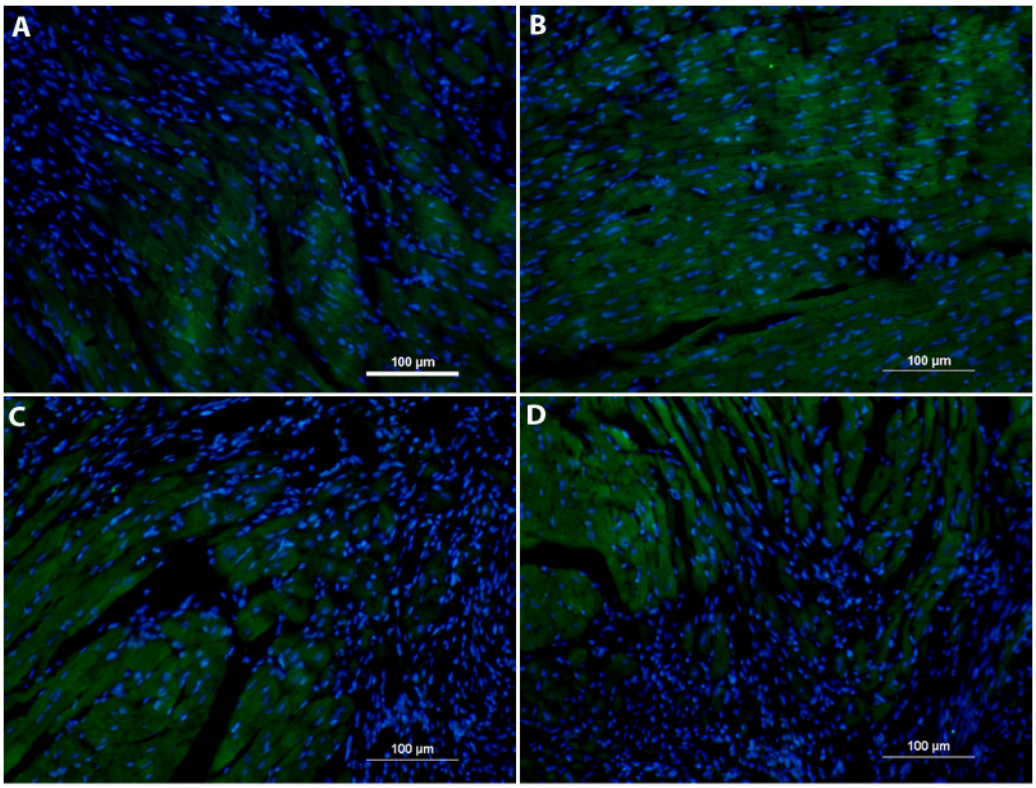

Figure 30. Cell Engraftment Assessment by anti-GFP Staining using Immunofluorescence Technique. Panel (A) is a representative image of negative control of saline treated sample. Panel (B) saline treated sample treated with both the primary and secondary antibodies. Images (C) and (D) were empty-cell and IGF-1Ea-cell transplanted hearts respectively. Images were acquired at the border zone. Scale bars are 100µm and DAPI was used for staining cell nuclei.

Through immunohistochemical analyses, immunoreactivity was observed to the GFP antibody in cells-injected hearts (Figure 31 , panels B and C). Saline-injected hearts presented a pale aspecific staining for GFP (panel A) whereas, IGF-1Ea and empty-cells injected hearts showed specific staining for GFP (left lane, panels B-C compared to the centre lane B-C). The IGF-1Ea-cells injected hearts showed higher number of GFP positive cell clusters than the empty-cells injected hearts (right lane, panels B and C). The quantification of engrafted cells was performed only visually on tissue sections. For better understanding of the amount of engrafted cells, future study should utilize quantification methods that involve isolation of cells after transplantation. One such approach could be FACS analysis and sorting of the transplanted cells. Although GFP positive cells were retained in the scar tissue of the transplanted hearts, they did not appear to integrate physically with the recipient tissue. They were in clusters and presented a spherical shape (right lane, panels B and C). Negative controls (centre lane, panels A-C) were treated only with biotin-conjugated secondary antibody. The results showed herein were produced from two animals per group (n=2). The figure below shows representative images for the different treatment groups.

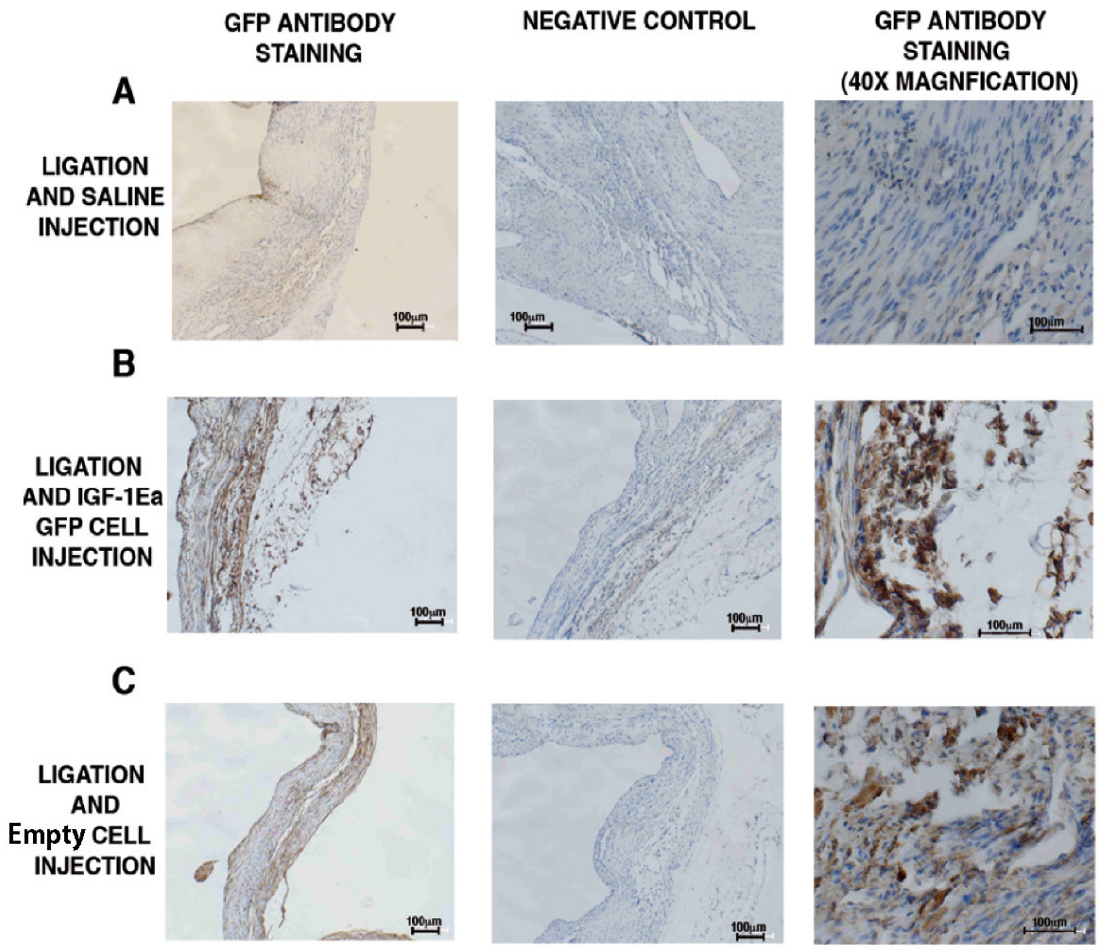

Figure 31. Cell Engraftment Assessment by anti-GFP Staining using Immunohistochemical Technique. Panel (A) are a representative images of saline treated sample. Panel (B) and (C) were IGF-1Ea- and empty-cells transplanted hearts respectively. For all the figures, left and central panels are taken at 10X magnification, whereas right panels at 40X magnification. Central panels showed control samples stained with only the secondary antibody. Images were acquired at the scar region. Scale bars are 100µm and haematoxylin was used for staining cell nuclei. n= 2 per sample type.

In summary, the immonohistochemical analysis showed that IGF-1Ea over-expressing cells engrafted better than the empty-cells, possibly due to their greater survival ability to deleterious environment previously observed *in vitro* (Chapter 3, Section III). However, the level of engraftment achieved did not confer function preservation at long-term and reduce scar size. Nevertheless, following the assessments of scar size and cell engraftment, the histological samples were utilized for capillary density analysis to examine whether injury and cell transplantation affected capillary density.

4.1.2.4.3 Capillary Density Assessment

Capillary density assessment was performed by immunohistochemical labelling of the endothelial cells by Isolectin B4. Three fields of 500um^2 area each per sample was considered for counting the Isolectin B4 positive capillaries at the border zone. Panel A shows a representative image of a border zone. Although there was a tendency for higher Isolectin B4 staining in the cell transplanted samples, no significant difference was observed between the capillary densities of the saline or cells transplanted groups, p=0.16. IGF-1Ea-cells transplanted hearts showed 79.10 +/- 21.70 Isolectin B4-positive capillaries (panel D), empty- cells transplanted hearts showed 64.50 +/- 20.80 (panel C) and saline-injected hearts showed 58.30 +/- 11.85 (Panel B). Figure below (Figure 32) illustrates these findings. The Isolectin B4 stained capillaries are stained brown, and nuclei blue.

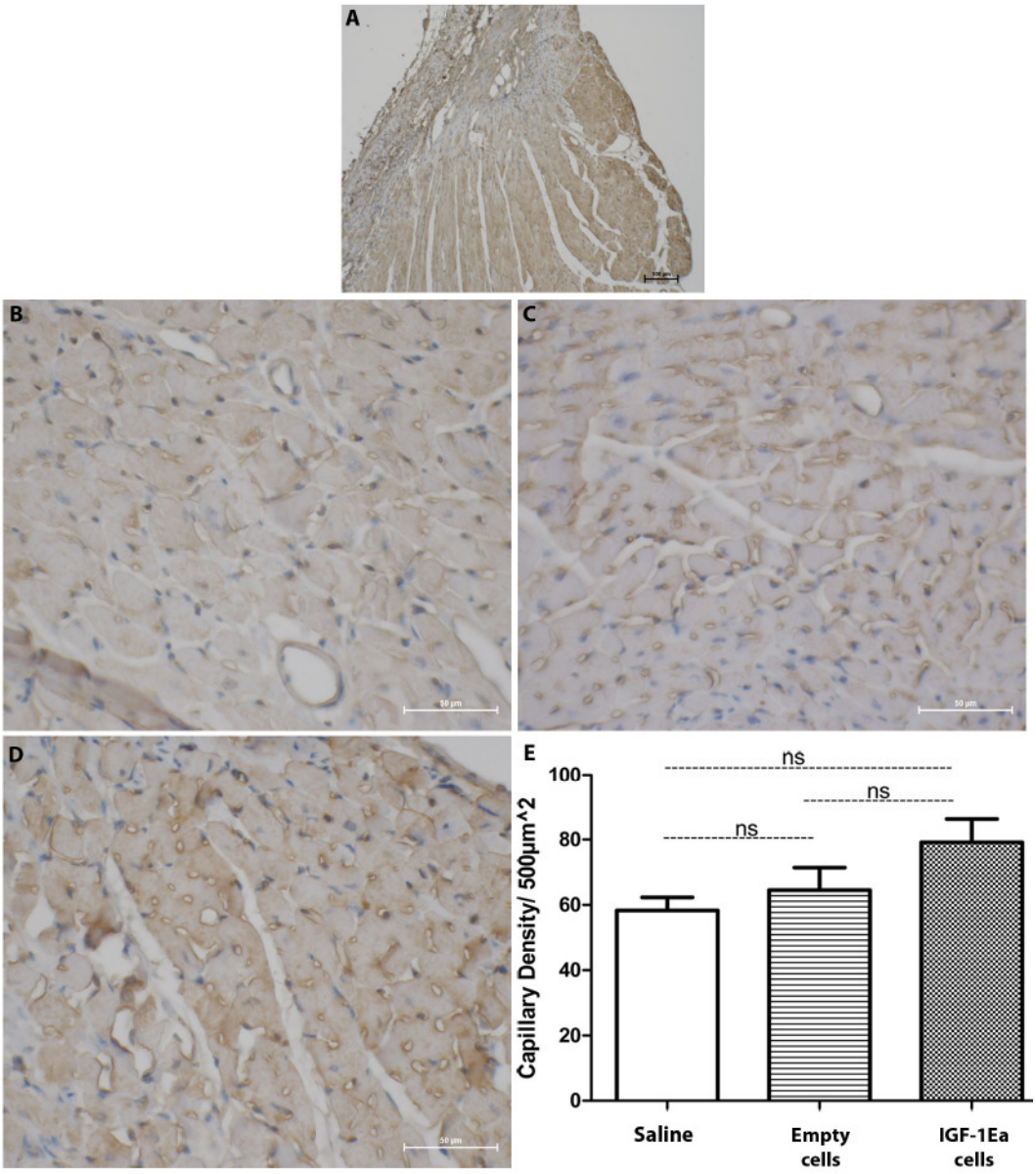

Figure 32. Capillary Density Assessment. Capillary density analysis was performed by Isolectin B4 immunohistochemical labelling of the 2 month tissue samples. Samples were 10um paraffin sections. Panel (A) is a representative image of the border zone, where the capillary density assessment was performed. Three fields of 500µm^2 area each were considered per sample for the assessment. Panels (B), (C) and (D) are representative images of one of the fields analyzed for Saline, empty-cells and IGF-1Ea-cells treated hearts respectively. Panel (D) illustrates the non-parametric one-way ANOVA analysis showing no significant difference in the capillary density between all of the three groups analyzed, p=0.16. n = 3 per group. Values are Mean +/-SEM. Scale bar for image (A) is 100µm and 50µm for the rest of the images.

The capillary density assessment also showed no significant difference between the different treatment groups, corroborating with the functional and scar size analyses. In addition to the histological analyses, long-term samples were examined also for the expression of the paracrine factors examined at short-term to understand whether there were changes in the expression profiles of these factors at long-term compared to the short-term time-point.

4.1.2.5 Molecular Analyses of Long-term Samples

Real time PCR analyses were performed with the 2-month infarction induced and cells/saline injected hearts to analyse at mRNA level, the expression of the paracrine factors IGF-1, Elastin, VEGFa, SDF-1, IL6 and IL10. No significant difference was observed between the WT control versus the infarcted cell/saline treated groups: p=0.08 for IGF-1, p= 0.08 for Elastin and p=0.17 IL6 genes. Interestingly, VEGFa expression was significantly higher in IGF-1Ea-cells transplanted hearts than the WT controls and the saline-treated hearts, p=0.02. No significant difference was observed in VEGFa expression between the empty-cells transplanted hearts compared to the WT and saline-treated hearts as well as between the IGF-1- and empty-cells transplanted hearts, p>0.05. SDF-1 expression on the other hand was significantly lower in IGF-1Ea transplanted hearts compared to all other groups. There was no difference in SDF-1 expression between all the other groups. IL10 mean relative expression was significantly higher in the empty-cells transplanted hearts compared to the WT controls, p=0.03 whereas there was no significant difference between all other groups. Statistical analyses were performed using the non-parametric one-way ANOVA (Kruskal-Wallis test) in Prism. Values are Mean +/- SEM. For all the treatment groups n = 3. The figure below (Figure 33) illustrates the findings.

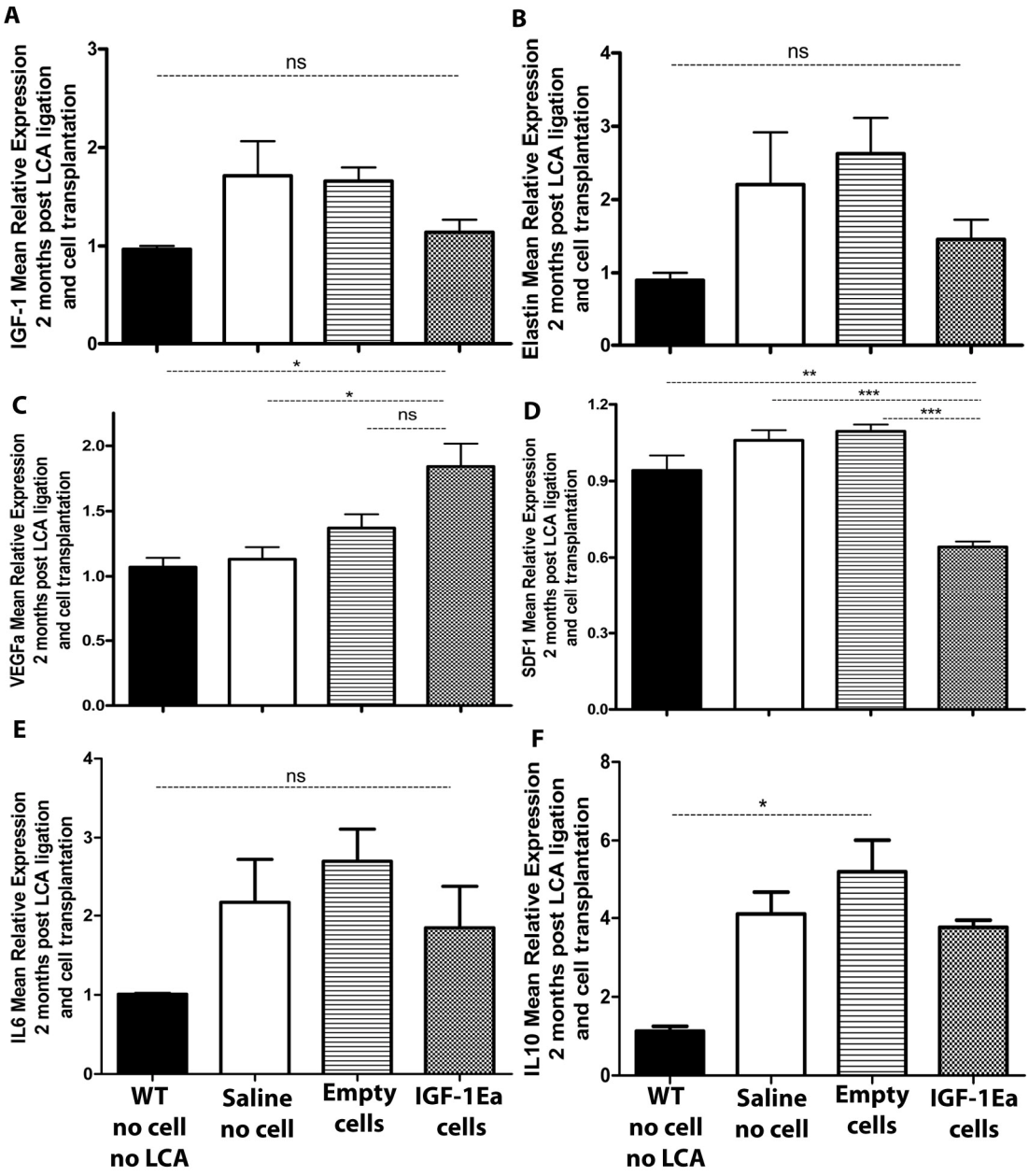

Figure 33. Mean Relative Paracrine Factors Expression with 2-month Samples. Real time PCR analyses were performed with 2 months post infarction and cells/saline treated hearts. For all the treatment groups n=3. (A) IGF-1, (B) Elastin, (C) VEGFa, (D) SDF-1, (E) IL6 and (F) IL10 mean relative expressions. No significant difference was observed between the WT control versus the infarcted cell/saline treated groups ($p>0.05$) for IGF-1, Elastin and IL6 genes. VEGFa expression was significantly higher in IGF-1Ea-cells transplanted hearts compared to the WT controls and the saline treated hearts, $p<0.05$. The SDF-1 expression was significantly lower in IGF-1Ea-cells transplanted hearts compared to all other groups, $p<0.01$= ** and $p<0.001$= *. There was no difference in SDF-1 expression between the other groups. IL10 mean relative expression was significantly higher in the empty-cells transplanted hearts compared to the WT controls, whereas there was no significant difference between all other groups. Statistical analyses were performed using the non-parametric One-way ANOVA test (Kruskal-Wallis test) in Prism. Values are Mean +/- SEM.**

Taking together the capillary density assessment and the molecular analysis on paracrine factor expression, transplantation of IGF-1Ea-cells modulated the transcript levels of pro-angiogenic factors, VEGFa and SDF-1 without altering capillary density. The activity of

these factors could therefore be important after injury induction in regulating the response of cardiomyocytes, rather than endothelial cells. It has been previously shown that VEGFa and SDF-1 may contribute to cardiomyocyte hypertrophy [221, 222]. In cardiomyocytes, VEGF drives cardiac hypertrophy or its regression, depending on its binding to VEGF2R (also known as KDR) or VEGF1R (also known as Flt-1), respectively Therefore, molecular and histological analyses were carried out to examine the properties of the native cells after injury and cell/saline injection.

4.1.2.6 Molecular and Histological Analysis of the Recipient Tissue for Hypertrophic Response

The histological analysis examined cell-cross sectional area of the border zone cells and the molecular analysis investigated expression of VEGF2R (KDR) at protein level and beta Myosin Heavy Chain (bMHC) and skeletal actin (aSK) at mRNA levels as markers of hypertrophy. Real time PCR analyses were conducted to quantify expression levels of aSK and bMHC (Figure 34**,** panels A and B). The data showed that aSK expression was significantly up-regulated in the empty cell-injected hearts compared to the WT, IGF-1Ea-cell and saline-injected hearts (Panel A**).** bMHC expression on the other hand, was significantly up-regulated in saline treated animals compared to the WT controls and the IGF-1Ea-cells injected animals (Panel B). Although not significant, the empty-cells transplanted samples also showed reduced bMHC expression compared to the saline injected hearts.

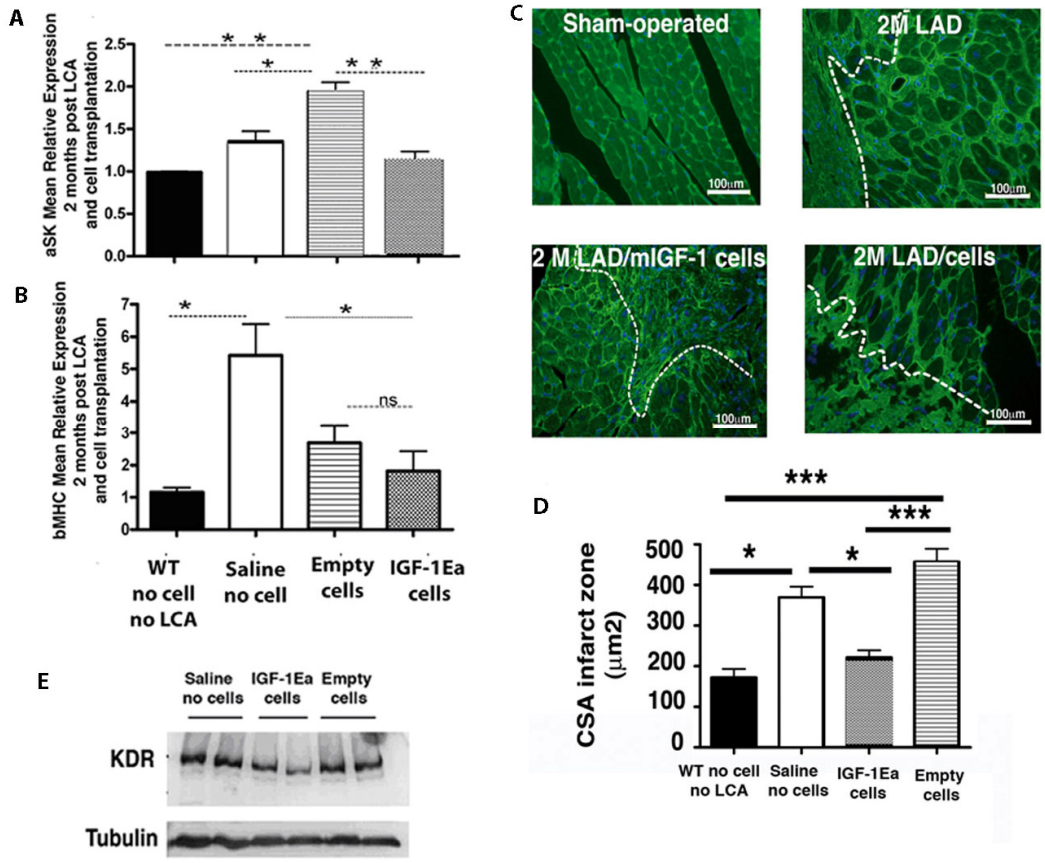

Figure 34. Molecular and Histological Analyses for Hypertrophic Response. Real time PCR analyses were performed with 2 months post infarction (LAD ligation) and cells/saline treated hearts. For all the treatment groups n=3. (A) aSK and (B) bMHC. Real time PCR was performed with Applied Biosystems probes as indicated in Material and Methods. Panel (C) shows analysis of cross-sectional area (CSA) of cardiomyocytes measured by Wheat Germ Agglutinin staining on 5 µm tissue samples of WT, saline, empty- and IGF-1Ea-cells (mIGF-1) injected hearts. The open lines mark the border for the scar from the non-scar tissue. Nuclei were stained with Hoechst dye. Images were acquired by a Nikon digital Camera DXM1200F. Statistical analyses were performed using the One-way ANOVA in Prism and shown in Panel D. Values are Mean +/- SEM. (E) KDR expression by western blot analysis. KDR was normalized with alpha-tubulin and its quantification was performed with n=2 per experimental group.* indicates p<0.05, ** p<0.01 and *** p<0.001.

The response to hypertrophy in cardiomyocytes exposed to VEGFa expression could be explained by the regulation of VEGFa receptor KDR. Western blot analysis showed mildly lower KDR expression for IGF-1Ea-cells transplanted heart samples compared to the saline and empty-cells treated hearts (Panel E). Cross-sectional area (CSA) analysis showed that cardiomyocytes bordering the scar tissue in the hearts that received IGF-1Ea-cells had significantly lower CSA compared to the saline and the empty cell-injected hearts (Panels C and D). The CSA of cardiomyocytes bordering the scar tissue of the

empty-cells injected hearts on the contrary were significantly higher than the WT, saline and IGF-1Ea-cells treated hearts.

In summary, these data showed that myocardial infarction induced by occlusion of the left coronary artery led to left ventricular (LV) remodelling, which was marked by hypertrophic cells and up-regulation of hypertrophic markers. Transplantation of empty-cells had no effect on LV remodelling however, transplantation of IGF-1Ea-cells resulted in lower hypertrophy compared to the empty-cells transplanted hearts suggesting that IGF-1Ea cells might play a role on modulating LV remodelling by directly or indirectly involving VEGFa and/or SDF-1 molecules. As the molecular analysis of 2 month heart samples on IGF-1 transcript expression (Figure 28) did not show a difference between the empty- and IGF-1Ea-cells transplanted hearts, the observed LV remodelling effect however might be resulting from other factors than IGF-1Ea as a result of transduction of IGF-1Ea vector.

4.1.3 DISCUSSION

The objective of this chapter was to test if function of impaired hearts caused by myocardial infarction could be improved by transplantation of the IGF-1Ea transduced P19Cl6 cells. The myocardial infarction induction and cell transplantation were successfully performed. First analysis was performed on survival of surgical animals following myocardial infarction and cell transplantation. The total intra- and early post myocardial infarction mortality was considered as reported by Fuchs et al. to be occurring between 0 and 3 days following surgery [223]. It was found to be 34.92% in this study (22 out of 63). The total number of animals that survived the surgical procedure for up to 2 months was 35 out of 63, (55% survival rate for the procedure).

The echocardiographic analyses on Ejection Fraction, Fractional Shortening and Fractional Area Change revealed that cell transplantation mildly preserved cardiac function at short-term, although statistically not significant. The functions of hearts receiving the IGF-1Ea- and empty-cells were not significantly different from one another indicating that transplantation of both the cell types contributed similarly to heart function at short-term. Possible explanation for the lack of difference in functional preservation between the two cell types could be attributed to their similarities, for instance both the

transplanted empty and IGF-1Ea transduced cells expressed IGF-1 (Figure 19). Further analyses on the properties of the two cell types would be necessary to understand if the cells shared other features that led to this outcome. The long-term functional analyses showed further significant reduction in the function of the cell transplanted hearts to the level of the saline-injected hearts, indicating that cell transplantation did not preserve function at long-term.

Studies have reported that transplantation of cells leads to release of paracrine factors either directly from the transplanted cells or indirectly from the native tissue, resulting in better survival of the native tissue, reduction of scar size, enhanced homing of stem cell population from other sources and improved left ventricular systolic function. To investigate whether the paracrine factors described by previous studies to induce cardiac function recovery, such as IGF [224, 225], Elastin [29], SDF-1 [219], VEGFa [226], IL10 [227] and IL6 [228] were altered, mRNA level analyses were performed with both the short-term and the long-term samples. The tendency on function observed at short-term could not be conferred to the factors analyzed. It has been reported that release of specific factors, such as SDF-1, is time-dependent and increased levels of SDF-1 have been observed three days after myocardial infarct induction [222]. Therefore, earlier time points after myocardial infarct induction than 5 days should be analysed to explain the effect on short-term function we have observed. There was also no significant difference in the expression patterns of these molecules between the saline-treated versus the cells-treated hearts, suggesting that the tendency in preservation of function observed in this specific time-point was not induced by the particular factors. We can speculate that other factors of neurohumoral origin or released by the renin-angiotensin web system could have a higher impact in cardiac function by regulating contractility. Therefore, to understand what other factors, if any, than the ones analyzed could contribute to the tendency for short-term maintenance of function, a gene array analysis should be utilized. In addition, it would be imperative to analyze GFP gene expression to show that the cells engrafted at short-term as well as long-term at mRNA level, which would additionally support the histological observation that at long-term cells engrafted.

The cell engraftment analyses using immunofluorescence and immunolabeling techniques on paraffin sections were both challenging due to autofluorescence encountered from artefacts, which could be tackled in future by using the method described earlier in section

4.1.2.4.2. Despite the observed problem, transplanted GFP positive cells were detected in the scar tissue of some hearts, although quantification of the actual number of engrafted cells with certainty was not possible in the paraffin embedded tissue sections. The transplanted cells were not organized in a syncitium, indicating that integration with the remaining cardiomyocytes was not achieved. Intramyocardial injection of the cells was successful with regard to cell maintenance in the injured site and the combination of the pro-peptide IGF-1Ea enhanced homing of the transplanted cells, based on tissue observation. As seen in the *in vitro* analysis (Chapter 3), IGF-1Ea over-expression could have conferred higher protection to the cells from deleterious events *in vivo,* leading to their enhanced homing compared to the empty-cells. However, cells did not integrate and contribute to maintain long-term cardiac function, even having a ventricular origin. Given the relative lack of efficacy in this study and previous cardiac regeneration studies, it is clear that future cell therapy approach must improve the efficiency and integration of the transplanted cells to the injured tissue to achieve a lasting maintenance of function. Future analysis to quantify cell engraftment must also consider re-isolating the transplanted cells and conduct analyses to confirm their number and existence to avoid technical problems encountered by the present study, and most importantly for quantification which is not solely based on tissue observation.

Scar measurement analysis showed no significant difference in scar size between the cell-transplanted and the saline treated groups. Although cell tracing assessment was able to detect homing of the donor cells, the extent of homing was not enough to reduce scar size. Reduction of scar size could be obtained by improving retention of the transplanted cells. Study by Hattori et al. have reported that cells get instantly washed out upon transplantation via the coronary circulation leading to their lower availability for engraftment [229]. They reported that 30-50% of the injected cells were washed out of the heart within 10 minutes of cell injection. This study was supported by an *in vivo* study conducted on rats. Dow et al. injected directly into the left ventricular wall of either re-perfused or permanently occluded rat hearts [230]. The cell injections were performed at 15 and 75 minutes post treatments respectively with 5*10^6 cells. The study recovered the donor cells in both the heart and the lungs in 100% of the animals. Furthermore, cells were also discovered in capillaries, kidney and spleen suggesting that the direct injection of cardiomyocytes does not represent the ideal mode for cell transplantation studies. Taking these studies into account, it is likely that donor cells were instantly washed out in

this study, resulting into insufficient homing and lack of improvement in scar size. Therefore, future cell transplantation studies could be performed with cell sheets or 3D engineered tissues that are harder to disperse than single cells. Transplantation of 3D cell sheets would in addition also aid cell tracing analyses, which is still a big challenge for cell transplantation studies.

Despite homing of the donor cells, the capillary density, scar size and functional analyses were all unaffected by transplantation of cells. Analysis of the paracrine factors with the long-term samples on VEGFa, SDF-1 and IL10 however showed a significant difference between the saline- and the cell-injected hearts. VEGFa was up-regulated in IGF-1Ea cell-injected group compared to the other groups, whereas SDF-1 was significantly down-regulated. Moreover, the differential modulation of these pro-angiogenic factors did not correlate with capillary density, which showed no significant difference between the saline treated and cell transplanted groups. The activity of these factors could therefore be important after injury induction in regulating the response of other cell types, rather than endothelial cells. It has been previously shown that VEGFa and SDF-1 may contribute to cardiomyocyte hypertrophy [221, 222]. In cardiomyocytes, VEGF drives cardiac hypertrophy or its regression by regulating availability of VEGF1R or VEGF1R by binding to VEGF2R (also known as KDR) or VEGF1R (also known as Flt-1) [221]. Molecular and histological analyses on hypertrophic response of the recipient tissue revealed that IGF-1Ea cell transplantation led to less hypertrophic native cells and decreased bMHC, aSK and KDR expression. These findings suggested that transplantation of IGF-1Ea transduced cells may preserve cells from hypertrophy by modulating VEGFa and SDF-1 expression. However, to understand whether the observed lowering of hypertrophy was due to direct effect of IGF-1Ea cell transplantation on VEGFa and SDF-1 expression or indirect effect via involvement of other factors, further investigation employing inhibition of VEGFa and SDF-1 would be necessary. The molecular analysis of 2 month heart samples on IGF-1 transcript expression (Figure 32) did not show a difference between the empty- and IGF-1Ea-cells transplanted hearts. This suggested that the observed LV remodelling might be resulting from other factors released from the IGF-1Ea transduced cells. *In vitro* studies involving analysis of conditioned media from IGF-1Ea and empty-cells will be necessary to answer what other factors, might be involved to protect cells from hypertrophy. In addition, further analysis should be conducted to

understand whether IGF-1Ea alone could confer this beneficial effect or a combinatorial therapy employing cell and IGF-1Ea is necessary to achieve this.

The empty-cells transplanted hearts expressed significantly higher IL10 than the other treatment groups. IL10 could in part protect the heart from further damage. IL10 modulates endothelial cell proliferation and it has been shown to protect the heart from deleterious cardiovascular remodelling by decreasing the amount of T lymphocytes in cardiac tissue after infarct and by regulating cardiac hypertrophy [227]. Burchfield et al. [227] showed that transplantation of Bone Marrow Mononuclear Cells (BM-MNCs), which released IL10, contributed to improved LV function after myocardial infarction, by decreasing T lymphocyte accumulation, reducing reactive hypertrophy and myocardial collagen deposition. With respect to cell cross-sectional area measurement, hearts receiving empty-cells showed significantly higher area than the wild type and IGF-1Ea-cell transplanted hearts suggesting that transplantation of these cells, unlike IGF-1Ea cells, did not preserve native cells from hypertrophy. Increased IL10 expression in the empty-cells transplanted hearts therefore did not lower cardiomyocyte hypertrophy. The lack of reduction on cardiac hypertrophy correlated with their long-term functional analyses that there was no preservation of function. Even though IGF-1Ea cell transplanted hearts showed lower hypertrophy than the empty-cells transplanted hearts, functional analyses at long-term for IGF-1Ea cells transplanted hearts also did not show any maintenance of function suggesting that reduction of hypertrophy alone probably does not confer better function.

In summary, the present study was able to achieve a tendency for maintenance of function at short-term upon both the empty- and IGF-1Ea-cells transplantation. It was however not able to show similar effect at long-term, although the cell transplanted hearts continued to show a tendency for better function than the saline-injected hearts. Nonetheless, combinatorial P19Cl6 and IGF-1Ea therapy was able to confer protection to cardiac cells from hypertrophy that could be beneficial to the recipient hearts. Therefore, this study proposes a novel mechanism that could regulate cardiac repair and induce beneficial cardiovascular remodelling in cell/ growth factor therapy. However, regeneration of the scar tissue to improve its function is still a challenge to be met. Figure below (Figure 35) shows the mechanism proposed by our hypertrophy analysis.

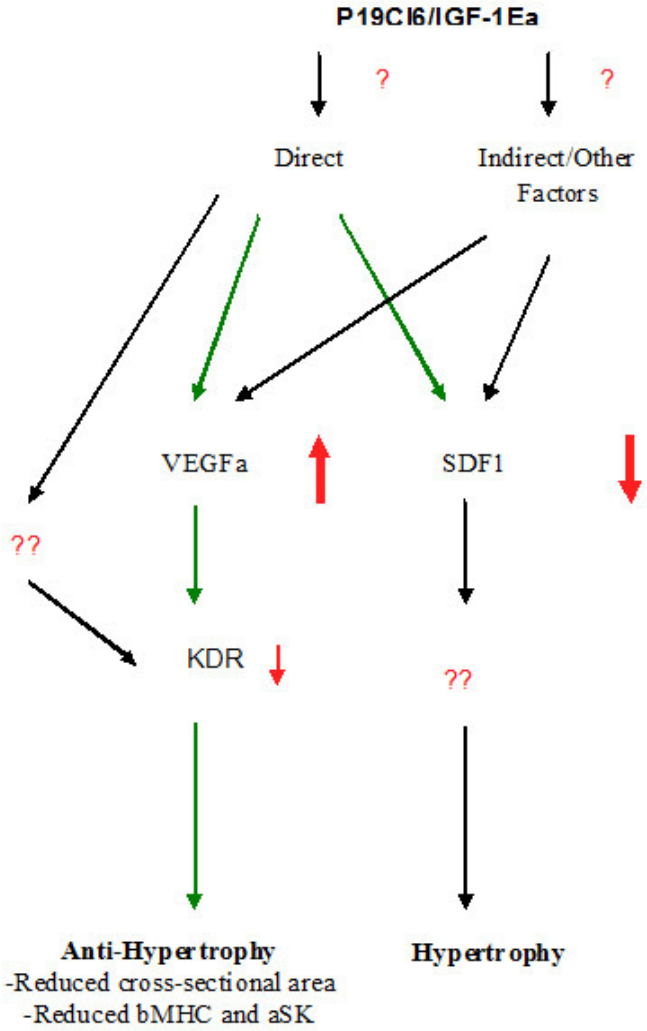

Figure 35. Mechanism of P19Cl6 cells and IGF-1Ea mediated amelioration of injured tissue. IGF-1Ea over-expressing cells conferred protection against hypertrophic response. IGF-1Ea-cell transplantation decreased cardiomyocytes cross-sectional area and induced a molecular signaling modulating the expression of vascular endothelial growth factor (VEGFa) and stromal-derived factor 1 (SDF-1). Down-regulation of SDF-1, up-regulation of VEGFa expression and down-regulation of VEGF2R (KDR) led to a differential cellular response independently of vessel formation and possibly regulating hypertrophic signaling. The green arrows show the signaling mechanism observed so far. Direct pathway refers to pathway that is conferred directly by IGF-1Ea and indirect pathway by involving other factors between IGF-1Ea and VEGFa/SDF1, which regulate expression of VEGFa and SDF1 upon interaction with IGF-1Ea. A direct regulation of KDR promoter by IGF-1Ea protein can not be excluded.

CHAPTER 5

5.1 GENERAL DISCUSSION

This was the first study that attempted to engineer pluripotent P19Cl6 cells to express IGF-1Ea for cell-based regeneration of infarcted hearts. The study utilized cell-based delivery of IGF-1Ea instead of pharmaco- or gene-therapy to obtain a controlled and sustained expression of the gene. The principal objectives addressed were: (i) stable transduction of P19Cl6-MLC2v-GFP cells with IGF-1Ea gene and tetracycline regulation of the gene expression, (ii) study the effect of IGF-1Ea transduction on properties of the engineered cells, (iii) test feasibility of the engineered cells for cell therapy in an *in vitro* system and (iv) test if transplantation of IGF-1Ea over-expressing cells improves function of the injured hearts and if they are superior to the control cells.

I was successful in engineering P19Cl6-MLC2v-GFP cells over-expressing IGF-1Ea through stable transduction of the gene using a lentiviral vector. Tetracycline -regulated expression of IGF-1Ea could not be accomplished in the P19Cl6 cells but was achieved in HT1080 cells, the reasons for which remain unknown. Nevertheless, the gene expression was successfully achieved at high amount in a constitutive manner, which fulfilled the goal of producing sustained IGF-1Ea expression. The engineered cells maintained efficient differentiation into ventricular cardiac myocytes. The resulting cardiac myocytes exhibited structured organization of the sarcomeric alpha actinin protein that is vital for contractile function and the differentiated cell clusters showed calcium induced calcium release mechanism, which is essential for conducting electromechanical function. Additionally, in vitro analyses revealed that the IGF-1Ea over-expression conferred increased survival to the cells against prolonged hypoxia exposure. Likewise, the IGF-1Ea conditioned media was efficient to protect neonatal cardiac myocytes from apoptosis, indicating that the constitutively expressed IGF-1Ea granted more than self-protection. . Taken together, the *in vitro* data indicated that IGF-1Ea-transduced cells represented an attractive candidate for cell therapy. With the exogenous delivery of the cells and potential prevention of further damage from IGF-1Ea over-expression, the transplantation of the IGF-1Ea transduced cells appeared to hold potential for preserving function of hearts after infarction.

As the *in vitro* analysis of the IGF-1Ea-transduced cells on their feasibility for cell transplantation therapy proved successful, the engineered cells were then transplanted into

allogeneic wild type murine hearts with acute myocardial infarction. The goals here were to analyze whether the impairment of function owing to the injury could be prevented by cell transplantation and if IGF-1Ea over-expressing cells were superior to the control cells with regard to efficiency of engraftment, tissue regeneration, scar size reduction and function preservation.

Functional analyses were conducted at short- and long-term (5 days and 2 months respectively) post-infarction induction and cell transplantation. The short-term analyses revealed a trend for prevention of deterioration of function for cell transplanted animals compared to the saline treated animals, but there was no significant difference between the empty-cells treated compared to the IGF-1Ea-cells transplanted hearts, suggesting that the observed effect on function was merely a result of cell transplantation and not IGF-1Ea expression. The absence of differences in function between the IGF-1Ea-cells and the empty-cells transplanted hearts could have resulted from the *in vitro* observation (Figure 19) that also the control cells produced high amounts of endogenous IGF-1 following their differentiation. This outcome was not initially anticipated. Therefore, to be able to deduce that the observed functional maintenance in short-term studies was solely due to cell transplantation and not due to IGF-1Ea expression, future studies must utilize an additional cell type as a control that is unable to produce IGF-1 upon their differentiation.

The effect of cell transplantation on function at short-term was further investigated at molecular level. Cell transplantation studies utilizing foetal cardiomyocytes [231-233], ESC [67-69, 234, 235], skeletal myoblasts [56, 57, 236], MSC [43, 45-47, 237-239], CPC [36] and iPS cells [60-62] have been conducted in various model systems. Some of these studies have demonstrated that the transplanted cells differentiated into cardiomyocytes and survived after cell transplantation [67, 69, 71, 233, 240], subsequently improving function of the injured hearts. However, in some of these studies, the improved function could not be directly linked to the transplanted cells and their number therefore a paracrine effect has been suggested [43, 45-48]. Therefore, to understand the tendency in short-term maintenance of function, paracrine effect was investigated at molecular level.

Paracrine factors namely, IGF-1, Elastin, VEGFa, SDF-1, IL6 and IL10 were analyzed by qRT-PCR. Interestingly, the expression of none of these factors was significantly different in the cell transplanted compared to the saline treated hearts. Similarly, there was also no

significant difference in their expressions between the injured and the wild type controls, although a tendency was observed for increased expressions of IGF-1, Elastin, IL6 and IL10 in all the injured hearts, independent of cell or saline transplantation. This tendency was merely due to injury as there was no difference in expressions of these factors between the saline treated compared to the cells transplanted hearts. It is reported in several studies that some of the paracrine factors studied here are modulated by induction of myocardial infarction. Circulating levels of IL6 are up-regulated post-myocardial infarction [223], where the level peaks at days 1 and 2 and remains higher than the physiological level even after 12 weeks [241]. Similarly, Reiss et al. reported in an acute myocardial infarction model, enhanced expression of both IGF-1 receptor and IGF-1 from 12h up to 7 days post injury induction [242].

Taking the findings of these studies, it is possible to conclude that the observed tendency for up-regulation of some of these factors was due to injury. Comparing the short-term functional analyses to the short-term molecular analyses, the observed tendency for maintenance of function with cell transplantation could not be linked to the examined paracrine factors. The reason for this observation in function could be due to paracrine factors other than the ones investigated, which could be understood better with a gene array analysis. It could very well be due to engraftment of cells, which was not analyzed at short-term. Histological analysis at 2 months showed homing of the transplanted cells therefore, the tendency for maintenance of function was most likely due to cell homing. It is important to emphasize however that the number of animals used for the molecular analyses was only 3 per group, which resulted into a very high standard deviation. Therefore, future study should employ more animals per experimental group to account for the variability, which results from individual differences and LCA ligation. In addition, at 5-day time-point, the functional analysis is not very reliable as the injured tissue is undergoing remodelling events that lead to immense disturbance in data acquisition. Therefore, it is likely that the tendency in function maintenance observed at short-term is due to great variability in data acquisition rather than a true observation.

At long-term however, even the tendency for maintenance of function observed at the short term analyses was lost, which could have resulted from numerous factors. It could be due to insufficient engraftment of the transplanted cells, lack of coupling of the transplanted cells with the host tissue or due to expansion of the damage such that the

transplanted cells suffered from the expansion. The cell tracing analyses showed that the transplanted cells were retained in the tissue and that IGF-1Ea over-expression enhanced cell homing. However, coupling of the donor cells with the host myocardium was not achieved and the cells remained in the scar tissue as separate cell clusters. Therefore, the deterioration of long-term function observed in this study could be attributed to lack of coupling of the transplanted cells with the recipient tissue.

Cell transplantation studies show discrepancies regarding engraftment of transplanted cells and functional improvement. Studies that utilized fetal, neonatal rat and embryonic cardiomyocytes transplantation into infarcted rat hearts reported engraftment of all of these cell types [232, 243, 244]. On the contrary, Watanabe et al. when transplanted fetal and neonatal pig cardiomyocytes and cardiac-derived HL-1 cell line into injured and uninjured pig hearts, found no survival and grafting of the transplanted cells [75]. Very recently however, more studies have shown long-term engraftment and enhancement of function [71, 93, 245]. However, van Laake [93] reported that even with long-term survival of the graft, the observed maintenance of function was lost at 12 weeks suggesting that the graft size could still be a limiting factor. The discrepancies observed in these studies might have resulted from differences in their animal models, donor cell types and their differentiation states, and on the status of the host myocardium at the time of cell transplantation and grafting.

Taking these discrepancies into consideration Reinecke et al. [246] studied the effects of developmental state of donor cells and of myocardium at the time of engraftment. They injected fetal, neonatal and adult cardiomyocytes into both cryo-injured and uninjured hearts and reported that the adult cells did not survive in any of the grating tissues at day 6 of analyses. They then analyzed the adult cell engraftment at day 1 and identified only few surviving cells. The neonatal and fetal cardiomyocytes however successfully formed grafts in both injured and the uninjured hearts indicating that the developmental stage of donor cells does influence graft survival. In contrast to the above study, Smits et al. [245] reported that transplantation of human cardiomyocyte progenitor cells and the cardiomyocyte progenitor cells-derived cardiomyocytes into immunodeficient mice following myocardial infarction. They observed no significant difference in the grafting efficiencies of the differentiated and the undifferentiated cells, observing only 3.5 +/- 1.8% and 3.0 +/- 0.8% cells engraftment for undifferentiated and differentiated cells

respectively. These studies displayed discrepancies on engraftment of differentiated versus the undifferentiated cells. Van Laake et al. [93] observed long-term engraftment of donor cells in immunodeficient mice with improvement of function in the cardiaomyocyte engrafted animals compared to non-cardiomyocytes engrafted. However, at long-term the conferred improvement in function by cardiomyocytes dropped to the same level as the non-cardiomyocytes engrafted hearts indicating lack of prolonged improvement of function, even with the evidence of cell engraftment. This study utilized fully differentiated ventricular cardiomyocytes as donor cells. Cells were successfully retained in the scar tissue but were not able to integrate in the host myocardium and confer lasting function preservation as described in van Laake et al. [93].

Interestingly, Hattori et al. [229] demonstrated that co-transplantation of ES-derived cardiomyocytes with fibroblast synergistically enhanced the survival of cardiomyocytes. They reported that when highly enriched cardiomyocytes generated from ES cells were transplanted together with embryonic fibroblasts into immunodeficient mouse hearts, histological analyses revealed that <1% of cardiomyocytes and 50% of the fibroblasts remained in the injured myocardium 24 hour after transplantation. This study clearly demonstrated the importance of adhesive qualities of cells for transplantation. Similarly, Kolossov et al. reported that transplantation of 3*(10^4) to 3*(10^5) ES cell-derived cardiomyocytes into syngeneic infarcted murine hearts resulted in poor engraftment of the cells [67]. This observation was altered when they transplanted ES-cell derived cardiomyocytes co-cultured with syngeneic fibroblast, highlighting the role of fibroblast cells in facilitating engraftment. In the same study, transplantation of the later cell type improved function of the infarcted hearts compared to the sham injected controls at 3-4 weeks post surgery. In a different approach to cell injection, Laflamme et al. [92], introduced a pro-survival cocktail cell therapy whereby they injected cells together with pro-survival molecules such as IGF-1, cyclosporine A, pinacidil together with Matrigel and observed enhanced survival of the cells, attenuation of ventricular dilation and preserved regional and global contractile function.

In retrospect, transplantation of highly enriched ventricular cardiomyocytes into allogeneic infarcted wild type mice, without any adhesive molecules possibly was one of the weaknesses that led to insufficient engraftment of the cells in the present study. Although the transplanted cells utilized by this study also expressed one of the survival

factors (IGF-1Ea) described by Laflamme [92], IGF-1, probably more than one factor is required for better engraftment and survival of the transplanted cells to be able to confer lasting preservation of function.

Hattori et al. also analyzed the mechanisms that could underlie the loss of transplanted cells leading to their lower availability for engraftment [229]. They investigated the amount of cells that get instantly washed out upon their transplantation via the coronary circulation. Murine hearts were re-perfused ex vivo and injected with highly enriched, GFP labelled cardiomyocytes. They then collected fluid drained out of the coronary sinus to count the drained labelled cells. From seven different experiments, it was reported that 30-50% of the injected cells were washed out of the heart within 10 minutes of cell injection. This study was supported by an *in vivo* study conducted on rats. Dow et al. injected directly into the left ventricular wall of either re-perfused or permanently occluded rat hearts [230]. The cell injections were performed at 15 and 75 minutes post treatments respectively with 5*10^6 cells. The study recovered the donor cells in both the heart and the lungs in 100% of the animals. Furthermore, cells were also discovered in capillaries, kidney and spleen suggesting that the direct injection of cardiomyocytes does not represent the ideal mode for cell transplantation studies. Additionally this approach holds a risk of dispersing the injected cells into other organs in the body. Although cell tracing were not carried out in other organs than the hearts, in the present study the loss of function at long-term could be due to loss of cells into coronary circulation leading to lower amount of cells for engraftment. To minimize this problem, cell transplantation could be performed with cell sheets or 3D engineered tissues that are harder to disperse than single cells. Transplantation of 3D cell sheets would in addition also aid cell tracing analyses, which is still a challenge for a lot of cell transplantation studies.

Amelioration of the regional function of hearts after injury could be achieved by re-vascularization and decreasing pathological hypertrophy. Although efficiency of contractile cell engraftment holds potential for overall function improvement, a study by van Laake et al. suggests that improvement of cardiac function correlates with vascularity rather than graft size [247]. They reported that transplantation of human ES cells derived cardiomyocytes enhanced vascularisation and improved function of the recipient hearts after myocardial infarction and interestingly smaller graft size conferred better functional outcome than bigger grafts. Smits et al. [245] transplanted human Cardiomyocyte

Progenitor Cells (hCMPC) and hCMPC-derived cardiomyocytes (hCMPC-CM) in infarcted murine hearts and reported that transplantation of these cells lead to preservation of long-term function. They observed higher vessel density for hCPMCs than the hCPMCs derived cardiomyocytes transplanted hearts. Their further *in vitro* analyses confirmed that the undifferentiated progenitor cells-conditioned media contained VEGF whereas the differentiated cells-conditioned media did not. Both of van Laake and Smits et al. [245, 247] studies implicated that enhanced vessel density correlates with enhanced functional outcome, although in the study by Smits et al., the hCMPC-derived cell transplantation led to comparable enhancement of function to the undifferentiated progenitor cell transplanted hearts even though their vessel density was lower. This finding in general implicated that the differentiated and undifferentiated cells could possibly secrete different paracrine factors exerting dissimilar effects in modulating the injured tissue.

The current study conducted a capillary density assessment in the long-term samples and showed no significant difference in the capillary densities between the cells transplanted and the saline-injected groups. As Smits et al. [245] reported the reason for this could be that the donor cells in the present study were fully differentiated cells that did not release sufficient amount of pro-angiogenic factors for making new vessels. Interestingly, the mRNA analysis of VEGFa expression in the 2-month samples was significantly higher in IGF-1Ea transplanted hearts compared to the WT controls but not in the empty-cells transplanted hearts. Although not statistically significant, the IGF-1Ea-cells transplanted hearts also had a tendency for higher capillary density. It is therefore likely that the IGF-1Ea-cells released insufficient amount of paracrine factor VEGFa, to make adequate new vessels to maintain their function at long-term. The capillary density assessment in the present study correlates very well with the functional and the scar size analyses. The preservation of function was not lasting in the cell transplanted hearts as the scar size could not be reduced and vessel density enhanced.

The apparent discrepancy observed between no change in capillary density and increased VEGFa transcript expression in the IGF-1Ea samples can be explained by considering the pleiotropic function of VEGFa. Apart from being pro-angiogenic factor, VEGFa is implicated in modulating hypertrophy. Hearts transplanted with IGF-1Ea cells showed significantly higher and lower expression of VEGFa and SDF-1 respectively. Although the actual mechanism of IGF-1Ea mediated modulation of VEGFa and SDF-1 expression

has not been found, the IGF-1Ea cell transplanted hearts showed down-regulation of VEGF receptor, KDR, down-regulation of aSK and bMHC in IGF-1Ea-cell transplanted hearts suggesting that IGF-1Ea cell transplantation may directly or indirectly confer protection against LV remodelling. It is not known how SDF-1 could contribute to the IGF1-Ea-induced modulation of hypertrophy therefore further study in our laboratory will examine in detail this signaling.

Although the hearts receiving IGF-1Ea-cells showed lower hypertrophic response than the hearts transplanted with empty –cells, this effect was not sufficient to confer a preservation of long-term function. Nonetheless, this study proposed a novel mechanism that could regulate cardiac repair and induce beneficial cardiovascular remodelling in cell/ growth factor therapy. However, for regeneration of the scar tissue to improve overall function, sufficient homing and integration of new contractile muscle mass would be necessary and modulation of hypertrophic response alone seemed not sufficient to achieve this.

5.2 LIMITATIONS AND FUTURE DIRECTION

Cell-based gene therapy of *IGF-1Ea* transduced P19Cl6-MLC2v-GFP cells was not able to confer lasting preservation of function of infarcted murine hearts. There are several factors which could have led to this outcome. One of the major limitations of the study was small number of subjects for in vivo cell transplantation, which led to high standard deviation within groups. The small number of subjects resulted from very high mortality observed from permanent LCA ligation utilized by the study to induce myocardial infarction. To improve the number of animals for similar study in future one should either improve animal survival by employing alternative myocardial infarction models such as the cryo-injury, cardiotoxin-injury or temporary ischemia- reperfusion models that have lower mortality or alternatively increase the total number of animals for the study. The temporary LCA ligation- reperfusion model will not only confer higher survival but will also be clinically more relevant than the permanent occlusion model.

Although the use of P19Cl6 cells for therapy was mainly a proof of principle, future studies should utilize safer cells such as embryonic, cardiac progenitor or iPS cells, which are clinically relevant as opposed to the carcinoma cells. In addition, the study observed

insufficient engraftment of the transplanted cells, which could have resulted from the use of allogeneic transplantation approach. The allogeneic transplantation model required long-term immunosuppression and long-term immunosuppression in mice has been described to be very difficult without inducing toxicity and local irritation (mentioned in [220]). Due to the adverse effects that could potentially be obtained from immunosuppression alone, the fate of the transplanted is very difficult to address in an allogeneic model. Therefore, future cell transplantation study should be carried out in immunodeficient mice. The insufficient engraftment could also have resulted from the differentiation state of the transplanted cells and the number of donor cells for transplantation. Future studies should therefore comprise donor cells of immature, mid-mature and fully mature types, in various numbers to investigate the optimal differentiation state and number for enhanced engraftment, as a previous study suggests that immature cells such as foetal cardiomyocytes survive better after injection in the hearts than the adult cardiomyocytes [246].

Previous study from our laboratory on transgenic mice over-expressing IGF-1Ea in the heart showed that the hearts preserved their function after injury, formed smaller scar and showed lower cell death compared to wild type hearts [77]. Despite the inability of this study to distinguish the endogenous and exogenously expressed IGF-1, the present study observed an increase in IGF-1 expression (although not significant, $p=0.08$) in all the injury induced hearts, independent of cell injection. However, this natural induction of IGF-1 was not able to protect the hearts from deleterious events caused by MI. This leads to hypotheses that (i) IGF-1 expression possibly confers prevention of damage rather than cure to MI-induced injury, (ii) if IGF-1 does have curative function, it is possible that persistent expression of the gene is important for protection as it is the case in transgenic mice but this might not be the case in the wild type after infarction and (iii) alternatively, it might be the level of IGF-1 expression after injury induction that is not enough in the wild type hearts to confer protection. To test these hypotheses, future cell therapy study could be conducted on transgenic mice over-expressing IGF-1Ea versus wild type animals. In addition, to address the inability of the present study to distinguish endogenous and exogenously introduced IGF-1, a custom RT-qPCR probe needs to be designed. The commercially available probe of rat IGF-1, which was used in this study was not specific to the species. Therefore for future work, a custom designed probe that incorporates parts of the vector backbone, is necessary.

The detection of IGF-1Ea did not only suffer from lack of rat IGF-1Ea specific RT-qPCR probe but also from species- and isoform- specific antibody. Despite several trials using western blot and direct ELISA methods, it was not possible to test at protein level, production of IGF-1Ea by the transduced cells. Although the *in vitro* cell survival assessment clearly showed that the IGF-1Ea transduced cells had a positive effect on cell survival compared to the empty-vector transduced cell, this effect could not be directly linked to IGF-1Ea expression. To prove that the transduced cells produced IGF-1Ea that was able to confer an effect, a functional assay should be considered in future. The functional assay could analyze expression of downstream molecules of IGF-1Ea signalling such as Akt, PDK1 or MAPkinases, following treatment of the untransduced cells with conditioned media from IGF-1Ea transduced cells.

In general, timing and method of delivery still are challenges for cell therapy studies. The current study utilized an intramyocardial route for cell injection. Intramyocardial route, although has high efficiency of cell delivery compared to other available methods, encounters instant wash-out of cells as the heart is continuously active while transplantation is being performed. Therefore, future cell transplantation could utilize transiently unloaded hearts for cell transplantation. Clinically it is relevant and feasible to transiently relax the heart with LVAD device until the transplanted cells have fully engrafted. In addition, cell transplanted acutely after induction of injury might not survive the unfavourable environment therefore future studies could avoid the hostile initial inflammatory phase by using a later time-point for transplantation. However, the decision on the timing of cell transplantation will depend on the objective of the study. The objective of the current study was to deliver survival factor IGF-1Ea to confer better survival of the transplanted and the native at-risk cells therefore it was vital to deliver the gene earlier on in the event of injury induction to protect the surviving cells.

For improving cell-engraftment, a tissue engineering approach combining different cell types or cell sheets seeded on scaffolds (3D tissue patch) might be better than transplanting single cells, to provide cell-cell contact and adherence to the transplanted cells to prevent easy wash-out upon their transplantation. The 3D tissue transplantation approach can potentially improve integration of the transplanted cells to the native tissue, as well as improve cell engraftment and quantification assessments that follow

transplantation. In addition, cell therapy studies to-date have shown improvement or preservation of function following cell transplantation without being able to relate the effects on function to the amount of cell engraftment. Although the present study did not observe any effect on function following cell transplantation, it would be vital in our future studies to include strategies which will be able to demonstrate this clearly. The strategy could either be surgical removal of the transplanted grafts or *in vivo* destruction of the transplanted cells by activating suicidal genes, consequently leading to loss of observed improvement or maintenance of function.

5.3 CONCLUDING REMARKS

This study was able to generate pluripotent cells over-expressing IGF-1Ea that conferred greater survival to hypoxia induced injury than the control cells. The engineered cells maintained their undifferentiated state and very efficient differentiation capacity towards ventricular cardiac myocytes lineage, generating large quantities of cells optimal for the cell transplantation study. In addition, the cells generated cardiomyocytes that were functionally active and exhibited a mature phenotype.

Taken together, the engineered cells displayed some of the major qualities that cells for transplantation studies must posses, making them suitable candidate for proof of principle, cell therapy approach. However, in future one should use safer cells to be able to securely translate the findings to clinical research. Upon allogeneic transplantation into wild type murine infarcted hearts, there was a trend for maintenance of function at short-term. Paracrine factor analyses revealed only a tendency for their enhanced expression, which could only be linked to injury and not cell transplantation. The reasons for tendency in maintenance of function at short-term could be due to cell engraftment and/or involvement of other paracrine factors than the ones examined. At long-term however, the tendency for maintenance of function was lost to the level of the control hearts. Cell tracing assessment revealed engraftment of the transplanted cells, although the cells failed to couple with the recipient tissue. Scar size and capillary density analyses revealed no significant difference between the cells treated hearts compared to the saline only treated hearts, corroborating with the functional data. Interestingly, IGF-1Ea-cell transplantation led to reduced LV remodelling of the recipient tissue, the mechanism for which is under investigation. The modulation of hypertrophic response however was not sufficient to confer lasting

maintenance of function to the injured hearts. This study nevertheless demonstrated a novel pathway via injection of IGF-1Ea over-expressing cells that has potential to maintain cardiac tissue after injury. The proposed signaling mechanism could potentially confer improvement of the passive function but for regeneration of the active function, efficient homing and integration of new contractile muscle mass is necessary.

REFERENCES

1. Dahlof, B., *Cardiovascular disease risk factors: epidemiology and risk assessment.* Am J Cardiol. **105**(3A-9A).
2. WHO. [cited 2010 13 10]; Available from: http://www.who.int/cardiovascular_diseases/en/.
3. Yamagishi, H., et al., *Molecular Embryology for an understanding of congenital heart diseases.* Anat Sci Int, 2009. **84**: p. 88-94.
4. AHA. [cited 2010 14 10]; Available from: http://www.americanheart.org/presenter.jhtml?identifier=4565.
5. Plageman, T.F. and K.E. Yutzey, *Microarray analysis of Tbx5-induced genes expressed in the developing heart.* Dev Dyn, 2006. **235**: p. 2868-2880.
6. Olson, E.N., *Gene regulatory networks in the evolution and development of the heart.* . Science, 2006. **313**: p. 1922-1927.
7. Watt, A.J., et al., *GATA4 is essential for formation of the proepicardium and regulates cardiogenesis.* Proc Natl Acad Sci U S A, 2004. **101**: p. 12573-12578.
8. Zigelman, C.Z. and P.M. Edelstein, *Aortic valve stenosis.* Anasthesiol Clin, 2009. **27**: p. 519-532.
9. Yosefy, C. and A. Ben Barak, *Floppy mitral valve/mitral valve prolapse and genetics.* J Heart Valve Dis, 2007. **16**: p. 590-595.
10. Fairweather, D. and S. Frisancho-Kiss, *Mast cells and inflammatory heart disease: potential drug targets.* Cardiovasc Hematol Disord Drug Targets, 2008. **8**: p. 80-90.
11. Fairweather, D. and N.R. Rose, *Inflammatory heart disease: a role of cytokines.* Lupus, 2005. **14**: p. 646-651.
12. Pavlopoulos, H. and P. Nihoyannopoulos, *The constellation of hypertensive heart disease.* Hellenic J Cardiol, 2008(49): p. 92-99.
13. Mettler, B.A. and B.B. Peeler, *Congenital heart disease surgery in the adult.* Surg Clin North Am, 2009. **89**: p. 1021-1032.
14. Kubes, P. and D.N. Granger, *Leukocyte-endothelial cell interaction evoked by mast cells.* . **Cardiovascular Research**, 1996. **32**.
15. Hill, J.H. and P.A. Ward, *The phlogistic role of C3 leukotactic fragment in myocardial infarcts of rats.* . J Exp Med, 1971: p. 885-890.
16. Nikolaos, G., et al., *The inflammatory response in myocardial infarction.* Cardiovasc Res, 2002. **53**: p. 31 –47.
17. Nikolaos, G., et al., *The inflammatory response in myocardial infarction.* Cardiovascular Research 2002. **53**: p. 31 –47.
18. Mourkioti, F. and N. Rosenthal, *IGF-1, inflammation and stem cells: interactions during muscle regeneration.* Trends Immunol, 2005. **26**(10): p. 535-42.
19. Leri, A., et al., *Myocardial regeneration and stem cell repair.* Curr Probl Cardiol, 2008. **33**(3): p. 91-153.
20. Zweier, J.L., *Measurement of superoxide-derived free radicals in the reperfused heart. Evidence for a free radical mechanism of reperfusion injury.* J Biol Chem, 1988. **263**(3): p. 1353-7.
21. Frazier, O.H., *First use of an untethered, vented electric left ventricular assist device for long-term support.* Circulation, 1994. **89**: p. 2908-2914.
22. Birks, E.J., *Current and future status of the left ventricular device (LVAD)s in the UK.* British Journal of Cardiology. , 2005. **12**: p. 333-335.
23. Poss, K.D., *Advances in understanding tissue regenerative capacity and mechanisms in animals.* Nat Rev Genet, 2010. **11**: p. 13.

24. Morgan, T.H., *Experimental studies of the regeneration of Planaria maculata.* Dev. Genes Evol., 1898. **7**: p. 364-397.
25. Reddien, P.W. and A. Sanchez Alvardo, *Fundamentals of planarian regeneration.* Annu. Rev. Cell Dev. Biol., 2004. **20**: p. 725-757.
26. Bosch, T.C., *Why polyps regenerate and we don't: towards a cellular and molecular framework for Hydra regeneration.* Dev Biol, 2007. **303**: p. 421-433.
27. Gaudette, G.R. and I.S. Cohen, *Cardiac regeneration: materials can improve the passive properties of myocardium, but cell therapy must do more.* Circulation, 2006. **114**(24): p. 2575-7.
28. Cohen, I.S. and G.R. Gaudette, *Regenerating the heart: new progress in gene/cell therapy to restore normal mechanical and electrical function.* Dialogues in cardiovascular medicine, 2009. **14**: p. 7-21.
29. Mizuno, T., et al., *Elastin stabilizes an infarct and preserves ventricular function.* Circulation, 2005. **112**(9 Suppl): p. I81-8.
30. Matsubayashi, K., et al., *Improved left ventricular aneurysm repair with bioengineered vascular smooth muscle grafts.* Circulation, 2003. **108 Suppl 1**: p. II219-25.
31. Fujimoto, K.L., et al., *An elastic, biodegradable cardiac patch induces contractile smooth muscle and improves cardiac remodeling and function in subacute myocardial infarction.* J Am Coll Cardiol, 2007. **49**(23): p. 2292-300.
32. Berry, M.F., et al., *Mesenchymal stem cell injection after myocardial infarction improves myocardial compliance.* Am J Physiol Heart Circ Physiol, 2006. **290**(6): p. H2196-203.
33. Lyon, A. and S. Harding, *The potential of cardiac stem cell therapy for heart failure.* Curr Opin Pharmacol, 2007. **7**(2): p. 164-70.
34. Flink, I.L., *Cell cycle reentry of ventricular and atrial cardiomyocytes and cells within the epicardium following amputation of the ventricular apex in the axolotl, Amblystoma mexicanum: confocal microscopic immunofluorescent image analysis of bromodeoxyuridine-labeled nuclei.* Anat Embryol (Berl), 2002. **205**(3): p. 235-44.
35. Poss, K.D., L.G. Wilson, and M.T. Keating, *Heart regeneration in zebrafish.* Science, 2002. **298**(5601): p. 2188-90.
36. Beltrami, A., et al., *Evidence That Human Cardiac Myocytes Divide after Myocardial Infarction* N Engl J Med, 2001. **344:1750-1757**.
37. Bergmann, O., et al., *Evidence for cardiomyocyte renewal in humans.* Science, 2009. **324**(5923): p. 98-102.
38. Potapova, I.A., et al., *Enhanced recovery of mechanical function in the canine heart by seeding an extracellular matrix patch with mesenchymal stem cells committed to a cardiac lineage.* Am J Physiol Heart Circ Physiol, 2008. **295**(6): p. H2257-63.
39. Planat-Benard, V., et al., *Spontaneous cardiomyocyte differentiation from adipose tissue stroma cells.* Circ Res, 2004. **94**(2): p. 223-9.
40. Messina, E., et al., *Isolation and expansion of adult cardiac stem cells from human and murine heart.* Circ Res, 2004. **95**(9): p. 911-21.
41. Schenk, S., et al., *Monocyte chemotactic protein-3 is a myocardial mesenchymal stem cell homing factor.* Stem Cells, 2007. **25**(1): p. 245-51.
42. Aghi, M., et al., *Tumor stromal-derived factor-1 recruits vascular progenitors to mitotic neovasculature, where microenvironment influences their differentiated phenotypes.* Cancer Res, 2006. **66**(18): p. 9054-64.

43. Assmus, B., et al., *Transcoronary transplantation of progenitor cells after myocardial infarction.* N Engl J Med, 2006. **355**(12): p. 1222-32.
44. Janssens, S., et al., *Autologous bone marrow-derived stem-cell transfer in patients with ST-segment elevation myocardial infarction: double-blind, randomised controlled trial.* Lancet, 2006. **367**(9505): p. 113-21.
45. Lunde, K., et al., *Intracoronary injection of mononuclear bone marrow cells in acute myocardial infarction.* N Engl J Med, 2006. **355**(12): p. 1199-209.
46. Meyer, G.P., et al., *Intracoronary bone marrow cell transfer after myocardial infarction: eighteen months' follow-up data from the randomized, controlled BOOST (BOne marrOw transfer to enhance ST-elevation infarct regeneration) trial.* Circulation, 2006. **113**(10): p. 1287-94.
47. Schachinger, V., et al., *Intracoronary bone marrow-derived progenitor cells in acute myocardial infarction.* N Engl J Med, 2006. **355**(12): p. 1210-21.
48. Wollert, K.C., et al., *Intracoronary autologous bone-marrow cell transfer after myocardial infarction: the BOOST randomised controlled clinical trial.* Lancet, 2004. **364**(9429): p. 141-8.
49. Martin-Rendon, E., et al., *Autologous bone marrow stem cells to treat acute myocardial infarction: a systematic review.* Eur Heart J, 2008. **29**(15): p. 1807-18.
50. Mills, J.S. and S.V. Rao, *REPAIR-AMI: stem cells for acute myocardial infarction.* Future Cardiol, 2007. **3**(2): p. 137-40.
51. Drexler, H., G.P. Meyer, and K.C. Wollert, *Bone-marrow-derived cell transfer after ST-elevation myocardial infarction: lessons from the BOOST trial.* Nat Clin Pract Cardiovasc Med, 2006. **3 Suppl 1**: p. S65-8.
52. Yousef, M., et al., *The BALANCE Study: clinical benefit and long-term outcome after intracoronary autologous bone marrow cell transplantation in patients with acute myocardial infarction.* J Am Coll Cardiol, 2009. **53**(24): p. 2262-9.
53. Urbanek, K., et al., *Myocardial regeneration by activation of multipotent cardiac stem cells in ischemic heart failure.* Proc Natl Acad Sci U S A, 2005. **102**(24): p. 8692-7.
54. Partridge, T., *Reenthronement of the muscle satellite cell.* Cell, 2004. **119**(4): p. 447-8.
55. Campion, D.R., *The muscle satellite cell: a review.* Int Rev Cytol, 1984. **87**: p. 225-51.
56. Reinecke, H., et al., *Electromechanical coupling between skeletal and cardiac muscle. Implications for infarct repair.* J Cell Biol, 2000. **149**(3): p. 731-40.
57. Smits, P.C., et al., *Catheter-based intramyocardial injection of autologous skeletal myoblasts as a primary treatment of ischemic heart failure: clinical experience with six-month follow-up.* J Am Coll Cardiol, 2003. **42**(12): p. 2063-9.
58. Menasche, P., et al., *Myoblast transplantation for heart failure.* Lancet, 2001. **357**(9252): p. 279-80.
59. Dib, N., et al., *Feasibility and safety of autologous myoblast transplantation in patients with ischemic cardiomyopathy.* Cell Transplant, 2005. **14**(1): p. 11-9.
60. Takahashi, K., et al., *Induction of pluripotent stem cells from adult human fibroblasts by defined factors.* Cell, 2007. **131**(5): p. 861-72.
61. Narazaki, G., et al., *Directed and systematic differentiation of cardiovascular cells from mouse induced pluripotent stem cells.* Circulation, 2008. **118**(5): p. 498-506.
62. Mauritz, C., et al., *Generation of functional murine cardiac myocytes from induced pluripotent stem cells.* Circulation, 2008. **118**(5): p. 507-17.
63. Okita, K., et al., *Generation of mouse induced pluripotent stem cells without viral vectors.* Science, 2008. **322**(5903): p. 949-53.

64. Stadtfeld, M., et al., *Induced pluripotent stem cells generated without viral integration.* Science, 2008. **322**(5903): p. 945-9.
65. Woltjen, K., et al., *piggyBac transposition reprograms fibroblasts to induced pluripotent stem cells.* Nature, 2009. **458**(7239): p. 766-70.
66. Nelson, T.J., et al., *Repair of acute myocardial infarction by human stemness factors induced pluripotent stem cells.* Circulation, 2009. **120**(5): p. 408-16.
67. Kolossov, E., et al., *Engraftment of engineered ES cell-derived cardiomyocytes but not BM cells restores contractile function to the infarcted myocardium.* J Exp Med, 2006. **203**(10): p. 2315-27.
68. Hodgson, D.M., et al., *Stable benefit of embryonic stem cell therapy in myocardial infarction.* Am J Physiol Heart Circ Physiol, 2004. **287**(2): p. H471-9.
69. Singla, D.K., et al., *Transplantation of embryonic stem cells into the infarcted mouse heart: formation of multiple cell types.* J Mol Cell Cardiol, 2006. **40**(1): p. 195-200.
70. Menard, C., et al., *Transplantation of cardiac-committed mouse embryonic stem cells to infarcted sheep myocardium: a preclinical study.* Lancet, 2005. **366**(9490): p. 1005-12.
71. Kehat, I., et al., *Electromechanical integration of cardiomyocytes derived from human embryonic stem cells.* Nat Biotechnol, 2004. **22**(10): p. 1282-9.
72. Murry, C.E., H. Reinecke, and L.M. Pabon, *Regeneration gaps: observations on stem cells and cardiac repair.* J Am Coll Cardiol, 2006. **47**(9): p. 1777-85.
73. Barbash, I.M., et al., *Systemic delivery of bone marrow-derived mesenchymal stem cells to the infarcted myocardium: feasibility, cell migration, and body distribution.* Circulation, 2003. **108**(7): p. 863-8.
74. Hou, D., et al., *Radiolabeled cell distribution after intramyocardial, intracoronary, and interstitial retrograde coronary venous delivery: implications for current clinical trials.* Circulation, 2005. **112**(9 Suppl): p. I150-6.
75. Watanabe, E., et al., *Cardiomyocyte transplantation in a porcine myocardial infarction model.* Cell Transplant, 1998. **7**(3): p. 239-46.
76. Hammond, H.K. and T. Tang, *Gene therapy for myocardial infarction-associated congestive heart failure: how far have we got?* Dialogues in cardiovascular medicine, 2009. **14**: p. 29-36.
77. Santini, M.P., et al., *Enhancing repair of the mammalian heart.* Circ Res, 2007. **100**(12): p. 1732-40.
78. Chao, W., et al., *Strategic advantages of insulin-like growth factor-I expression for cardioprotection.* J Gene Med, 2003. **5**(4): p. 277-86.
79. van den Bos, E.J., et al., *A novel model of cryoinjury-induced myocardial infarction in the mouse: a comparison with coronary artery ligation.* Am J Physiol Heart Circ Physiol, 2005. **289**(3): p. H1291-300.
80. Gavira, J.J., et al., *Repeated implantation of skeletal myoblast in a swine model of chronic myocardial infarction.* Eur Heart J. **31**(8): p. 1013-21.
81. van Amerongen, M.J., et al., *Cryoinjury: a model of myocardial regeneration.* Cardiovasc Pathol, 2008. **17**(1): p. 23-31.
82. Duerr, G.D., et al., *Comparison of myocardial remodeling between cryoinfarction and reperfused infarction in mice.* J Biomed Biotechnol. **2011**: p. 961298.
83. Ye, L., et al., *Nanoparticle based delivery of hypoxia-regulated VEGF transgene system combined with myoblast engraftment for myocardial repair.* Biomaterials. **32**(9): p. 2424-31.

84. Ahmed, R.P.H., *Cardiac tumorgenic potential of induced pluripotent stem cells in an immunocompetent host with myocardial infarction.* Regenerative Medicine, 2011. **6**: p. 171-178.
85. Tang, X.L., et al., *Intracoronary administration of cardiac progenitor cells alleviates left ventricular dysfunction in rats with a 30-day-old infarction.* Circulation. **121**(2): p. 293-305.
86. Padin-Iruegas, M.E., et al., *Cardiac progenitor cells and biotinylated insulin-like growth factor-1 nanofibers improve endogenous and exogenous myocardial regeneration after infarction.* Circulation, 2009. **120**(10): p. 876-87.
87. Matsuura, K., et al., *Transplantation of cardiac progenitor cells ameliorates cardiac dysfunction after myocardial infarction in mice.* J Clin Invest, 2009. **119**(8): p. 2204-17.
88. Cho, J., et al., *Myocardial injection with GSK-3beta-overexpressing bone marrow-derived mesenchymal stem cells attenuates cardiac dysfunction after myocardial infarction.* Circ Res. **108**(4): p. 478-89.
89. Zhang, X., et al., *Combined transplantation of endothelial progenitor cells and mesenchymal stem cells into a rat model of isoproterenol-induced myocardial injury.* Arch Cardiovasc Dis, 2008. **101**(5): p. 333-42.
90. Christoforou, N., et al., *Implantation of mouse embryonic stem cell-derived cardiac progenitor cells preserves function of infarcted murine hearts.* PLoS One. **5**(7): p. e11536.
91. Caspi, O., et al., *Transplantation of human embryonic stem cell-derived cardiomyocytes improves myocardial performance in infarcted rat hearts.* J Am Coll Cardiol, 2007. **50**(19): p. 1884-93.
92. Laflamme, M.A., et al., *Cardiomyocytes derived from human embryonic stem cells in pro-survival factors enhance function of infarcted rat hearts.* Nat Biotechnol, 2007. **25**(9): p. 1015-24.
93. van Laake, L.W., et al., *Human embryonic stem cell-derived cardiomyocytes survive and mature in the mouse heart and transiently improve function after myocardial infarction.* Stem Cell Res, 2007. **1**(1): p. 9-24.
94. Rossant, J. and M.W. McBurney, *The developmental potential of a euploid male teratocarcinoma cell line after blastocyst injection.* J Embryol Exp Morphol, 1982. **70**: p. 99-112.
95. Edwards, M.K., J.F. Harris, and M.W. McBurney, *Induced muscle differentiation in an embryonal carcinoma cell line.* Mol Cell Biol, 1983. **3**(12): p. 2280-6.
96. Jones-Villeneuve, E.M., et al., *Retinoic acid-induced neural differentiation of embryonal carcinoma cells.* Mol Cell Biol, 1983. **3**(12): p. 2271-9.
97. Habara-Ohkubo, A., *Differentiation of beating cardiac muscle cells from a derivative of P19 embryonal carcinoma cells.* Cell Struct Funct, 1996. **21**(2): p. 101-10.
98. van der Heyden, M.A. and L.H. Defize, *Twenty one years of P19 cells: what an embryonal carcinoma cell line taught us about cardiomyocyte differentiation.* Cardiovasc Res, 2003. **58**(2): p. 292-302.
99. McBurney, M.W., *P19 embryonal carcinoma cells.* Int J Dev Biol, 1993. **37**(1): p. 135-40.
100. Moore, J.C., et al., *A P19Cl6 GFP reporter line to quantify cardiomyocyte differentiation of stem cells.* Int J Dev Biol, 2004. **48**(1): p. 47-55.
101. Adelstein, R.S. and E. Eisenberg, *Regulation and kinetics of the actin-myosin-ATP interaction.* Annu.Rev.Biochem, 1980(49): p. 921-956.

102. Barton, P.J. and M.E. Buckingham, *The myosin alkali light chain proteins and their genes.* Biochem J, 1985. **231**(2): p. 249-61.
103. Lee, K.J., et al., *Myosin light chain-2 luciferase transgenic mice reveal distinct regulatory programs for cardiac and skeletal muscle-specific expression of a single contractile protein gene.* J Biol Chem, 1992. **267**(22): p. 15875-85.
104. Jones-Villeneuve, E.M., et al., *Retinoic acid induces embryonal carcinoma cells to differentiate into neurons and glial cells.* J Cell Biol, 1982. **94**(2): p. 253-62.
105. Paquin, J., et al., *Oxytocin induces differentiation of P19 embryonic stem cells to cardiomyocytes.* Proc Natl Acad Sci U S A, 2002. **99**(14): p. 9550-5.
106. Martin, G.R. and M.J. Evans, *The morphology and growth of a pluripotent teratocarcinoma cell line and its derivatives in tissue culture.* Cell, 1974. **2**(3): p. 163-72.
107. Martin, G.R. and M.J. Evans, *Differentiation of clonal lines of teratocarcinoma cells: formation of embryoid bodies in vitro.* Proc Natl Acad Sci U S A, 1975. **72**(4): p. 1441-5.
108. Strickland, S. and V. Mahdavi, *The induction of differentiation in teratocarcinoma stem cells by retinoic acid.* Cell, 1978. **15**(2): p. 393-403.
109. McBurney, M.W., et al., *Control of muscle and neuronal differentiation in a cultured embryonal carcinoma cell line.* Nature, 1982. **299**(5879): p. 165-7.
110. Friend, C., et al., *Hemoglobin synthesis in murine virus-induced leukemic cells in vitro: stimulation of erythroid differentiation by dimethyl sulfoxide.* Proc Natl Acad Sci USA, 1976(68): p. 378-382.
111. Tralka, T.S. and A.S. Rabson, *Cilia formation in cultures of human lung cancer cells treated with dimethyl sulfoxide.* J Natl Cancer Inst, 1976. **57**(6): p. 1383-8.
112. Lako, M., et al., *Characterisation of Wnt gene expression during the differentiation of murine embryonic stem cells in vitro: role of Wnt3 in enhancing haematopoietic differentiation.* Mech Dev, 2001. **103**(1-2): p. 49-59.
113. Morley, P. and J.F. Whitfield, *The differentiation inducer, dimethyl sulfoxide, transiently increases the intracellular calcium ion concentration in various cell types.* J Cell Physiol, 1993. **156**(2): p. 219-25.
114. Wilton, S. and I. Skerjanc, *Factors in serum regulate muscle development in P19 cells.* In Vitro Cell Dev Biol Anim, 1999. **35**(4): p. 175-7.
115. Scuhltheiss, T.M., J.B. Burch, and A.B. Lassar, *A role of bone morphogenetic proteins in the induction of cardiac myogenesis.* Genes Dev, 1997(11): p. 451-462.
116. Monzen, K., et al., *Bone morphogenic proteins induce cardiomyocyte differentiation through the mitogen-activated protein kinase kinase kinase TAK1 and cardiac transcription factors Csx/Nkx-2.5 and GATA-4.* Mol Cell Biol, 1999(19): p. 7096-7105.
117. Jamali, M., et al., *BMP signaling regulates Nkx2-5 activity during cardiomyogenesis.* FEBS Lett, 2001. **509**(1): p. 126-30.
118. Rudnicki, M.A., et al., *Actin and myosin expression during development of cardiac muscle from cultured embryonal carcinoma cells.* Dev Biol, 1990. **138**(2): p. 348-58.
119. Arreola, J., S. Spires, and T. Begenisich, *Na+ channels in cardiac and neuronal cells derived from a mouse embryonal carcinoma cell line.* J Physiol, 1993. **472**: p. 289-303.
120. van der Heyden, M.A., et al., *P19 embryonal carcinoma cells: a suitable model system for cardiac electrophysiological differentiation at the molecular and functional level.* Cardiovasc Res, 2003. **58**(2): p. 410-22.

121. Wobus, A.M., et al., *Cardiomyocyte-like cells differentiated in vitro from embryonic carcinoma cells P19 are characterized by functional expression of adrenoceptors and Ca2+ channels.* In Vitro Cell Dev Biol Anim, 1994. **30A**(7): p. 425-34.
122. Musaro, A., et al., *Localized Igf-1 transgene expression sustains hypertrophy and regeneration in senescent skeletal muscle.* Nat Genet, 2001. **27**(2): p. 195-200.
123. Barton, E.R., et al., *Muscle-specific expression of insulin-like growth factor I counters muscle decline in mdx mice.* J Cell Biol, 2002. **157**(1): p. 137-48.
124. Jones, J.I. and D.R. Clemmons, *Insulin-like growth factors and their binding proteins: biological actions.* Endocr Rev, 1995. **16**(1): p. 3-34.
125. Clemmons, D.R., et al., *Role of insulin-like growth factor binding proteins in the control of IGF actions.* Prog Growth Factor Res, 1995. **6**(2-4): p. 357-66.
126. Shimatsu, A. and P. Rotwein, *Mosaic evolution of the insulin-like growth factors. Organization, sequence, and expression of the rat insulin-like growth factor I gene.* J Biol Chem, 1987. **262**(16): p. 7894-900.
127. Shavlakadze, T., et al., *Targeted expression of insulin-like growth factor-I reduces early myofiber necrosis in dystrophic mdx mice.* Mol Ther, 2004. **10**(5): p. 829-43.
128. Simmons, J.G., et al., *Multiple transcription start sites in the rat insulin-like growth factor-I gene give rise to IGF-I mRNAs that encode different IGF-I precursors and are processed differently in vitro.* Growth Factors, 1993. **9**(3): p. 205-21.
129. Yang, H., et al., *Alternative leader sequences in insulin-like growth factor I mRNAs modulate translational efficiency and encode multiple signal peptides.* Mol Endocrinol, 1995. **9**(10): p. 1380-95.
130. Roberts, C.T., Jr., et al., *Molecular cloning of rat insulin-like growth factor I complementary deoxyribonucleic acids: differential messenger ribonucleic acid processing and regulation by growth hormone in extrahepatic tissues.* Mol Endocrinol, 1987. **1**(3): p. 243-8.
131. Musaro, A., et al., *Stem cell-mediated muscle regeneration is enhanced by local isoform of insulin-like growth factor 1.* Proc Natl Acad Sci U S A, 2004. **101**(5): p. 1206-10.
132. Liu, J.P., et al., *Mice carrying null mutations of the genes encoding insulin-like growth factor I (Igf-1) and type 1 IGF receptor (Igf1r).* Cell, 1993. **75**(1): p. 59-72.
133. Ludwig, T., et al., *Mouse mutants lacking the type 2 IGF receptor (IGF2R) are rescued from perinatal lethality in Igf2 and Igf1r null backgrounds.* Dev Biol, 1996. **177**(2): p. 517-35.
134. Barres, B.A., et al., *Cell death and control of cell survival in the oligodendrocyte lineage.* Cell, 1992. **70**(1): p. 31-46.
135. Werther, G.A., H. Cheesman, and V. Russo, *Olfactory bulb organ culture is supported by combined insulin-like growth factor-I and basic fibroblast growth factor.* Brain Res, 1993. **617**(2): p. 339-42.
136. Llorens-Martin, M., I. Torres-Aleman, and J.L. Trejo, *Mechanisms mediating brain plasticity: IGF1 and adult hippocampal neurogenesis.* Neuroscientist, 2009. **15**(2): p. 134-48.
137. Ni, W., et al., *Impaired brain development and reduced astrocyte response to injury in transgenic mice expressing IGF binding protein-1.* Brain Res, 1997. **769**(1): p. 97-107.
138. Mathews, L.S., et al., *Growth enhancement of transgenic mice expressing human insulin-like growth factor I.* Endocrinology, 1988. **123**(6): p. 2827-33.

139. Bikle, D., et al., *The skeletal structure of insulin-like growth factor I-deficient mice.* J Bone Miner Res, 2001. **16**(12): p. 2320-9.
140. Zhang, M., et al., *Osteoblast-specific knockout of the insulin-like growth factor (IGF) receptor gene reveals an essential role of IGF signaling in bone matrix mineralization.* J Biol Chem, 2002. **277**(46): p. 44005-12.
141. Shavlakadze, T., et al., *Reconciling data from transgenic mice that overexpress IGF-I specifically in skeletal muscle.* Growth Horm IGF Res, 2005. **15**(1): p. 4-18.
142. Yang, S.Y. and G. Goldspink, *Different roles of the IGF-I Ec peptide (MGF) and mature IGF-I in myoblast proliferation and differentiation.* FEBS Lett, 2002. **522**(1-3): p. 156-60.
143. Hameed, M., et al., *Expression of IGF-I splice variants in young and old human skeletal muscle after high resistance exercise.* J Physiol, 2003. **547**(Pt 1): p. 247-54.
144. Hill, M. and G. Goldspink, *Expression and splicing of the insulin-like growth factor gene in rodent muscle is associated with muscle satellite (stem) cell activation following local tissue damage.* J Physiol, 2003. **549**(Pt 2): p. 409-18.
145. Musaro, A., et al., *IGF-1 induces skeletal myocyte hypertrophy through calcineurin in association with GATA-2 and NF-ATc1.* Nature, 1999. **400**(6744): p. 581-5.
146. Renganathan, M., M.L. Messi, and O. Delbono, *Overexpression of IGF-1 exclusively in skeletal muscle prevents age-related decline in the number of dihydropyridine receptors.* J Biol Chem, 1998. **273**(44): p. 28845-51.
147. Ito, H., et al., *Insulin-like growth factor-I induces hypertrophy with enhanced expression of muscle specific genes in cultured rat cardiomyocytes.* Circulation, 1993. **87**(5): p. 1715-21.
148. Fuller, S.J., J.R. Mynett, and P.H. Sugden, *Stimulation of cardiac protein synthesis by insulin-like growth factors.* Biochem J, 1992. **282 (Pt 1)**: p. 85-90.
149. Chen, W.H., N.S. Pellegata, and P.H. Wang, *Coordinated effects of insulin-like growth factor I on inhibitory pathways of cell cycle progression in cultured cardiac muscle cells.* Endocrinology, 1995. **136**(11): p. 5240-3.
150. Reiss, K., et al., *Overexpression of insulin-like growth factor-1 in the heart is coupled with myocyte proliferation in transgenic mice.* Proc Natl Acad Sci U S A, 1996. **93**(16): p. 8630-5.
151. Amato, G., et al., *Body composition, bone metabolism, and heart structure and function in growth hormone (GH)-deficient adults before and after GH replacement therapy at low doses.* J Clin Endocrinol Metab, 1993. **77**(6): p. 1671-6.
152. Cittadini, A., et al., *Insulin-like growth factor-1 but not growth hormone augments mammalian myocardial contractility by sensitizing the myofilament to Ca2+ through a wortmannin-sensitive pathway: studies in rat and ferret isolated muscles.* Circ Res, 1998. **83**(1): p. 50-9.
153. Duerr, R.L., et al., *Insulin-like growth factor-1 enhances ventricular hypertrophy and function during the onset of experimental cardiac failure.* J Clin Invest, 1995. **95**(2): p. 619-27.
154. Donath, M.Y., et al., *Acute cardiovascular effects of insulin-like growth factor I in patients with chronic heart failure.* J Clin Endocrinol Metab, 1998. **83**(9): p. 3177-83.
155. Donath, M.Y., et al., *Cardiovascular and metabolic effects of insulin-like growth factor I at rest and during exercise in humans.* J Clin Endocrinol Metab, 1996. **81**(11): p. 4089-94.

156. Freestone, N.S., S. Ribaric, and W.T. Mason, *The effect of insulin-like growth factor-1 on adult rat cardiac contractility.* Mol Cell Biochem, 1996. **163-164**: p. 223-9.
157. Ren, J., et al., *Altered inotropic response to IGF-I in diabetic rat heart: influence of intracellular Ca2+ and NO.* Am J Physiol, 1998. **275**(3 Pt 2): p. H823-30.
158. Florini, J.R., D.Z. Ewton, and S.A. Coolican, *Growth hormone and the insulin-like growth factor system in myogenesis.* Endocr Rev, 1996. **17**(5): p. 481-517.
159. Ren, J., W.K. Samson, and J.R. Sowers, *Insulin-like growth factor I as a cardiac hormone: physiological and pathophysiological implications in heart disease.* J Mol Cell Cardiol, 1999. **31**(11): p. 2049-61.
160. Solem, M.L. and A.P. Thomas, *Modulation of cardiac Ca2+ channels by IGF1.* Biochem Biophys Res Commun, 1998. **252**(1): p. 151-5.
161. Anversa, P., et al., *Myocyte cell death and ventricular remodeling.* Curr Opin Nephrol Hypertens, 1997. **6**(2): p. 169-76.
162. Buerke, M., et al., *Cardioprotective effect of insulin-like growth factor I in myocardial ischemia followed by reperfusion.* Proc Natl Acad Sci U S A, 1995. **92**(17): p. 8031-5.
163. Li, Q., et al., *Overexpression of insulin-like growth factor-1 in mice protects from myocyte death after infarction, attenuating ventricular dilation, wall stress, and cardiac hypertrophy.* J Clin Invest, 1997. **100**(8): p. 1991-9.
164. Butler, A.A., et al., *Insulin-like growth factor-I receptor signal transduction: at the interface between physiology and cell biology.* Comp Biochem Physiol B Biochem Mol Biol, 1998. **121**(1): p. 19-26.
165. White, M.F., *The IRS-signalling system: a network of docking proteins that mediate insulin action.* Mol Cell Biochem, 1998. **182**(1-2): p. 3-11.
166. Craparo, A., T.J. O'Neill, and T.A. Gustafson, *Non-SH2 domains within insulin receptor substrate-1 and SHC mediate their phosphotyrosine-dependent interaction with the NPEY motif of the insulin-like growth factor I receptor.* J Biol Chem, 1995. **270**(26): p. 15639-43.
167. Coolican, S.A., et al., *The mitogenic and myogenic actions of insulin-like growth factors utilize distinct signaling pathways.* J Biol Chem, 1997. **272**(10): p. 6653-62.
168. Giorgetti, S., et al., *The insulin and insulin-like growth factor-I receptor substrate IRS-1 associates with and activates phosphatidylinositol 3-kinase in vitro.* J Biol Chem, 1993. **268**(10): p. 7358-64.
169. Kaliman, P., et al., *Phosphatidylinositol 3-kinase inhibitors block differentiation of skeletal muscle cells.* J Biol Chem, 1996. **271**(32): p. 19146-51.
170. Kaliman, P., et al., *Insulin-like growth factors require phosphatidylinositol 3-kinase to signal myogenesis: dominant negative p85 expression blocks differentiation of L6E9 muscle cells.* Mol Endocrinol, 1998. **12**(1): p. 66-77.
171. Pinset, C., et al., *Wortmannin inhibits IGF-dependent differentiation in the mouse myogenic cell line C2.* C R Acad Sci III, 1997. **320**(5): p. 367-74.
172. Datta, S.R., A. Brunet, and M.E. Greenberg, *Cellular survival: a play in three Akts.* Genes Dev, 1999. **13**(22): p. 2905-27.
173. Nabeshima, Y., et al., *Myogenin gene disruption results in perinatal lethality because of severe muscle defect.* Nature, 1993. **364**(6437): p. 532-5.
174. Tamir, Y. and E. Bengal, *Phosphoinositide 3-kinase induces the transcriptional activity of MEF2 proteins during muscle differentiation.* J Biol Chem, 2000. **275**(44): p. 34424-32.

175. Rommel, C., et al., *Mediation of IGF-1-induced skeletal myotube hypertrophy by PI(3)K/Akt/mTOR and PI(3)K/Akt/GSK3 pathways.* Nat Cell Biol, 2001. **3**(11): p. 1009-13.
176. Lai, K.M., et al., *Conditional activation of akt in adult skeletal muscle induces rapid hypertrophy.* Mol Cell Biol, 2004. **24**(21): p. 9295-304.
177. Song, Y.H., et al., *Insulin-like growth factor I-mediated skeletal muscle hypertrophy is characterized by increased mTOR-p70S6K signaling without increased Akt phosphorylation.* J Investig Med, 2005. **53**(3): p. 135-42.
178. Datta, S.R., et al., *Akt phosphorylation of BAD couples survival signals to the cell-intrinsic death machinery.* Cell, 1997. **91**(2): p. 231-41.
179. Minshall, C., et al., *IL-4 and insulin-like growth factor-I inhibit the decline in Bcl-2 and promote the survival of IL-3-deprived myeloid progenitors.* J Immunol, 1997. **159**(3): p. 1225-32.
180. Minshall, C., et al., *Phosphatidylinositol 3'-kinase, but not S6-kinase, is required for insulin-like growth factor-I and IL-4 to maintain expression of Bcl-2 and promote survival of myeloid progenitors.* J Immunol, 1999. **162**(8): p. 4542-9.
181. Parrizas, M. and D. LeRoith, *Insulin-like growth factor-1 inhibition of apoptosis is associated with increased expression of the bcl-xL gene product.* Endocrinology, 1997. **138**(3): p. 1355-8.
182. Parrizas, M., A.R. Saltiel, and D. LeRoith, *Insulin-like growth factor 1 inhibits apoptosis using the phosphatidylinositol 3'-kinase and mitogen-activated protein kinase pathways.* J Biol Chem, 1997. **272**(1): p. 154-61.
183. Peruzzi, F., et al., *Multiple signaling pathways of the insulin-like growth factor 1 receptor in protection from apoptosis.* Mol Cell Biol, 1999. **19**(10): p. 7203-15.
184. Crabtree, G.R., *Generic signals and specific outcomes: signaling through Ca2+, calcineurin, and NF-AT.* Cell, 1999. **96**(5): p. 611-4.
185. Semsarian, C., et al., *Skeletal muscle hypertrophy is mediated by a Ca2+-dependent calcineurin signalling pathway.* Nature, 1999. **400**(6744): p. 576-81.
186. Bodine, S.C., et al., *Akt/mTOR pathway is a crucial regulator of skeletal muscle hypertrophy and can prevent muscle atrophy in vivo.* Nat Cell Biol, 2001. **3**(11): p. 1014-9.
187. Invitrogen, *ViraPower T-Rex Lentiviral Expression System User Manual*. 2004.
188. Biosystems, A., *Relative quantification of gene expression: ABI PRISM 7700 Sequence Detection system*, A. Biosystems, Editor. 1997.
189. NCBI. *Rat IGF-1Ea mRNA Sequence*. 2010 15-09-2010]; Rat IGF-1Ea mRNA Sequence]. Available from: **<http://www.ncbi.nlm.nih.gov/nuccore/XM_216875.1?report=genbank>**
190. Bonfoco, E., et al., *Apoptosis and necrosis: two distinct events induced, respectively, by mild and intense insults with N-methyl-D-aspartate or nitric oxide/superoxide in cortical cell cultures.* Proc Natl Acad Sci U S A, 1995. **92**(16): p. 7162-6.
191. Uchide, N., et al., *Lactate dehydrogenase leakage as a marker for apoptotic cell degradation induced by influenza virus infection in human fetal membrane cells.* Intervirology, 2009. **52**(3): p. 164-73.
192. Decker, T. and M.L. Lohmann-Matthes, *A quick and simple method for the quantitation of lactate dehydrogenase release in measurements of cellular cytotoxicity and tumor necrosis factor (TNF) activity.* J Immunol Methods, 1988. **115**(1): p. 61-9.

193. Lappalainen, K., et al., *Comparison of cell proliferation and toxicity assays using two cationic liposomes.* Pharm Res, 1994. **11**(8): p. 1127-31.
194. Nachlas, M.M., et al., *The determination of lactic dehydrogenase with a tetrazolium salt.* Anal Biochem, 1960. **1**: p. 317-26.
195. Suzuki, T., et al., *DNA staining for fluorescence and laser confocal microscopy.* J Histochem Cytochem, 1997. **45**(1): p. 49-53.
196. Rabinovitch, P. *Introduction to Cell Cycle Analysis*. [cited 2010 10-09]; Available from: www.phnxflow.com/Introduction%20to%20Cell%20Cycle%20Analysis.pdf.
197. Tarnavski, O., et al., *Mouse cardiac surgery: comprehensive techniques for the generation of mouse models of human diseases and their application for genomic studies.* Physiol Genomics, 2004. **16**(3): p. 349-60.
198. Takagawa, J., et al., *Myocardial infarct size measurement in the mouse chronic infarction model: comparison of area- and length-based approaches.* J Appl Physiol, 2007. **102**(6): p. 2104-11.
199. Ismail, J.A., et al., *Immunohistologic labeling of murine endothelium.* Cardiovasc Pathol, 2003. **12**(2): p. 82-90.
200. Romano, G., *Current development of lentiviral-mediated gene transfer.* Drug News Perspect, 2005. **18**(2): p. 128-34.
201. Gould, D.J. and Y. Chernajovsky, *Endogenous GATA factors bind the core sequence of the tetO and influence gene regulation with the tetracycline system.* Mol Ther, 2004. **10**(1): p. 127-38.
202. Niwa, H., J. Miyazaki, and A.G. Smith, *Quantitative expression of Oct-3/4 defines differentiation, dedifferentiation or self-renewal of ES cells.* Nat Genet, 2000. **24**(4): p. 372-6.
203. Rabinovsky, E.D., et al., *Targeted expression of IGF-1 transgene to skeletal muscle accelerates muscle and motor neuron regeneration.* FASEB J, 2003. **17**(1): p. 53-5.
204. Russo, V.C., et al., *The insulin-like growth factor system and its pleiotropic functions in brain.* Endocr Rev, 2005. **26**(7): p. 916-43.
205. An, C., et al., *IGF-1 and BMP-2 induces differentiation of adipose-derived mesenchymal stem cells into chondrocytes-like cells.* Ann Biomed Eng. **38**(4): p. 1647-54.
206. Winn, N.S., *The differential Role of Insulin-like Growth Factor-1 Isoforms in Skeletal muscle*. 2006, Heidelberg University.
207. Klinz, F., et al., *Inhibition of phosphatidylinositol-3-kinase blocks development of functional embryonic cardiomyocytes.* Exp Cell Res, 1999. **247**(1): p. 79-83.
208. Sauer, H., et al., *Role of reactive oxygen species and phosphatidylinositol 3-kinase in cardiomyocyte differentiation of embryonic stem cells.* FEBS Lett, 2000. **476**(3): p. 218-23.
209. McDevitt, T.C., M.A. Laflamme, and C.E. Murry, *Proliferation of cardiomyocytes derived from human embryonic stem cells is mediated via the IGF/PI 3-kinase/Akt signaling pathway.* J Mol Cell Cardiol, 2005. **39**(6): p. 865-73.
210. Lazarides, E. and K. Burridge, *Alpha-actinin: immunofluorescent localization of a muscle structural protein in nonmuscle cells.* Cell, 1975. **6**(3): p. 289-98.
211. Goncharova, E.J., Z. Kam, and B. Geiger, *The involvement of adherens junction components in myofibrillogenesis in cultured cardiac myocytes.* Development, 1992. **114**(1): p. 173-83.
212. Williams, A.J., *The functions of two species of calcium channel in cardiac muscle excitation-contraction coupling.* Eur Heart J, 1997. **18 Suppl A**: p. A27-35.

213. Satin, J., et al., *Calcium handling in human embryonic stem cell-derived cardiomyocytes.* Stem Cells, 2008. **26**(8): p. 1961-72.
214. Klabunde, R.E., *Cardiovascular Physiology Concepts*. 2005, Lippincott Williams & Wilkins.
215. Information, P., *Rhod Calcium Indicators*, M.P.I.D. Technologies, Editor. 2010.
216. Bers, D.M., *Calcium cycling and signaling in cardiac myocytes.* Annu Rev Physiol, 2008. **70**: p. 23-49.
217. Guyette, J.P., I.S. Cohen, and G.R. Gaudette, *Strategies for regeneration of heart muscle.* Crit Rev Eukaryot Gene Expr. **20**(1): p. 35-50.
218. Burchfield, J.S. and S. Dimmeler, *Role of paracrine factors in stem and progenitor cell mediated cardiac repair and tissue fibrosis.* Fibrogenesis Tissue Repair, 2008. **1**(1): p. 4.
219. Abbott, J.D., et al., *Stromal cell-derived factor-1alpha plays a critical role in stem cell recruitment to the heart after myocardial infarction but is not sufficient to induce homing in the absence of injury.* Circulation, 2004. **110**(21): p. 3300-5.
220. van Laake, L.W., et al., *Monitoring of cell therapy and assessment of cardiac function using magnetic resonance imaging in a mouse model of myocardial infarction.* Nat. Protocols, 2007. **2**(10): p. 2551-2567.
221. Zhou, Y., K. Bourcy, and Y.J. Kang, *Copper-induced regression of cardiomyocyte hypertrophy is associated with enhanced vascular endothelial growth factor receptor-1 signalling pathway.* Cardiovasc Res, 2009. **84**(1): p. 54-63.
222. Bettink, S.I., et al., *Integrin-linked kinase is a central mediator in angiotensin II type 1- and chemokine receptor CXCR4 signaling in myocardial hypertrophy.* Biochem Biophys Res Commun. **397**(2): p. 208-13.
223. Fuchs, M., et al., *Role of interleukin-6 for LV remodeling and survival after experimental myocardial infarction.* FASEB J, 2003. **17**(14): p. 2118-20.
224. Uemura, R., et al., *Bone marrow stem cells prevent left ventricular remodeling of ischemic heart through paracrine signaling.* Circ Res, 2006. **98**(11): p. 1414-21.
225. Urbanek, K., et al., *Cardiac stem cells possess growth factor-receptor systems that after activation regenerate the infarcted myocardium, improving ventricular function and long-term survival.* Circ Res, 2005. **97**(7): p. 663-73.
226. Markel, T.A., et al., *VEGF is critical for stem cell-mediated cardioprotection and a crucial paracrine factor for defining the age threshold in adult and neonatal stem cell function.* Am J Physiol Heart Circ Physiol, 2008. **295**(6): p. H2308-14.
227. Burchfield, J.S., et al., *Interleukin-10 from transplanted bone marrow mononuclear cells contributes to cardiac protection after myocardial infarction.* Circ Res, 2008. **103**(2): p. 203-11.
228. Kinnaird, T., et al., *Marrow-derived stromal cells express genes encoding a broad spectrum of arteriogenic cytokines and promote in vitro and in vivo arteriogenesis through paracrine mechanisms.* Circ Res, 2004. **94**(5): p. 678-85.
229. Hattori, F., et al., *Nongenetic method for purifying stem cell-derived cardiomyocytes.* Nat Methods. **7**(1): p. 61-6.
230. Dow, J., et al., *Washout of transplanted cells from the heart: a potential new hurdle for cell transplantation therapy.* Cardiovasc Res, 2005. **67**(2): p. 301-7.
231. Soonpaa, M.H., et al., *Formation of nascent intercalated disks between grafted fetal cardiomyocytes and host myocardium.* Science, 1994. **264**(5155): p. 98-101.
232. Leor, J., et al., *Transplantation of fetal myocardial tissue into the infarcted myocardium of rat. A potential method for repair of infarcted myocardium?* Circulation, 1996. **94**(9 Suppl): p. II332-6.

233. Li, R.K., et al., *In vivo survival and function of transplanted rat cardiomyocytes.* Circ Res, 1996. **78**(2): p. 283-8.
234. Doetschman, T.C., et al., *The in vitro development of blastocyst-derived embryonic stem cell lines: formation of visceral yolk sac, blood islands and myocardium.* J Embryol Exp Morphol, 1985. **87**: p. 27-45.
235. Maltsev, V.A., et al., *Embryonic stem cells differentiate in vitro into cardiomyocytes representing sinusnodal, atrial and ventricular cell types.* Mech Dev, 1993. **44**(1): p. 41-50.
236. Pouzet, B., J.T. Vilquin, and P. Menasche, *[Myocardial implantation of muscle cells].* Presse Med, 2002. **31**(33): p. 1569-76.
237. Fukuda, K., *Use of adult marrow mesenchymal stem cells for regeneration of cardiomyocytes.* Bone Marrow Transplant, 2003. **32 Suppl 1**: p. S25-7.
238. Jackson, K.A., et al., *Regeneration of ischemic cardiac muscle and vascular endothelium by adult stem cells.* J Clin Invest, 2001. **107**(11): p. 1395-402.
239. Orlic, D., et al., *Bone marrow cells regenerate infarcted myocardium.* Nature, 2001. **410**(6829): p. 701-5.
240. Murry, C.E., et al., *Skeletal myoblast transplantation for repair of myocardial necrosis.* J Clin Invest, 1996. **98**(11): p. 2512-23.
241. Gabriel, A.S., et al., *IL-6 levels in acute and post myocardial infarction: their relation to CRP levels, infarction size, left ventricular systolic function, and heart failure.* Eur J Intern Med, 2004. **15**(8): p. 523-528.
242. Reiss, K., et al., *Acute myocardial infarction leads to upregulation of the IGF-1 autocrine system, DNA replication, and nuclear mitotic division in the remaining viable cardiac myocytes.* Exp Cell Res, 1994. **213**(2): p. 463-72.
243. Scorsin, M., et al., *Can grafted cardiomyocytes colonize peri-infarct myocardial areas?* Circulation, 1996. **94**(9 Suppl): p. II337-40.
244. Connold, A.L., et al., *The survival of embryonic cardiomyocytes transplanted into damaged host rat myocardium.* J Muscle Res Cell Motil, 1997. **18**(1): p. 63-70.
245. Smits, A.M., et al., *Human cardiomyocyte progenitor cell transplantation preserves long-term function of the infarcted mouse myocardium.* Cardiovasc Res, 2009. **83**(3): p. 527-35.
246. Reinecke, H., et al., *Survival, integration, and differentiation of cardiomyocyte grafts: a study in normal and injured rat hearts.* Circulation, 1999. **100**(2): p. 193-202.
247. van Laake, L.W., et al., *Improvement of mouse cardiac function by hESC-derived cardiomyocytes correlates with vascularity but not graft size.* Stem Cell Res, 2009. **3**(2-3): p. 106-12.